Forces on Bars in High-Consistency Mill-Scale Refiners

by

Dustin James Olender
B.Sc., Queen's University, 2001
M.A.Sc., Royal Military College of Canada, 2004

A Dissertation Submitted in Partial Fulfillment of the
Requirements for the Degree of

DOCTOR of PHILOSOPHY

in the Department of Mechanical Engineering

December 20, 2007

Forces on Bars in High-Consistency Mill-Scale Refiners

by

Dustin James Olender

Supervisory Committee

Dr. Peter Wild, Supervisor
(Department of Mechanical Engineering)

Dr. Brad Buckham, Departmental Member
(Department of Mechanical Engineering)

Dr. David Sinton, Departmental Member
(Department of Mechanical Engineering

Dr. Rolf Lueck, Outside Member
(School of Earth and Ocean Sciences)

Supervisory Committee

Dr. Peter Wild, Supervisor (Department of Mechanical Engineering)

Dr. Brad Buckham, Departmental Member (Department of Mechanical Engineering)

Dr. David Sinton, Departmental Member (Department of Mechanical Engineering

Dr. Rolf Lueck, Outside Member (School of Earth and Ocean Sciences)

Abstract

Refiners are used in the pulp and paper industry to separate wood chips into individual fibres and to develop the morphology of fibres to be suitable for the type and grade of paper to be produced. Within a refiner are discs, at least one of which rotates at high speed and all of which are lined with radial patterns of bars on their opposing surfaces. As the chips and fibres are accelerated through the refiner, compressive and shear forces are applied to them by the bars as the opposed discs cross each other. Experiments have shown that the contact mechanics of bar-crossings are a significant factor in the development of fibre properties. To investigate the contact mechanics in operating refiners, a prototype piezoelectric-based sensor was developed to measure the forces applied by the bars. This work re-designs the prototype sensor to function at the mill-scale, and validates the design in two trials. Performance during these trials is presented along with an in-depth analysis of the recorded data.

Arrays of force sensors were installed in two single-disc refiners: a pilot-scale machine operating as a primary stage, and a mill-scale machine operating as a rejects stage. In the rejects refiner, mean forces were highest at the periphery of the refining zone, while in the primary stage, mean forces were higher at the sensor closest to the refiner axis. Higher coefficients of friction were measured in the primary stage refiner,

which also showed less active bar-crossings. Distributions of peak force values were generated for a range of standard operating conditions. Primary stage refining showed near decreasing exponential distributions, while rejects refining showed skewed normal distributions. These results indicate a fundamental difference in the behavior of these refiners, which is explained in terms of the processing stage of the wood fibre and scale of the refiner.

Past laboratory experiments in a single-bar refiner have shown that pulp consistency can greatly affect the contact mechanics of bar-crossing impacts. The effect was observed as a positive correlation between the coefficient of friction and the mass fraction of fibre in the stock, known as the consistency. In the present work, a similar correlation was found in the primary stage refiner, but only in the sensor closest to the refiner axis. No significant changes in the coefficient of friction were observed in the rejects refiner; however, only a small range of consistencies was tested. These initial findings suggest relationships found in past laboratory tests may translate to larger-scale equipment.

The clashing of plates during refining accelerates bar wear, and delays production. An investigation of the ability of the sensor to predict plate clash was conducted. The force sensors consistently provided advanced warning of a clash event, many seconds before the accelerometer-based plate protection system currently in use by the mill. A sensitivity study showed that the new system was able to outperform the accelerometer system over a range of detection settings, and that the accelerometer could not be tuned to match the performance of the new system.

Table of Contents

List of Figures

Nomenclature

Symbols

Cn	consistency of the feedstock (%)
$\mathbf{C}$	centrifugal force acting on annular mass of pulp (N)
$\mathbf{F_{r1}}$	radial friction force from first disc acting on annular mass of pulp (N)
$\mathbf{F_{r2}}$	radial friction force from second disc acting on annular mass of pulp (N)
$\mathbf{F_{t1}}$	tangential friction force acting on annular mass of pulp (N)
m_f	mass of fibre in feedstock (kg)
m_w	mass of water in feedstock (kg)
$\mathbf{S}$	steam-induced drag force acting on annular mass of pulp (N)
T	gap between plates (mm)
$\mathbf{T}$	normal force acting on an annular mass of pulp (N)
μ_{teq}	equivalent tangential coefficient of friction
W	floc grammage (g/m^2)

Nomenclature

Acronyms

TMP thermomechanical pulp

RFS refiner force sensor

HC high-consistency

LC low-consistency

FRF frequency response function

Definitions

Defibration – separation of wood chips into individual fibres

Fibrillation – brushing and collapsing of fibre walls during refining

Floc –fibres that have grouped together after having been separated from their original wood matrix

Grammage – a measure of the apparent density of a physical sheet of paper, also referred to as the basis weight

Residence Time – amount of time that the fibre remains in between the plates during operation

Shive – a term used to describe a fragment of a chip, which is often the result of having passed through the refiner relatively unprocessed

Acknowledgments

I would first like to thank my supervisor, Dr. Peter Wild, for many things, but the most important, would be for providing strong leadership, and showing me what it takes to bring a project of this magnitude through to completion. I would also like to thank the other researchers and engineers whom I worked closely with: Peter Byrnes, Brett Prairie, Paul Francescutti, Daniel Ouellet, and John Senger. Your work ethic and engineering skills are top notch, and I learned, and continue to learn, a great deal from you.

When one embarks on an academic quest such as this, it is absolutely necessary to have a supportive network of friends and family to help, and really, to enjoy life outside of research along the way. My deep thanks to those in my life who have made this time so rich.

Chapter 1

Introduction

Although the production of lower-grades of paper, specifically newsprint, is in decline in North America due to stagnant or diminishing demand, much of this lost capacity is shifting to meet demand in other parts of the planet, notably South America and Asia [1]. The use of mechanical energy to develop wood into pulp, for producing paper for conventional uses, or as a substrate for newer products [2], will thus remain a global activity into the foreseeable future. Canada in particular has a serious interest in mechanical refining, as it currently leads the world in the commercial production of mechanical pulp [3] and retains a massive knowledge-base as a result.

The popularity of the process is a result of its high yield, low cost, and relatively environmentally friendly nature. Mechanical refining produces a long, flexible fibre that is strong, but lacks the brightness of chemically derived pulps. Mechanical pulps are typically combined with expensive chemical pulps to reach desired quality grades. The one drawback of mechanical pulping is the amount of electrical energy it consumes. Current energy requirements are between 1500 – 3000 kWh/t, and the bulk of this energy is consumed during refining [4].

More efficient use of energy is thus the primary goal of research into mechanical refining, a process which has advanced significantly over the past four decades. Possibly due to the poor accessibility of the refining zone, which is completely enclosed and pressurized, energy-based quantifiers that rely on global process parameters such as gross power, have emerged to estimate refiner performance. These methodologies largely ignore the mechanical interactions experienced by the wood fibre within the refiner, in favor of a more black box approach. To provide explanations to many aspects of the process which remain unknown, or disputed, researchers are investigating the contact mechanics which govern the process.

One such endeavor is the Refiner Force Sensor Project, whose aim has been to develop a sensor capable of measuring the forces imparted to wood fibre within the refiner. Data from this sensor has provided insight into many aspects of refining [5, 6], but only in the context of experimental, or pilot-scale refiners. In this work, the prototype sensor is redesigned, qualifying a new generation of sensor that is capable of measuring localized bar forces in a mill-scale refiner. The results of an in-depth analysis of the data are presented.

1.1 Background

All refiners operate on the same principle, having two or more axially aligned discs, at least one of which is driven (*i.e.* the *rotor*) and rotates at high speeds. Replaceable *plate segments*, lined with radially oriented bars, are mounted to the surface of the discs, and it is these bars that perform the mechanical action. Bars wear during normal operation and are typically replaced after many hundreds of hours of operation.

A mixture of wood chips and water is fed into the gap between the plates at the rotational axis. Under many tons of axial thrust, the gap is closed to 1-2 millimeters, causing the bars to impose cyclic compression and shear on the wood fibre passing through the gap. As the fibres are worked and separated, they become pulp and tend to accumulate in bundles, called “flocs”. A depiction of a floc being captured between a rotor and stator bar is shown in Figure 1.1. As these flocs of fibres make contact with the rotor they are accelerated and forced to flow to the disc periphery. The immense frictional forces that occur generate heat, which eases the separation of the wood fibres, while also producing steam, which is a driving force in the process. This combination of treatments defines the thermomechanical pulp (TMP) refiner. Additional chemical and thermal pre-treatments are often employed to varying degrees [7].

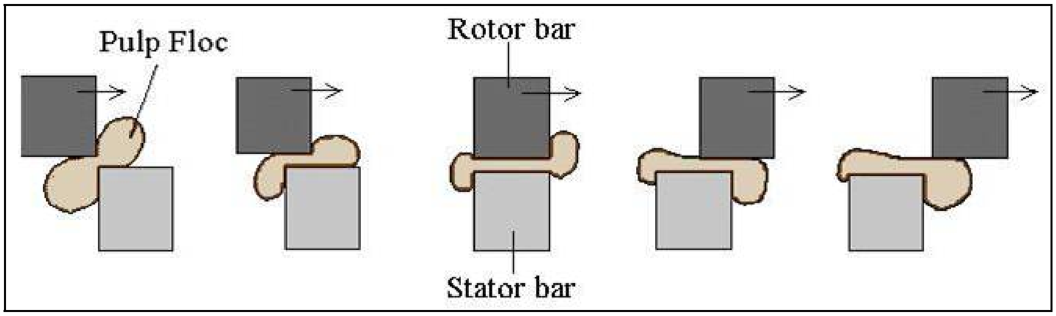

Figure 1.1: Schematic of a bar-crossing [32].

The single-disc type is the simplest mechanical configuration of the refiner discussed above, and is shown schematically in Figure 1.2. It is composed of one rotor, and one stationary disc or *stator*. Stock, being composed of wood material and water, is fed through the eye of the stator by a ribbon-feeder. The open construction of the ribbon-feeder is such that it allows venting of steam without disrupting the flow of material into the refiner. The capacity of the refiner is usually discussed in terms of the *production rate*, measured in tonnes of pulp produced per day (t/d).

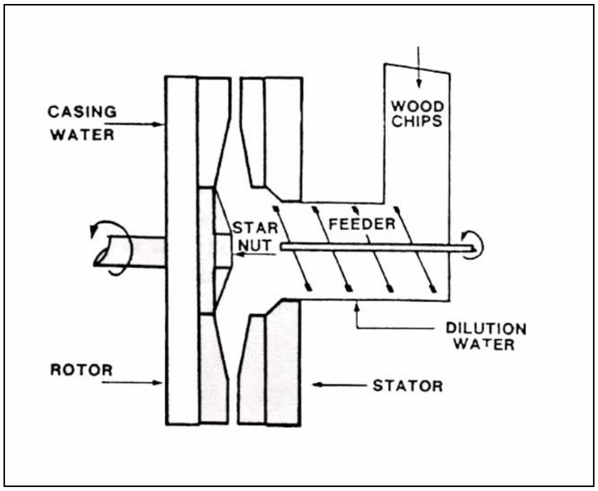

Figure 1.2: Schematic of a single-disc type refiner [7].

To impart the forces necessary to develop the wood fibre, the discs within the refiner must be operated at close proximity. This configuration is difficult to achieve mechanically, and results in frequent collisions between the discs, referred to as *plate clashes* [8]. Even with control systems in place to protect against plate clashing, these clashes still occur regularly in operation, accelerating the wear of bars and causing production delays. The phenomenon is poorly understood, but it is widely believed that plate clashes are the result of an interruption in the flow of pulp within the refiner [9].

All refiner designs allow for the addition of dilution water during operation, which, as shown in Figure 1.2, can be injected at the ribbon-feeder, or directly into the casing. The amount of water in the stock is an important process parameter, which is measured as consistency. *Consistency*, *Cn*, is defined as the percentage, by weight, of wood fibre in the fibre and water mixture. This is shown in Equation 1,

$$Cn = \frac{m_f}{m_f + m_w} \times 100\% , \qquad (1)$$

where m_f is the mass of wood fibre (kg), and m_w is the mass of water (kg).

The primary stages of refining are performed at consistencies greater than 20%, which is considered *high-consistency* (HC), in which the stock is still in the form of freshly cut chips or coarse fibres. A consistency of 50% marks the upper barrier of high-consistency refining, beyond this point, chips would have to be heated to remove further moisture. Later stages of refining are performed at consistencies below 5%, which is considered *low-consistency* (LC), in which the texture of the pulp is similar to that of porridge. Mechanical pulps often do not receive LC refining, in contrast to chemical pulps, which greatly benefit from this process [10]. LC refining is a milder form of refining and consumes approximately an order of magnitude less energy than HC refining. It is therefore in the primary HC stages of refining where most of the energy is consumed in producing mechanical pulps, and where the overall character of the pulp is developed.

The plate segments discussed earlier are critical to the refining process, as they contain the pattern of bars that directly perform the refining action. A typical first-stage plate segment is shown in Figure 1.3, alongside a photograph of an open Andritz 45-1B single-disc type refiner. The plate shown has three sections containing progressively finer bars: the breaker-bar section, intermediate section and fine bar section.

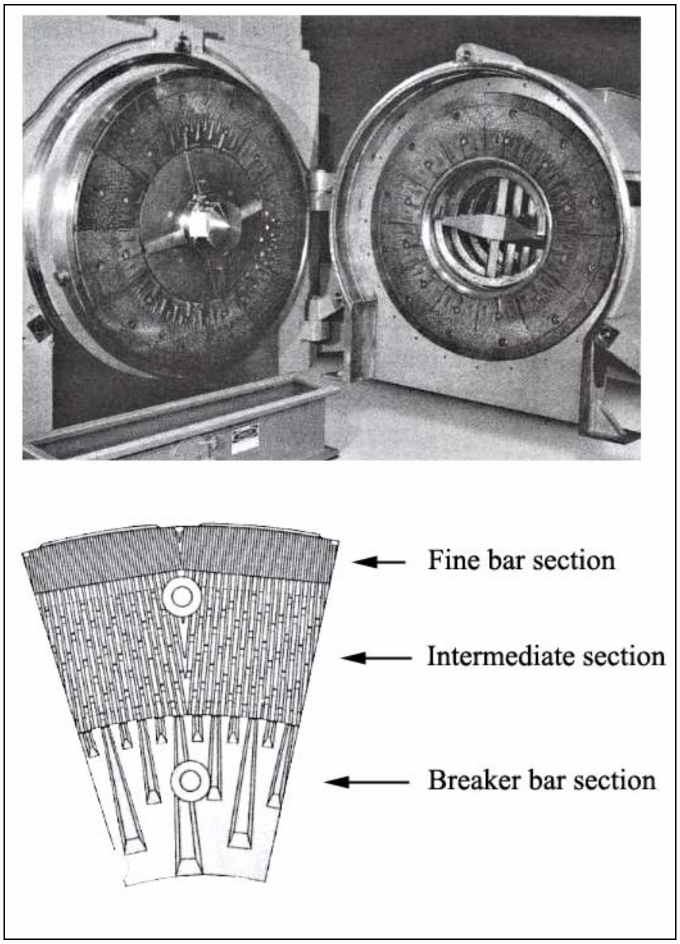

Figure 1.3: Andritz 45-1B single-disc refiner with stator door open and a typical first-stage plate segment, showing the three different zones of refining bars [7].

A number of studies have tracked the development of wood fibre across the plates by means of radially spaced sampling ports [11, 12, 13], or other techniques [14]. These studies have indicated that each section of the plate is associated with a specific stage of fibre development. It is known that the breaker-bar section decomposes the wood chips into a coarsely reduced form, referred to as *shives*. A cross-sectional view of the plate would also reveal a taper in the breaker bar section leading up to the intermediate and fine bar sections, which are ground relatively flat. It is thus in the intermediate and fine bar sections where the smallest plate gaps occur, and where most of the energy is consumed [14]. A further function of the breaker bars is to supply a continuous feed of coarse material to this small gap region, commonly referred to as the *refining zone*. Within the refining zone, the idealized function of the intermediate section is to separate the wood into individual fibres. This process is called *defibration*, and is also accompanied by actions which negatively affect fibre quality, such as fibre cutting. The idealized function of the fine bar section is *fibrillation*, or the brushing of the walls of individual fibres. The morphology that is developed in the fibre is critical for building the bonds necessary to produce paper [7].

The level of refining is presently measured in terms of energy-based quantifiers, the most basic of which is the *specific energy*. Specific energy is defined as the energy consumed by the motor, divided by the production rate, having units of kilowatt-hours per ton (kWh/t). Wide variations in pulp properties can occur at the same level of specific energy [15], and, therefore, specific energy alone is insufficient to completely describe the refining action. It was proposed [16] that variations of standard operating parameters, such as motor load, production rate, consistency and rotational speed can be used to change the amount of time the pulp spends in the refining zone, known as the *residence time*, without a change in specific energy. This would affect the amount of energy actually delivered to the pulp.

Residence time of the pulp in the refining zone is a quantity not easily measured in practice, and theoretical models have attempted to fill this void. The most widely accepted model of pulp flow for an HC refiner was developed by Miles and May [16, 17, 18]. In this model, a force balance is used to predict the radial velocity of an annular mass of pulp, shown in Figure 1.4a. Many forces contribute to the motion of pulp in the refiner (shown in Figure 1.4b): centrifugal forces, **C**; radial friction $\mathbf{F_{r1}}$ and $\mathbf{F_{r2}}$, which retards the pulp flow; and steam flow-induced drag **S**, which can act radially inward or outward from the steam stagnation point. Tangential friction, $\mathbf{F_{t1}}$, which is created by the normal force acting on the pulp, **T**, is also considered. The model is based on a number of assumptions, which are summarized here:

(i) a small amount of pulp is stagnant in the grooves of the stator, but the bulk of the pulp network rotates with the rotor;

(ii) tangential friction forces are independent of consistency, refiner speed and radius;

(iii) radial friction is assumed constant, and chosen to be the same as wet wood on steel;

(iv) steamflow-induced drag retards pulp flow close to the axis and assists pulp flow toward the periphery, and is considered to have no net effect.

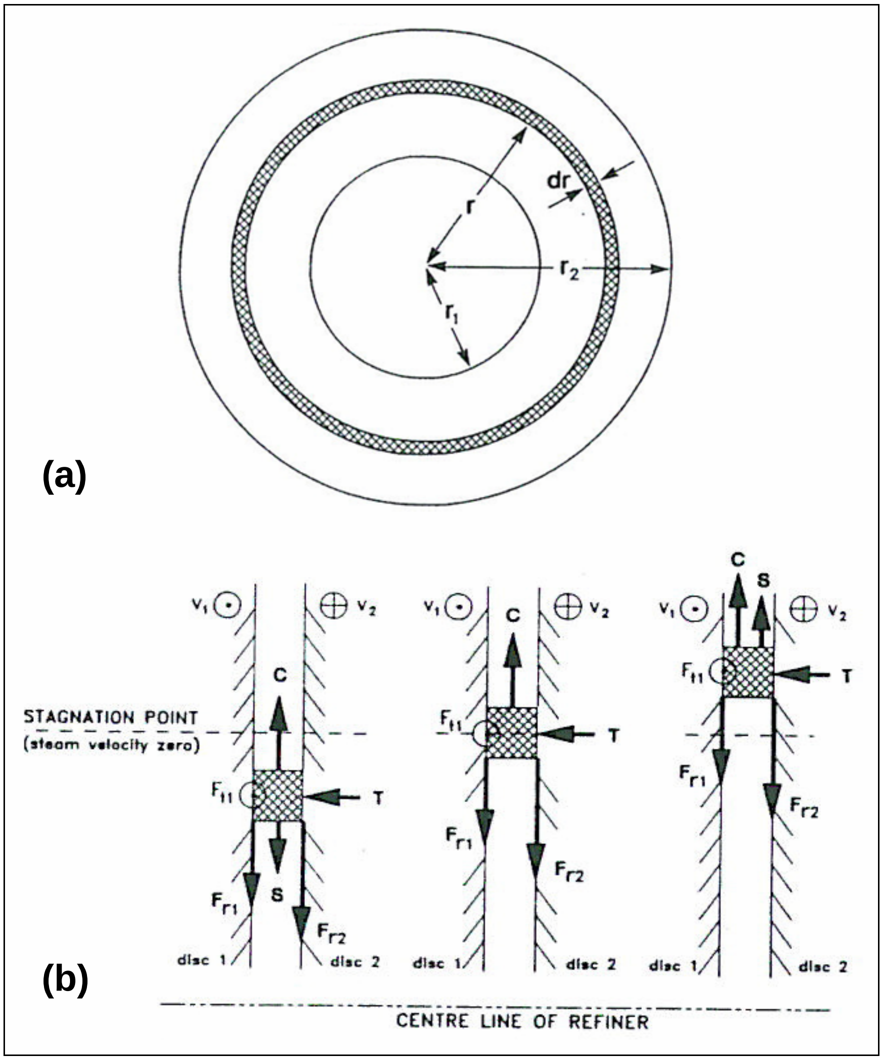

Figure 1.4: Miles and May Model of pulp flow: (a) annular mass of pulp, and (b) a free-body diagram of all forces acting on the annular mass [16].

The Miles and May model offers an explanation for the effects of many process parameters, including the effect of consistency. The model predicts that increasing the water content (decreasing consistency) between the plates increases the centripetal acceleration and therefore, force necessary to retain the pulp at a given radius, which causes more rapid expulsion from the refining zone. Alami *et al.* [19] and, separately, Murton [20] have shown that a reduction in consistency to approximately 36 % will reduce the specific energy needed to produce a certain pulp quality. The efficiency gains surrounding this behavior were primarily explained by the effect of consistency on residence time predicted by the Miles and May model. It was assumed that pulp residence time is too high, and that the work performed on the pulp during this extended time period is not useful.

In an attempt to verify these and other gains made under the auspices of the Miles and May model, a number of experiments have been performed to physically measure the residence time of pulp in the refining zone. Experiments were performed in a lab-scale refiner by Ouellet *et al.* [21], which used dyes in combination with optical sensors, and in tests in mill-scale refiners by Harkonen *et al.* [22] and separately, by Murton and Duffy [23], both of which used radioactive tracers. In all cases, it was found that empirical measurements of residence time did not support those predicted by the Miles and May model. For example, Murton and Duffy found that consistency had no effect on the residence time of the pulp [23]. Murton and Duffy partially attribute the failings of the model to an inadequacy of energy-based quantifiers to fully explain the effect of the refining action, which do not account for forces experienced by the pulp in the refining zone. In any case, these experimental findings underscore a controversy in the literature over residence time, and fundamental aspects of refiner operation.

Research into the contact mechanics of bar-crossings continues to offer new insight into these aspects of refining. Studies of the mechanisms of fibre development [24], fibre quantity in the refining zone [25], and recent tribological tests [26] are all notable in this regard.

Measurements of bar forces also fall within this area of research, and were first made in LC refiners in the 1970s [27, 28]. More recently, Senger and Ouellet [29] measured the normal and shear forces experienced by flocs in a single-bar laboratory refiner, which was designed to simulate bar-crossing impacts. Senger and Ouellet define the equivalent tangential coefficient of friction for this work, symbolized as μ_{teq}, which is defined as the average shear force, divided by the average normal force over an impact. Senger and Ouellet report that μ_{teq} is dependent on the sharpness of the bar, the thickness or *grammage* of the floc, and on the consistency of the floc. In particular, it was found that μ_{teq} increased proportionally with consistency when values over ~35% were tested; below this value μ_{teq} was relatively constant. The graph of μ_{teq} versus consistency is reproduced in Figure 1.5a. Four series of experiments are shown, during which plate gap T and floc grammage W were held constant.

Senger and Ouellet make the connection to earlier work by Alami *et al*. [19] and Murton [20] in which it was shown that a change in the energy-quality relationship was found when refining consistency was increased above 36 %, as shown in Figure 1.5b. In this case, the quality of the pulp was determined using an index of common metrics of the refined pulp. These metrics include, for example, the ability of the pulp suspension to drain through a screen and standardized orifice, which is known as the *freeness*; the presence of unrefined wood fragments that has escaped refining, which are known as *shives*; and also, the percentage of fibres over a certain minimum length. Higher quality pulps drain slower, have fewer shives, and have a high percentage of long, uncut fibres.

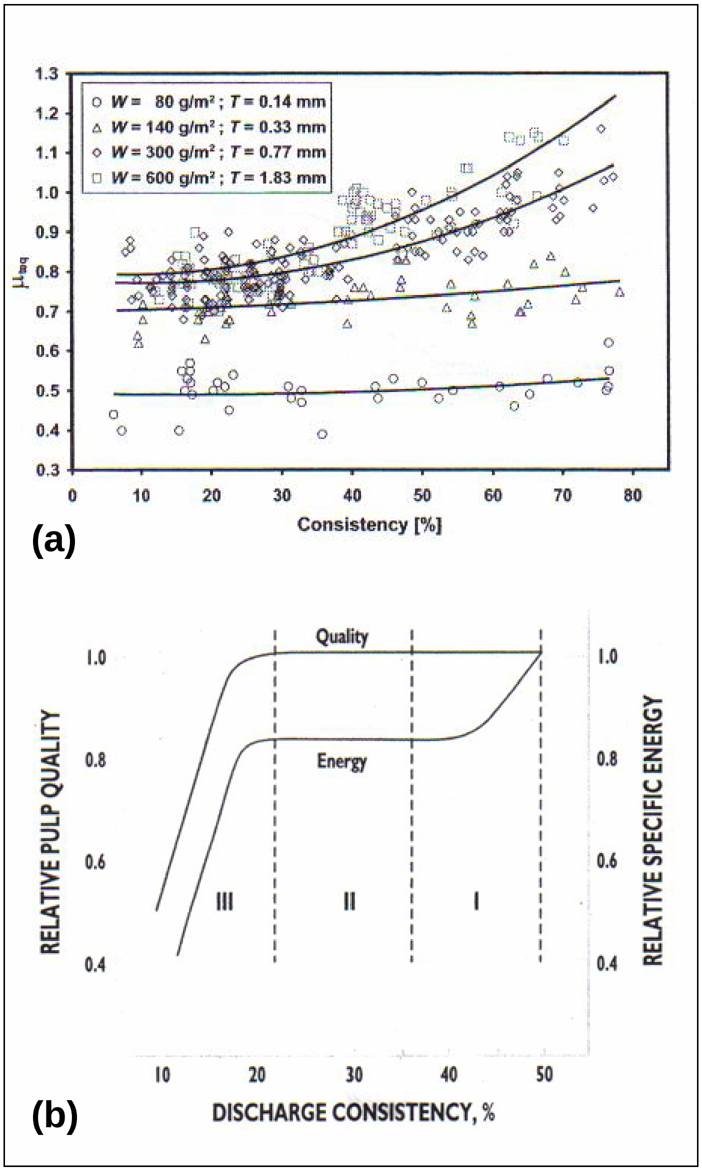

Figure 1.5: (a) Effect of consistency on equivalent tangential coefficient of friction found by Senger and Ouellet in single-bar refiner [29], and (b) relationship between pulp quality and discharge consistency found by Alami et al. [19].

Alami *et al.* had proposed that a decrease in residence time was responsible for the shift in refiner performance in region I and II, but the work of Senger and Ouellet suggest this might be better explained by the effect of consistency on μ_{teq}. The single-bar laboratory experiments were a major motivation for further exploration of the forces that are developed during bar-crossing impacts. These experiments renewed interest in the ploughing component of the forces that are generated over the first half of a bar-crossing impact as a major driver of pulp quality; the first researchers to make note of this were Goncharov *et al.* [27, 28].

Backlund [30] made measurements of shear forces over a small circular section of the refining zone in a mill-scale chip refiner. A commercial piezoelectric-based sensor was retrofitted to make these measurements; however, because of its size, individual bar-crossing impacts could not be resolved. Measurements of larger time-scale forces were successfully made, and the author reported that the highest shear forces were measured at the periphery of the refining zone. Backlund proposed that this increasing radial force trend is caused by the decreasing gap, and increasing tangential velocity of crossing bars, as one moves radially outwards in the refining zone.

Initial work on a prototype refiner force sensor (RFS), which is the focus of this work, was undertaken by Bankes [31] and Siadat [32]. A photograph of the first generation sensor, RFS1, is shown in Figure 1.6, along with a cross-sectional view. The RFS was designed to measure the forces experienced by refiner bars during individual bar-crossing events. The probe part extends into the refining zone, replacing a small section of refiner bar and imparts vertical loads to the piezo-ceramic elements below. This work determined the sensing element, the basic geometry of the probe and supporting components, and tested the method used to resolve normal and shear forces from the resultant.

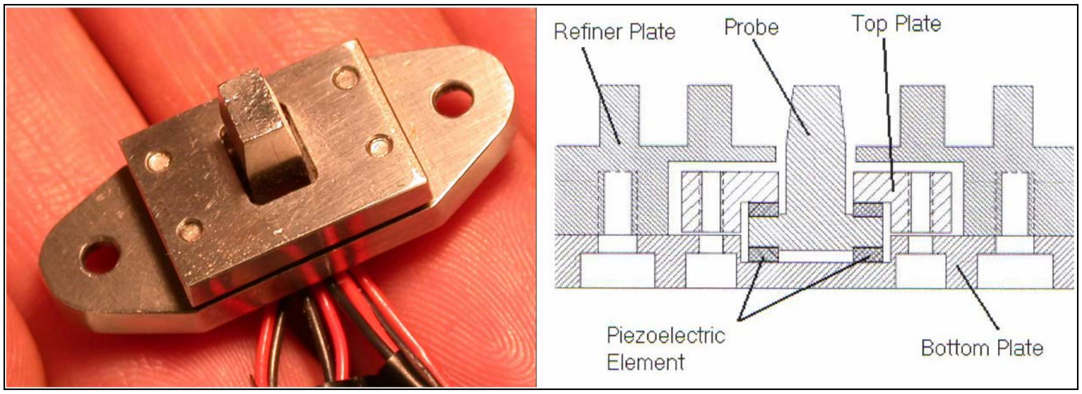

Figure 1.6: A photograph and cross-section of the first generation sensor: RFS1.

The RFS1 was tested in a laboratory-scale refiner, where it was recognized that resonance was a major design issue. Olmstead sought to address this problem in the second generation design [33], which was tested in a laboratory-scale refiner [34].

To perform in larger-scale refiners, it was recognized that the sensor would need an even wider dynamic range, and further improved durability. Senger *et al.* miniaturized the RFS2 design, and further increased the stiffness of the housing, and fixation of the sensor to the refiner plate. These improvements are discussed in more detail in Appendix A. Figure 1.7 shows series of normal and shear force impacts from the innermost and outermost sensors in an initial pilot-scale trial of the third generation sensor at the FPInnovations – Paprican Laboratory in Pt. Claire, QC. The asymmetry visible in the force profiles is caused by ploughing of the fibres as bars initially meet, as was initially discovered by Goncharov [28].

Both pulp and chips were used as feedstock during these trials and it was noted that for wood chips, impacts would last for several bar crossings. It was further observed that the distribution of forces followed a decreasing exponential distribution, which suggested substantial heterogeneity of the regularity of impacts within the refining zone.

This distribution had been suggested earlier [35] and later theorized [36] in the context of LC refining.

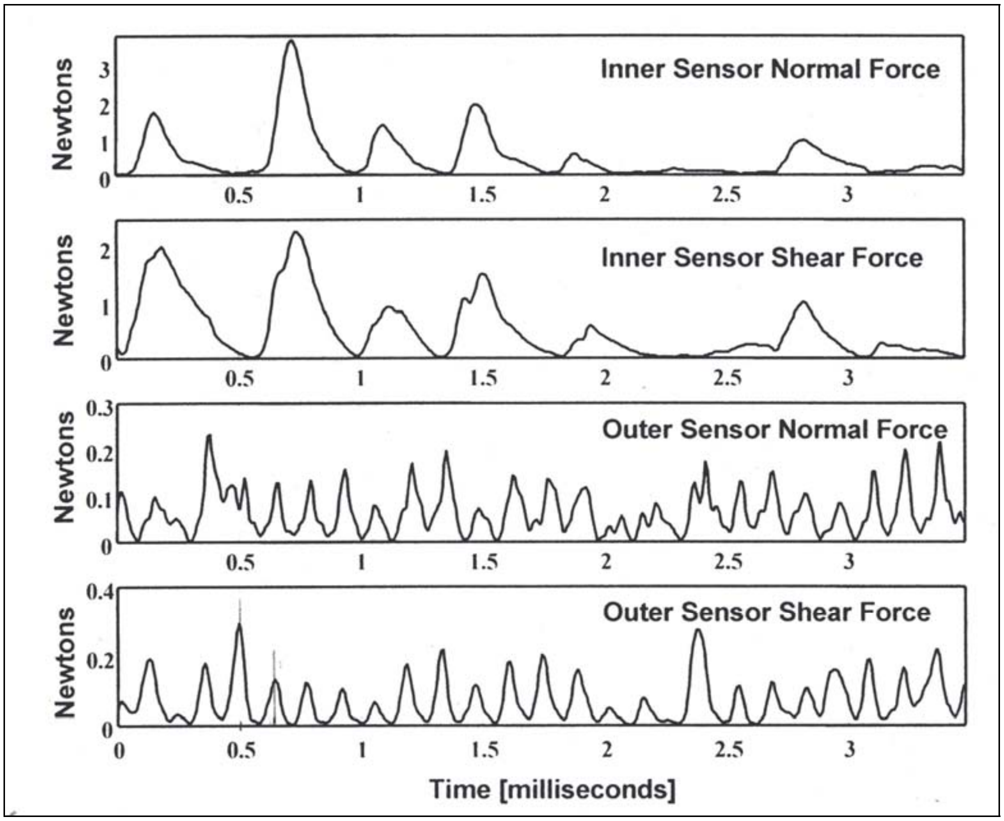

Figure 1.7: Normal and shear forces measured by RFS3 during bar-crossing impacts in a pilot-scale refiner [5].

The RFS3 was later tested in a 36-inch diameter, pressurized, single-disc refiner at the Andritz Research Facility in Springfield, Ohio (a photograph of this refiner is found in Figure 3.1). Unfortunately, force data could not reliably be measured due to resonance artifacts and an unexplained failure of all sensors in the second day of testing. But it was discovered that in combination, the array of sensors that were installed could still be used to track the movement of pulp in the refining zone and provide an estimate of mean residence time [15].

1.2 Objectives of this Dissertation

The overall objective of this work is to advance understanding of mechanical wood-chip refining by the exploration of bar-crossing contact mechanics in mill-scale refiners. The first objective is, therefore, to have a sensor capable of making bar-force measurements for an extended period of time in a mill-scale refiner. A better understanding of the general characteristics of mill-scale bar forces follows as a second objective. A further objective is to elucidate the effects of process parameters, such as consistency, on bar forces, and to explore how this interaction affects refiner operation. The final objective is to investigate the use of data from the sensor for improving process control.

1.3 Methods of this Dissertation

To achieve the stated objectives it was first necessary to diagnose modes of failure in the previous sensor design, and to then improve the design of the sensor to alleviate, or completely remove, these modes. Based on this diagnosis, a sensor was redesigned and tested in early 2005 in a large pilot-scale refiner at the Andritz Ltd. Research Facility in Springfield, OH, United States. The collected signals indicated that the new sensor was capable of sustained force measurement in mill-scale refiners.

A second trial took place at a Catalyst Paper Corp. mill in Port Alberni, BC, Canada in late 2005. Sensors were installed in an operating refiner over the entire life of a set of plates, a period of nearly three months, during which time a number of experiments were performed.

1.4 Contributions of this Dissertation

Forces during individual bar-crossing impacts in mechanical refiners, which impart the necessary forces to break apart wood chips and develop specific fibre morphologies for use in making paper have been measured. These measurements are taken with a force sensor technology, based on previous work, which has been further developed by the author to perform in mill-scale refiners. Trials in a pilot-scale HC refiner were carried out over a range of operating conditions, and for the first time, trials in a mill-scale HC refiner were carried out over a range of operating conditions.

The first contribution of this work is the design of a fourth generation force sensor. This new design improves dynamic range by increasing the stiffness of the sensor assembly, and the method of fixating the sensor to the refiner plate. Sensor durability is improved by incorporating mechanical seals, and by introducing wiring passages that are laden with silicone. The new sensor was able to accurately measure bar forces, and showed a marginal drop in sensitivity over the extended trial in the mill-scale refiner.

For the second contribution, frequency distributions of peak forces and other useful metrics, including an estimate of the fraction of bar-crossings in which fibre is captured and worked, are studied. This information provides new insight into the fundamental differences that occur in operation in refiners of different stage and scale. The effect of consistency on bar forces is also studied, and largely confirms that trends found in experimental setups apply to larger-scale refiners.

In the final contribution, the ability of the sensor to predict refiner plate clash is investigated. A number of plate clashes were successfully recorded during the extended trial at the mill. The signal data from these sensors leading up to and during these clash events is compared to signals from the existing plate clash protection system in use at the mill. Different combinations of sensors, and methods of processing the signals, are evaluated to find a configuration most sensitive to plate clash. Using the sensor data, a method is found that significantly improves warning times of plate clashes, and is less sensitive to threshold settings.

1.5 Dissertation Organization

The contributions of this thesis are presented in four papers:

- A Piezoelectric Force Sensor for Mill-Scale Chip Refiners (OLENDER, D., WILD, P., and BYRNES, P., Under review, Proc. IMechE, Part E, Journal of Process Mechanical Engineering);
- Forces on Bars in High-Consistency Mill-Scale Refiners: Trends in Primary and Rejects Stage Refiners (OLENDER, D., WILD, P., BYRNES, P., OUELLET, D., and SABOURIN, M., Published, Journal of Pulp and Paper Science, 33(3):163-171 2007);
- Forces on Bars in High-Consistency Mill-Scale Refiners: Effect of Consistency (OLENDER, D., WILD, P., BYRNES, P., OUELLET, D., and SABOURIN, M., Under review, Journal of Pulp and Paper Science);
- Refiner Plate Clash Detection Using an Embedded Force Sensor (OLENDER, D., FRANCESCUTTI, P., WILD, P., and BYRNES, P., Published, Nordic Pulp and Paper Research Journal, 22(1):124-130 2007).

These papers are contained in appendices A, B, C and D, respectively. The body of the dissertation contains four chapters, 2 to 5, which describe the papers in the appendices, including the methodology, and a discussion of significant findings. Chapter 6 presents the conclusions of the combined papers, and outlines potential future work.

1.6 Other Relevant Publications

During the course of this work, the author also contributed to other research which made use of the force sensor, and is therefore relevant. A number of publications stem from this research, and are listed below:

- A Technique to Measure Mean Residence Time in TMP Refiners Based on Inherent Process Fluctuations (SENGER, J., OUELLET, D., WILD, P., SABOURIN, M., and OLENDER, D., Published, Journal of Pulp and Paper Science, 32(2):83-89 2006);

- Forces During Bar-Crossing Events in Low-Consistency Refining: Effect of Refiner Tram (PRAIRIE, B., WILD, P., BYRNES, P., OLENDER, D., OUELLET, D., and FRANCIS, B., Published, Pulp and Paper Canada, 108(9):T153-T156 2007);

- Forces During Bar-Crossing Events in Low-Consistency Refining: Distributions and Relations to Specific Edge Load (PRAIRIE, B., WILD, P., BYRNES, P., OLENDER, D., OUELLET, D., and FRANCIS, B., In press, Journal of Pulp and Paper Science).

The first paper reports on tests performed using the third generation force sensor. The author did not participate in the trials, but was involved in interpretation of the data, and assisted in writing the manuscript.

The latter two papers report on the installation of the new force sensor in a low-consistency refiner, which was undertaken as part of a Masters Thesis by another graduate student. The author assisted with the experiments, post-processing and interpretation of the data, and writing of the manuscripts.

Chapter 2

Fourth Generation Sensor (RFS4)

Key design improvements to the sensor are detailed in this chapter. A brief introduction to past RFS designs is first given to understand the principles of operation, and to understand the scope of the latest design enhancements.

2.1 Past Sensor Designs

The first two variants of the sensor, RFS1 and RFS2, are shown Figure 1a and 1b in Appendix A, respectively (denoted as Figure A.1a and Figure A.1b from here on in). During the design of these two sensors, the principle of operation was determined, including the choice of piezoelectric ceramics as sensing elements, and the basic geometry of the probe and supporting components. A circular housing captures the probe, sensing elements and the plug and setscrew assembly, which pre-loads the system. Bar forces are applied to the probe, which transfers load to the elements below, generating voltage signals. Normal and shear forces are resolved from these signals using constants obtained during calibration.

The third generation sensor, RFS3, shown in Figure A.1c, is smaller and stiffer than the RFS2. More mounting holes were also added to improve fixation between the sensor and refiner plate. This design was tested in a pilot-scale chip refiner (shown in Figure 3.1) over a week-long trial, where two major issues emerged: significant resonance-induced vibrations were observed in the force signal, and no signal could be recorded from any of the three sensors after one day of operation in the 150 °C and 0.5 MPa steam environment of the refiner.

Post-trial laboratory testing of the piezo elements recovered from these sensors revealed that they had been saturated with water. It was apparent that the epoxy used to pot the sensors had failed to protect the piezo elements.

2.2 The Fourth Generation Sensor: RFS4

To more effectively protect the piezo elements in the refining zone, the fourth generation sensor (as shown in Figure A.2) includes O-ring seals at the two principal orifices of the piezo compartment. Wiring is routed out of the sensor through two cylindrical passages, which are laden with silicone. These measures were effective at sealing the RFS4 in a 180 ºC and 1 MPa steam test environment.

To accommodate the O-ring, the base of the probe is cylindrical, and mates with the housing over a conical section, as seen in Figure A.2. A backing-screw assembly, shown in Figure A.3, is used to affix the sensor to the refiner plate, which replaces the cap screw configuration used in past designs. Other features were added to the design, and are more fully discussed in Appendix A.

2.3 Dynamic Behaviour

As a result of these modifications, the RFS4 has greater dynamic range than any of its predecessors, as shown in the frequency response functions (FRF) plotted in Figure A.4. In particular, the same plates and sensor locations were used in the installation of the third and fourth generation sensors in the pilot-scale refiner, allowing an opportunity to quantify the RFS4 performance, relative to the RFS3. As can be seen in Figure A.4, the RFS4 has a first natural frequency nearly 10 kHz greater than the RFS3.

The improvements to the dynamic range of the RFS4 are primarily attributed to the increased stiffness of the new conical probe geometry, and of the new method of fixation. Although the probe is more massive than past designs, it is more fully captured by the housing in three dimensions. The backing-screw assembly is credited with increasing stiffness by producing a more even, and higher force clamping of the RFS housing to the refiner plate.

2.4 Mill-Scale Trial Results and Discussion

The installed RFS4s successfully recorded force data over the entire life of the plates in a mill-scale refiner, a period of nearly three months. During this time the sensors were subjected to a 140 ºC steam environment, plate clashes, and interruptions in production. Post-trial calibration revealed a marginal loss in normal sensitivity, no greater than 10% in any one of the four installed sensors. The loss in shear sensitivity (by as much as 30%) was attributed to the wear in height of the probe, and associated reduction of the moment arm necessary to transmit torque to the piezo elements. It should also be noted that the probes of the sensors experienced accelerated rounding relative to the rest of the plate. This was due to the softness of the probes, which were made of AISI 316 stainless steel (HRB 80). In comparison, the plate was nickel-hardened, with a tested hardness of HRC 60.

Force profiles recorded by the RFS4 exhibited features known to exist from previous measurements of bar forces in smaller-scale setups. These features, such as the asymmetry in force profiles believed to be caused by ploughing, help to support the validity of the force signals collected during the mill-scale trials.

Chapter 3

Bar Force Trends

During commissioning of the RFS4 in the pilot-scale and mill-scale trials, a series of experiments were carried out to detect the effect of process conditions on bar forces. In particular, motor load, and production rate were tested. Refiner scale, stage of wood fibre refinement and radial location across the refining zone are also considered.

3.1 Experiments

The first trial of the RFS4 took place in Springfield, OH, USA, at an Andritz Inc. Research Facility. The pilot-scale refiner, as shown in Figure 3.1, is housed in a pressurized case, which reaches temperatures of 150 ºC and pressures of 0.4 MPa during refining. The refiner is a 36 in. diameter, single-disc type, and is powered by a variable-speed electric motor.

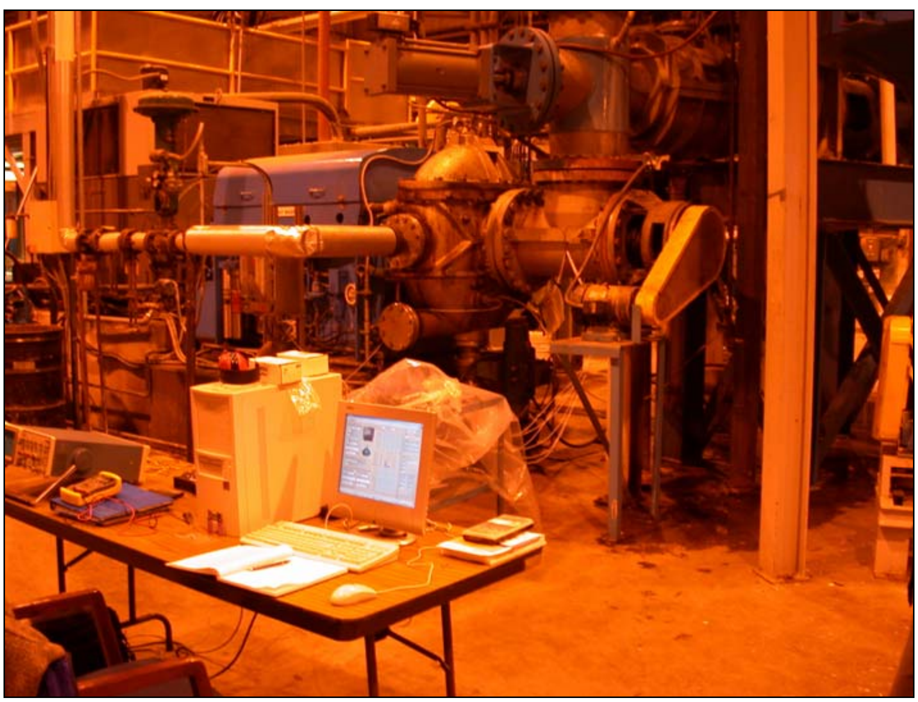

Figure 3.1: Refiner used in Springfield, OH with data acquisition equipment in foreground.

During the experiments in the Springfield trial, production rate was held constant, while four different levels of motor load were tested. Three production rates were tested in this manner, as shown in Table B.1. All other variables, such as dilution flow, were held constant.

The second trial of the RFS4 took place at a Catalyst Corp. Paper mill in Port Alberni, BC. The mill-scale refiner, as shown in **Figure 3.2**, is also a single-disc type. This refiner discharges to the atmosphere, and operates at temperatures of approximately 140 ºC within the refining zone. It is referred to as a *rejects* refiner because it processes pulp that has been rejected by filtering screens that follow the main processing lines. This is in contrast to the trial in Springfield, in which chips were processed. A new data acquisition system was purchased for the Port Alberni trial, because of its duration. This system is detailed in Appendix F.

Figure 3.2: Refiner used in Port Alberni, BC with charge amplifier enclosure (in grey) shown attached.

Table B.2 describes the experiments that were carried out during the Port Alberni trial, which took place immediately following the installation of the sensor array. In the first set of experiments, production rate was held constant while motor load was varied. In the second set of experiments, motor load was held constant while production rate was varied. All other process variables, such as dilution flow rate, were held constant. Experiments were performed at regular intervals of plate life, but these data were not included in this particular analysis due to the accelerated blunting of the probe relative to surrounding bars.

In both trials, multiple sensors were installed in one segment, but at different radial locations. The setup in Springfield is shown in Figure B.2, and the setup in Port Alberni is shown in Figure B.3. Sensors were enumerated S1, S2, S3, etc., from innermost to outermost radially. A detailed description of the installation is presented in Appendix B.

3.2 Signal Conditioning and Processing Techniques

Most sensor signals require conditioning, usually in the form of a filter to remove unwanted distortion. The RFS is a second-order instrument [39], and operates at frequencies high enough to warrant filtering of resonance-induced vibrations. Being a piezoelectric-based sensor, it is also necessary to compensate for the loss of low frequencies (*i.e.* DC components) in the signal.

A digital filter is created based on the inverse of the FRF collected during calibration. This filter is applied to the sensor signal to attenuate any magnitude distortion [40]. To compensate for the loss of the DC component, a compensation filter is also applied. Further compensation is still necessary, and the signal is manually offset based on the assumption that the signal returns to zero in between bar-crossing impacts. A more detailed description of the signal conditioning steps can be found in Appendix E.

Because of the quantity of acquired data, which involved many millions of bar-crossings, a program was written to automatically identify and characterize individual impacts. The algorithm consisted of applying a 4^{th}-order, low-pass filter to the conditioned signal (with a cut-off frequency near the bar-crossing frequency). This exposed the boundaries and peaks of each bar-crossing, to peak-finding algorithms. By phase-matching this heavily-filtered signal to the conditioned signal, it was then possible to isolate the boundaries of individual impacts.

Once an impact was isolated, its features, such as peak forces and μ_{teq}, were catalogued for later analysis. An indicator of the fraction of all crossings in which fibre was captured and worked was also defined through the *occurrence ratio* metric. The occurrence ratio is defined as the number of impacts recorded, divided by the theoretical number of impacts predicted by the bar-crossing frequency and sample duration.

3.3 Force Signals and Distributions

Sensor signals from the outer sensors (S3) in Springfield and Port Alberni are shown in Figure B.5a and B.5b. It was observed that in many cases, the force signal did not return to zero in between every impact. This signal feature was more apparent in Springfield data, and was explained in part by considering the relative bar angle between rotor and stator disc. With large relative angles, as was found in Springfield, it is possible for the approaching bar to contact the sensor probe before the receding bar has completely cleared. This produces a scenario where two rotor bars over-lap the sensor probe at once.

Further qualitative differences between the two signals were also observed. Impacts in Port Alberni were more regular and uniform in magnitude. In contrast, impacts in Springfield were less regular, consisting of many small-force impacts interspersed with relatively few large-force impacts. This aspect of the signals was more accurately quantified by building frequency distributions of peak forces collected from thousands of impacts, as seen in Figure B.6. Distributions of peak forces in Port Alberni were found to be skewed normal, while distributions in Springfield appeared closer to decreasing exponential. A Weibull curve-fit was applied to the distributions to estimate their exact shape.

The difference in distributions between the two refiners was attributed primarily to the difference in composition of the mixture being processed. In Springfield, the wood fibre consisted of unprocessed chips, and it is speculated that this induces glancing blows on the refiner bars, and creates voids within the flow. In Port Alberni, the rejected wood fibre has already been processed in two refining stages, and had lost much of its mechanical properties, such as strength. It is therefore more likely to provide an uninterrupted flow of material into the nip of crossing bars. Indeed, impacts recorded by Prairie *et al*. [6] in a low-consistency refiner, which processes a water-saturated slurry of pulp, were much more regular in time and uniform in shape than the impacts observed in the high-consistency refiners.

The scale of the refiner is thought to be another factor that affects the flow of material. Larger refiners have significantly higher production rates, and therefore process considerably more fibre per unit area. It was estimated in the work in Appendix B, that the rejects refiner in Port Alberni would have approximately twice as much material in the refining zone as the refiner in Springfield at any point in time.

The observation of different peak force distributions in these two refiners has potential implications for refining efficiency. Theoretical [35, 36] and empirical research [37] suggest the existence of an optimal level of forces to best develop fibres. A normal force distribution centered on this optimal force would provide a larger number of useful impacts than a decreasing exponential distribution, and would, thus, be more efficient. As a possible example of the efficiency gains, Sabourin *et al.* [38] has found that increasing the defibration of chips prior to first-stage refining decreased specific energy use by 11%.

3.4 General and Radial Trends

Mean levels of peak forces, equivalent tangential coefficient of friction and occurrence ratio, taken over all the experiments listed in these trials, for each sensor, provided radial trends on the contact mechanics in the refining zone. The average of the three sensor means, called the trial mean, provided information on more general trends between the two refiners.

Mean peak forces at each sensor, and trial means, are shown in Figure B.7 for both Springfield and Port Alberni trials. The trial mean peak forces in Port Alberni were found to be approximately 5 times higher than in Springfield, which matches the difference in power between the motors of the two machines, suggesting bar forces are proportional to motor load.

Higher equivalent tangential coefficients of friction were found in the chip refiner, as shown in Figure B.8, which is attributed to the mechanical properties of the chips, and smaller amount of lubricating water in the high-consistency mixture.

Trial mean occurrence ratios in the Springfield refiner were 20% less than those found in the Port Alberni refiner, as shown in Figure B.9. This was considered a further indication of the heterogeneity of the mixture in the chip refiner in Springfield. Both refiners showed their highest occurrence ratio in the middle of the plate, which is thought to be caused by an increase in local density of the fibres at the steam flow stagnation point.

The rejects refiner showed increasing forces with radius, while the chip refiner showed nearly constant or decreasing force trends with radius. One explanation for the difference in these trends considers that chips, or intact wood segments such as shives, induce larger force impacts than refined pulp for a given plate gap. In the chip refiner, the radial force trend is then driven by the chip to pulp transition, while in the rejects refiner, which is processing pulp, the radial force trend is driven by an increase in tangential velocity of crossing bars, or decreasing gap caused by taper of the plates.

Chapter 4

Effect of Consistency

The mass fraction of wood fibre in the refining feedstock, known as the consistency, is an important process parameter. The energy-quality relationship in refining is strongly affected by consistency. Part of this influence has been explained by its effect on the residence time of pulp in the refining zone [16]. Recent simulations in the laboratory have shown that consistency also greatly influences the coefficient of friction during bar-crossing impacts, and that a significant transition point in this relationship coincides with a major operational shift in refining [29]. During the pilot-scale and mill-scale trials discussed in previous chapters, experiments were carried out in which consistency was varied, to explore its effect on bar forces in larger-scale refiners.

4.1 Experiments

The experiments carried out in Springfield, OH, are listed in Table C.1. The dilution flow rate was used to alter the refining consistency, and was tested at four different rates, between 19 to 42 l/min (5 to 11 USGPM). Each dilution flow rate was also tested at two targeted levels of motor load. Consistencies measured at the discharge of the refiner ranged from approximately 20 to 55%.

The experiments performed in Port Alberni, BC, are listed in Table C.2. Both the dilution flow rate and pressure in the dewatering press were varied in separate tests to alter the refining consistency. Dilution flow rates were varied from 11 to 27 l/min (3 to 7 GPM), while the pressure in the dewatering press was varied from 10.3 MPa to 12.4 MPa (1500 to 1800 psig). No discharge consistency measurements were taken for these experiments. Discharge consistency measurements were taken at a later date using the same operating conditions. Discharge consistencies in those tests ranged from approximately 20 to 27%, which were below the 33% historical average discharge consistency for this refiner.

4.2 Signal Conditioning and Processing Techniques

The same conditioning steps discussed in Chapter 3 were taken to remove any magnitude distortion, and compensate for the loss of low frequency components in the force signals.

Programs from the previous study were used to process this data. As in the last study, only impacts with peak normal forces above the noise threshold (0.2 N) were included in distributions. These results are referred to as “low threshold” in this study. Additionally, very high-force impacts, representing less than 5% of recorded data were investigated. These high-force impacts were isolated using a high threshold that varied between 2 and 4 N.

The equivalent tangential coefficient of friction μ_{teq}, which is calculated by dividing the average shear force by the average normal force over an impact, was the main impact metric under consideration in this study.

4.3 Results and Discussion

Figure C.3, C.4, and C.5, show the results from the inner, middle and outer sensors respectively, in the Springfield experiments. Mean values of μ_{teq} measured at the inner sensor showed a positive correlation with discharge consistency at both low and high thresholds. Mean values of μ_{teq} measured at the middle and outer sensors showed this relationship only at the high threshold.

One hypothesis for the influence of consistency on μ_{teq} at the inner sensor, and not over most of impacts at the middle and outer sensors, is that the unprocessed wood fibre at the entrance to the refining zone in the Springfield refiner is more sensitive to water content. This could be a manifestation of the relationship found in experiments carried out by Senger and Ouellet in the laboratory [29], in which it was revealed that μ_{teq} has a positive correlation with floc grammage, or thickness, and that thicker flocs were more sensitive to changes in consistency. This also explains why high-force impacts in the middle and outer sensors, which likely involve thicker flocs, still show a positive correlation between μ_{teq} and consistency. In explaining these results, it is possible that the location of dilution water injection, which is closer to the entrance of the refining zone, also plays a role.

In Port Alberni, μ_{teq} was independent of the changes to dilution flow and the de-watering press pressure. Mean values of μ_{teq} at the inner, middle and outer sensors were 0.34±0.006, 0.64±0.015, and 0.53±0.017 respectively.

The lack of significant change in μ_{teq} in Port Alberni is not unexpected. Although process parameters were varied within their operational limits, the range of consistencies achieved during the experiments was limited. Furthermore, the tested consistencies were near 35%, a value which was shown by Senger and Ouellet [29] to be a transition point; below 35% there was no correlation between μ_{teq} and consistency.

Figure C.8 plots the mean values of μ_{teq} using the low threshold, but separates high and low motor load experiments. As seen in this figure, μ_{teq} at low motor loads is more sensitive to consistency and shows a higher coefficient of determination. This effect was not observed in the middle and outer sensors. Explanation of this finding is reserved until more data can be collected.

Chapter 5

Plate Clash

The signal from the RFS was investigated for potential use in a number of further applications. One successful application was the early prediction of plate clash. The mill-scale trial in Port Alberni offered an authentic environment to study this phenomenon, and to compare an RFS-based plate protection system to the plate protection system already in use by the mill.

5.1 Current Plate Protection System

The existing plate protection system relies on an accelerometer, which is mounted to the outboard bearing block of the refiner. Signals from the accelerometer are monitored within a specific frequency range known to be responsive to plate clash. An alarm is triggered if the running average of the acceleration exceeds a present threshold. The running average is calculated over a prescribed period, immediately preceding the last recorded acceleration. The system responds by notifying the operator and automatically increasing the plate gap.

The accelerometer signal was recorded in parallel with the RFS signal during the trial, and these signals are thus synchronous. A program was written to simulate when the accelerometer-based system would trigger an alarm. The simulated alarms are shown as dashed lines in Figure D.4. Note that acceleration drops after the alarm is triggered in two cases where a potential clash is averted. In the third case, an alarm is triggered, but the system is unable to stop the clash.

5.2 RFS Signal Pre-Processing

The two voltage signals from each RFS are sampled at 300 kS/s, and are then converted into normal and shear force signals. Manual inspection of these force signals showed that it was unnecessary to be sampling at such a high rate to record the build-up of forces on the plates that preceded a clash. Because of this, the sampled data was decimated to a more manageable size. The decimated data was the equivalent of using a sampling rate of 300 S/s. The decimated data was also rectified, to cast all points into the positive domain.

5.3 Clash Events

There were only nine full clash events recorded during the entire trial. All of these plate clashes were recorded during the set of experiments which immediately followed the installation of the sensors. Six of these events were interrupted by the existing plate protection system, while in the rest of the events actual contact occurred.

5.4 Detection Methods

Several methods of processing the decimated RFS data were considered to find the one most sensitive to predicting plate clash. The four most promising methods were referred to as: peak density, weighted peak density, running average and combined running average.

The peak density method makes use of a peak-finding algorithm. In this method, an alarm is triggered if a prescribed number of peaks exceed a present threshold within a certain period of time. The weighted peak density method is an extension of this technique, in which peaks are weighted, based on their magnitude.

The running average method is similar to the algorithm used by the accelerometer-based system. In this method, an alarm is triggered if the running average is greater than a threshold, which is the sum of a second running average, taken over a longer period, and an offset. This method is described diagrammatically in Figure D.7.

The combined running average method is based on the running average method. The average of the normal and shear forces are first calculated for each sensor, and then processed using the running average method described above. The average of the normal and shear forces from all four sensors is also calculated, and then processed similarly.

5.5 Results and Discussion

The performance of each of the methods of processing the RFS data, using optimum parameter settings, is presented in Table D.1. The lead-time refers to the improved warning time, in seconds, over the accelerometer-based system. The RFS-based detection methods are all superior to the accelerometer-based system producing, on average, lead-times of at least six seconds. The combined running average method, using the signals from the innermost sensor, S1, provided the most warning, producing an average lead-time of 11 seconds over all nine clash events.

The larger lead-times provided by the innermost sensor are attributed to the location of the sensor, which is radially inward from the steam stagnation point. If back-flowing steam is a contributor to the disruption of the pulp flow, as suggested in the literature [9], it might suggest a restriction of pulp flow radially inward from the stagnation point. This restriction could result in an accumulation of material in the inner part of the refining zone prior to a clash, which would explain the early rise in forces recorded by S1.

Two studies were performed to further evaluate the performance of the RFS-based system versus the accelerometer-based system. In the first case, the threshold in the accelerometer-based system was decreased to increase that system’s sensitivity. In the second case, the threshold of the RFS-based system was increased, to decrease the sensitivity of the system.

The results of the first study are presented in Figure D.9. They reveal that the accelerometer could not match the performance of the RFS for any event, other than one, without also causing false triggers. The results of the second study are shown in Figure D.10, and show that the RFS-based system could offer improved detection performance for a broad range of offset values.

Chapter 6

Conclusions and Future Work

The primary objective of this work was to create a sensor to make localized, high resolution measurements of bar forces within a mill-scale refiner over the entire life of a set of plates. A secondary objective was to investigate the nature of bar-crossing forces, including their general composition and distribution within the refining zone. A third objective was then to examine the effects that specific process parameters, such as refining consistency, have on bar forces. The final objective was to explore other possible applications of the sensor signal for improved process control.

A piezoelectric-based sensor designed to measure bar forces in a chip refiner has been further developed to withstand the harsh environment found at the mill-scale. Mechanical seals and more robust circuitry have been added to the sensor to protect against the high pressures and temperatures found in larger refiners. A wider dynamic range is necessary to measure bar-crossings that occur at higher frequencies, and is achieved through improvements to the sensor stiffness, and to the method of mounting the sensor.

Pilot and mill-scale refiner trials were carried out at the Andritz Inc. Research Facility in Springfield, OH, US, and at a Catalyst Paper Corp. mill in Port Alberni, BC, CAN, respectively, to qualify the latest design. The mill-scale trial is of particular significance, proving the sensors reliability over the entire life of a set of plate segments - a period of approximately 1800 hours of near continuous operation. Post trial calibration of the sensors revealed only marginal loss of sensitivity, after accounting for the wear of the probes. Force profiles from bar-crossing impacts at different radial locations in the refining zone were successfully captured, and resemble those observed in smaller-scale refiners.

Force signals from chip refining in Springfield were fundamentally different from those observed in rejects refining in Port Alberni. Bar forces in chip refining have larger coefficients of friction, and are irregular, in that many low-force impacts are interspersed with few high-force impacts. Further, fewer crossings were observed in which wood fibre was actually captured and worked. This heterogenic aspect of the signal was quantified by creating frequency distributions of the peak bar forces. These distributions were found to be nearly decreasing exponential. In rejects refining, bar force distributions were skewed normal, with impacts that were more uniform.

All of these findings can be, in part, attributed to the mechanical properties of the wood in the feedstock. Raw wood chips being refined in Springfield are far less compliant, for example, than the rejects-stage fibre in Port Alberni, and are less likely to promote regular flow of material into the nip of crossing bars. The mechanical properties of chips, and smaller transitional forms, such as shives, allow resistance to shearing. This provides a possible explanation for the recording of higher coefficients of friction in the chip refiner. It is also the loss of these mechanical properties of the wood in the chip refiner, as the chips transition to pulp, that is believed to drive the decrease in forces from the radially innermost to outermost sensor. In contrast, in Port Alberni, the increasing radial trend is believed to be driven by the kinematics and geometry of the refining zone: as fibres move radially outwards, an increase in tangential velocity of bar crossings and decreasing gap occur. These results highlight the complex nature of bar forces within the refining zone, and their relationship to the stage of refinement of the wood fibre and scale of the refiner. The existence of different distributions in particular provides a potential explanation for recently reported efficiency gains, and suggests an avenue for future process improvement.

The effect of consistency on bar forces was explored in both Springfield and Port Alberni trials to confirm the existence of relationships originally discovered in laboratory simulations [29]. Consistency was varied by altering dilution flow in both installations, and in the case of Port Alberni, also changing the pressure developed in the dewatering press. An increase in refining consistency in the chip refiner, measured at the discharge, was observed to cause an increase in the coefficient of friction over the bulk of the impacts at the inner sensor, but not at the middle or outer sensors. No significant changes were observed in the rejects refiner, but only a small range of consistencies could be tested. These initial findings can be interpreted as manifestation of the effects of consistency and floc thickness found in the laboratory, and suggest these relationships may translate to larger-scale equipment.

As described in the first chapter, plate clashes are still a regular occurrence in commercial refiners, causing accelerated bar wear, and disrupted production. During the extended trial in Port Alberni, a number of plate clashes were observed. The use of the sensor signal as a predictive tool, to detect the onset of these plate clashes was investigated. Several methods and sensor combinations were considered. It was found that the signal from the innermost sensor, using a straightforward approach which triggers an alarm if average forces go above a certain prescribed threshold, yielded the best performance. This system can predict all recorded plate clash events before the accelerometer-based system currently in use at the mill, with an average lead of 10.9 s. A sensitivity study confirmed that the accelerometer-based system could not match the performance of the sensor for any event, other than one, without also causing false triggers. The study also showed that the system could offer improved detection performance for a broad range of offset values. The finding that the innermost sensor was most sensitive to plate clash supports speculation that plate clashes were triggered by a build-up of fibre material in the inner part of the refining zone.

6.1 Future Work

The design and qualification of a robust sensor capable of measuring bar forces in commercial refiners is a useful research tool for scientists and engineers involved in mechanical refining. It is expected that more trials will be undertaken in the future, and should focus on the following areas:

- examination of the potential relationship between distributions of bar forces and their effects on the efficiency of mechanical treatment of fibres;
- continuation of research into the effect of specific process parameters, such as production rate and consistency on bar forces;
- investigation of the relationship between bar forces and developed pulp properties;
- expansion of plate clash trials, which evaluate the performance of the sensor over more clashes, preferably in another mill setting;
- revisitation of the use of the sensor in estimating mean residence time in the refining zone;
- evaluation of the effects of new tribological fluids within the refiner.

References

[1] GARNER, A., “20th Anniversary PWC Global Forest and Paper Industry Conference,” Pulp and Paper Canada, 108(7-8):26-27 (2007).

[2] PUSHPARAJ, V.L., SHAIJUMON, M., KUMAR, A., MURUGESAN, S., CI, L., VAJTAI, R., LINHARD, R.J., NALAMASU, O., and AJAYAN, P.M., “Flexible Energy Storage Devices Based on Nanocomposite Paper,” Proceedings of the National Academy of Sciences, USA 104, 13574-13577 (2007).

[3] YOUNG, R., TURNER, L., and BERG, R., “Regional Overview – Canada,” 2003-2004 Pulp and Paper Global Fact & Price Book,” W. Mies, Editor (2004).

[4] GRADIN, P.A., JOHANSSON, O., BERG, J.-E., and NYSTRÖM, S., "Measurement of the Power Distribution in a Single-Disc Refiner," Journal of Pulp and Paper Science, 25(11):384-387 (1999).

[5] SENGER, J., OLMSTEAD, M., OUELLET, D., and WILD, P., "Measurement of Normal and Shear Forces in the Refining Zone of a TMP Refiner," Journal of Pulp and Paper Science, 31(1):28-32 (2004).

[6] PRAIRIE, B., WILD, P., BYRNES, P., OLENDER, D., FRANCIS, D.W., and OUELLET, D., “Forces During Bar-Passing Events in Low Consistency Refining: Effects of Refiner Tram,” Pulp and Paper Canada, 109(9):T153-T156 (2007).

[7] KAPPEL, J., "Mechanical Pulps: From Wood to Bleached Pulp," Atlanta, GA: TAPPI Press (1999).

[8] DUMONT, G.A., and ASTROM, K.J., "Wood Chip Refiner Control," IEEE Control Systems Magazine, 8(2):38-43 (1988).

[9] ALLISON, B.J., CIARNIELLO, J.E., TESSIER, P.J.C., and DUMONT, G.A., "Dual Adaptive Control of Chip Refiner Motor Load," Automatica, 31(8):1169-1184 (1995).

[10] SMOOK, G.A., "Handbook of Pulp and Paper Terminology: A Guide to Industrial and Technical Usage," TAPPI Press (1990).

[11] ATACK, D., STATIONWALA, M.I. and KARNIS, A., "What Happens in Refining," Pulp and Paper Canada, 85(12):119-124 (1984).

[12] KARNIS, A., D. ATACK, and M.I. STATIONWALA, "What Happens in Refining - Part II," Pulp and Paper Canada, 87(11):54-59 (1984).

[13] STATIONWALA, M.I., ATACK, D. and KARNIS, A., "Effect of Refiner Plate Design on Pulp Fractionation and Strength Development," Journal of Pulp and Paper Science, 14(6):133-140 (1986).

[14] ATACK, D. and MAY, W.D., "Mechanical Reduction of Chips by Double-Disk Refining," Pulp and Paper Magazine Canada, 64(C):75-83, 118 (1963).

[15] SENGER, J., OUELLET, D., WILD, P., BYRNES, P., SABOURIN, M., and OLENDER D. "A Technique to Measure Mean Residence Time in TMP Refiners Based on Inherent Process Fluctuations," Journal of Pulp and Paper Science, 32(2):83-89 (2006).

[16] MILES, K.B. and MAY, W.D., "The Flow of Pulp in Chip Refiners," Journal of Pulp and Paper Science, 16(2):63-72 (1990).

[17] MILES, K.B., "A Simplified Method for Calculating the Residence Time and Refining Intensity in a Chip Refiner," Paperi ja Puu, 73(9):852-857 (1991).

[18] MILES, K.B. and W.D. MAY, "Predicting the Performance of a Chip Refiner: A Constitutive Approach," Journal of Pulp and Paper Science, 19(6):268-274 (1993).

[19] ALAMI, R., BOILEAU, I., HARRIS, G., LACHAUME, J., KARNIS, A., MILES, K., AND ROCHE, A., "Impact of Refining Intensity on Energy Reduction in Commercial Refiners: Effect of Primary-Stage Consistency," TAPPI Journal, 80(1): 185-193 (1997).

[20] MURTON, K.D. "Effect of Primary Stage Refining Consistency on TMP Pulp Quality and Energy Consumption," Appita Annual General Meeting, Melbourne, Australia (1997).

[21] OUELLET, D., BENNINGTON, C.P.J., SENGER, J.J., BORISOFF, J.F., and MARTISKAINEN, J.M., "Measurement of Pulp Residence Time in a High-Consistency Refiner," Journal of Pulp and Paper Science, 22(8):301-305 (1996).

[22] HARKONEN, E., HUUSARI, E., and RAVILA, P., "Residence Time of Fibre in a Single Disc Refiner," Pulp and Paper Canada, 101(11):45-50 (2000).

[23] MURTON, K. and G. DUFFY, "The Influence of Pulp Residence Time on Refining Intensity and Pulp Quality," Appita Journal, 58(1):64-71 (2005).

[24] OUELLET, D., BENNINGTON, C.P.J., and POTKINS, D., "Wood Comminution and Material Flow in a Laboratory Chip Refiner," Journal of Pulp and Paper Science, 21(12):415-421 (1995).

[25] ALAHAUTALA, T., LASSILA, E., HERNBERG, R., HARKONEN, E., AND VUORIO, P., “Optical Measurement of Pulp Quantity in a Rotating Disc Refiner,” Measurements Science and Technology, 15(11):2256-2261 (2004).

[26] SVENSSON, B.A., RUNDÖLF, M., AND H. HOGLUND, “Sliding Friction Between Wood and Steel in a Saturated Steam Environment,” Journal of Pulp and Paper Science, 32(1): 38-43 (2006).

[27] GONCHAROV, V.N., SMIRNOVA, E.A., SHEMYAKIN, E.V., "Method for the Determination of Stresses between Refiner Blades," Bumazh. Promst., 27:134-138 (1970).

[28] GONCHAROV, V.N., "Force Factors in a Disk Refiner and their Effect on the Beating Process," Bumazh. Promst., 12(5):12-14 (1971).

[29] SENGER, J.J. and OUELLET, D., "Factors Affecting the Shear Forces in High-Consistency Refining," Journal of Pulp and Paper Science, 28(11):364-368 (2002).

[30] BACKLUND, H.-O., "Measurement of Shear Force, Temperature Profiles and Fibre Development in Mill-Scale TMP Refiners," Ph.D. Thesis, Mid Sweden University: Sweden (2002).

[31] BANKES, A., "Design and Development of a Mechanical Wood Pulp Refiner Force Sensor. M.Sc. Thesis, Dept. of Mechanical Engineering, Queen's University, Kingston, ON (2000).

[32] SIADAT, A., BANKES, A., WILD, P.M., SENGER, J., AND OUELLET, D., “Development of a Piezoelectric Force Sensor for a Chip Refiner,” Proceedings of the Institute of Mechanical Engineers, Part E, Journal of Process Mechanical Engineering, 217:133-140 (2003).

[33] OLMSTEAD, M., "Development of a Second-Generation Sensor to Measure Forces Applied to the Bars of a Mechanical Wood-Pulp Refiner," Department of Mechanical Engineering, Queen's University, Kingston (2002).

[34] SENGER, J., SIADAT, A., OUELLET, D., WILD, P., "Measurement of Normal and Shear Forces During Refining Using a Piezoelectric Force Sensor," Preprints IMPC, PAPTAC, 403-407 (2003).

[35] GIERTZ, H.W., "A New Way to Look at the Beating Process," Norsk Skogindustri, 18(7):239-248 (1964).

[36] MAYADE, T.L., "Statistical Theory of Chemical Pulp Refining - An Innovative Combined Approach," Appita Journal, 50(3):237-244 (1997).

[37] VIFORR, S. AND SALMEN, L., “Optimal Shear/Compression Forces – A Way of Collapsing Coarse TMP Fiber,” Journal of Pulp and Paper Science, 33(1):22-28 (2007).

[38] SABOURIN, M.J., "Evaluation of a Compressive Pretreatment Process on TMP Properties and Energy Requirements," Pulp and Paper Canada, 101(2):50-56 (2000).

[39] DOEBELIN, E.O., "Measurement Systems: Application and Design," 4th ed. McGraw-Hill (1990).

[40] SMITH, S., "The Scientist and Engineer's Guide to Digital Signal Processing," 2nd Ed., California Technical Publishing (1999).

Appendix A

A Piezo-Electric Force Sensor for Mill-Scale Chip Refiners

(In press, will appear in:
Proceedings of the Institution of Mechanical Engineers,
Part E: Journal of Process Mechanical Engineering,
Professional Engineering Publishing, Vol. 222, No. 8, 2008)

A Piezoelectric Force Sensor for Mill-Scale Chip Refiners

D. Olender[1], P. Wild[1*] and P. Byrnes[2]

[1.]Department of Mechanical Engineering, University of Victoria, PO Box 3055 Victoria, BC, V8W 3P6, Canada
[2.]Herzberg Institute of Astrophysics, Victoria, BC, Canada

[*]Corresponding author (pwild@uvic.ca)

Abstract

Refiners are used in the pulp and paper industry to separate wood chips into individual fibres and to develop the morphology of fibres to be suitable for the type and grade of paper to be produced. Within a refiner are discs, at least one of which rotates at high speed and all of which are lined with radial patterns of bars on their opposed surfaces. A mixture of chips and water is accelerated radially through the space between the discs. Compressive and shear forces are applied to chips and fibres as the bars on the opposed discs cross each other. Experiments have shown that certain process variables can greatly affect the forces applied to chips or fibres when bars cross. These findings suggest that the contact mechanics of bar-crossings are a significant factor in the development of fibre properties. To investigate these contact mechanics in operating refiners, a piezoelectric-based sensor has been developed to measure the forces applied to the chips and fibres by the bars. The sensor replaces a small section of a refiner bar and is sensitive to both axial and tangential forces. This paper describes the evolution of the design of this sensor from a proof-of-concept prototype for a laboratory-scale refiner to the latest generation sensor for a mill-scale refiner. Performance during the most recent mill trials is presented.

Keywords

mechanical pulp, chip refiner, force, piezo, sensor

Introduction

Chip refiners are used in the pulp and paper industry to process wood chips into pulp for the production of paper. Refiners apply cyclic loads to wood chips, breaking apart the wood matrix and releasing individual fibres. Normal and shear stresses are repeatedly applied to intact chips, shives (*i.e.* chip fragments), and fibres as they are trapped in the nip between crossing bars. Although this interaction during repeated bar-crossings is critical to the refining process, it is not well understood. The complexity of the three-phase flow of water, steam and wood fibre, the speed of the interaction and the difficulty of making measurements in the hostile environment of the refiner, are among the factors that contribute to this lack of understanding.

In the current research, a sensor has been developed that enables direct measurement of forces during bar-crossing impacts. Data gathered with this sensor offer new insight into the fundamental mechanics of the refining process which, in turn, may lead to significant process improvements.

The development of a prototype piezoelectric-based sensor that measures forces in a chip refiner was reported previously by Siadat *et al.* [1]. This sensor replaced a small section of refining bar, and was sensitive to both normal and tangential shear forces during individual bar-crossing impacts. This prototype sensor was tested in an atmospheric laboratory-scale refiner. Three subsequent generations of the force sensor described by Siadat *et al.* [1] have since been designed, built and tested in increasingly large refiners, including both laboratory and pilot-scale refiners [2-4] and, most recently, a successful extended trial at a Catalyst Paper Corp. mill in Port Alberni, BC [5]. Development of the sensor design has required improvements in both durability and dynamic behavior. This paper describes the development of the design of the sensor, quantifying the improvements gained from each new build. Results that qualify the reliability and performance of the sensors are presented from trials in a refiner in an operational pulp mill.

Background

Mechanical refiners produce pulp that is suitable as furnish for many lower grades of paper, such as those used in newspapers or magazines. All refiners operate on the same principle, having two or more axially-aligned discs, at least one of which is driven (*i.e.* the *rotor*) and rotates at high speeds. Replaceable *plates*, lined with radially oriented bars, are mounted to the surface of the discs and it is these bars that perform the mechanical action. These bars wear in operation, and the plates are normally replaced after hundreds of hours of operation.

A mixture of wood chips and water is fed into the *gap* between the plates at the rotational axis. The mass fraction of wood in the feedstock is referred to as the *consistency*. Under many tons of axial thrust, the gap is closed to a fraction of a millimeter, causing the bars to impose cyclic compression and shear on the wood fibre passing through the gap. Operating the discs at such close proximity is necessary but mechanically difficult and collisions, referred to as *plate clashes* [6], are frequent. As the fibres are worked and separated they become pulp, and tend to accumulate in bundles in a process called *flocculation*. As these “flocs” make contact with the rotor they are also accelerated and forced to flow to the disc periphery. The immense frictional forces that occur generate heat, which is necessary to ease separation of the wood fibre, while also producing steam, which is a considerable driving force. This combination of treatments defines the thermomechanical pulp (TMP) refiner. Additional chemical and thermal pre-treatments are often employed in varying degrees [6].

Throughout the pulp and paper industry, refiners are being pushed to process as much wood fibre as possible to increase profit or, in some cases, to minimize losses. As operators increase the mass flow rate of wood fibre through their machines, target pulp quality must be maintained. Various control strategies are used to ensure that this is the case. One such strategy is to maintain a constant level of *specific energy*. Specific energy is calculated by dividing the power required to drive the rotor by the mass flow rate of fibre through the refiner. Specific energy is widely used as an indicator of performance but wide variations in pulp properties have been found at similar levels of this parameter [4, 7]. More sophisticated models of refiner operation take into account the average time the pulp spends in the refining zone, known as the *residence time* [8]. However, this parameter is difficult to measure and the limited empirical data that does exist does not support the prevailing model [4, 9].

Research into the contact mechanics of bar-crossings has shown promise in explaining the refining process further. Senger and Ouellet [10] investigated the effect of consistency on shear forces during bar-crossing impacts using a single-bar laboratory rig. It was discovered that trends in shear forces closely matched the energy-quality relationship with consistency seen in actual refiners. In a similar vein, Viforr and Salmen [11] studied the effect of shear and compression forces on coarse fiber mats between rollers. Their studies suggest an optimal ratio of shear and compressive force exists to efficiently develop fibres. Tribological tests have also been carried out by Svensson *et al.* [12], showing the effects of temperature and steam on the sliding contact of wood and metal. These laboratory studies demonstrate the potential significance of bar forces, but are limited in their scope because of their simulated nature.

Direct measurement of bar forces offers a means of verifying these studies. An early *in situ* measurement of bar forces was undertaken three decades ago by Goncharov [13] in a low-consistency (LC) refiner. These refiners process pulp slurry having a consistency below 5 %, in contrast to high-consistency (HC) refiners, which process raw wood material at consistencies of 20 % or more (medium consistency refiners operate between 5% and 20 %). LC refiners are typically smaller, and operate at lower speeds, temperatures and pressures. The sensor employed by Goncharov used a traditional bending beam load cell, with strain gauges as sensing elements, and replaced a small section of refiner bar. Limited by its first natural frequency, the sensor was only able to measure bar-crossings up to 1.3 kHz. As such, it was adequate to measure impact profiles at the low operating speeds of the LC refiner, and allowed the first observation of the rapid spike in force as crossing bars initially meet. Another notable attempt at force measurement was recently undertaken by Backlund [14] in a mill-scale chip refiner. In these experiments, a commercial piezo-electric based sensor was modified to measure shear forces over a circular section of the refining zone, spanning many bars. Because of its size, the sensor could only record an average shear force that took place over many bar-crossings.

This paper describes the development of the design of the refiner force sensor (RFS), whose aim was to accurately measure the forces experienced by chips, shives, flocs and fibres during individual bar-crossings in commercial chip refiners. Data acquired from these sensors have elucidated many aspects of the refining process that have until now, been hidden. For example, these sensors have been used to observe the effect of rotor run-out on bar forces [15], to make an estimate of the mean residence time of the pulp in the refining zone [4], and also to give advanced warning of plate clashes [16]. By recording many thousands of bar-crossings and studying their distributions, the general character of these impacts has also been revealed, including how their regularity and magnitude can vary due to machine scale and stage of refinement [5, 17].

Sensor Design

The first working prototype of the refiner force sensor, RFS1, shown in Figure 1a, was designed and built in the late 1990s [1, 18]. This work determined the principle of operation, including the sensing element, and the basic geometry of the probe and supporting components. As seen in cross-section in Figure 1a, the sensor probe replaces a short segment of refiner bar and transmits loads exerted on the tip of the probe to the piezoelectric elements. The RFS1 also allowed testing of the method used to resolve normal and shear forces from the resulting impact [1]. A 31 cm (12 in.) diameter laboratory chip refiner at FPInnovations - Paprican Division in Vancouver, BC, CA was used to test this early design.

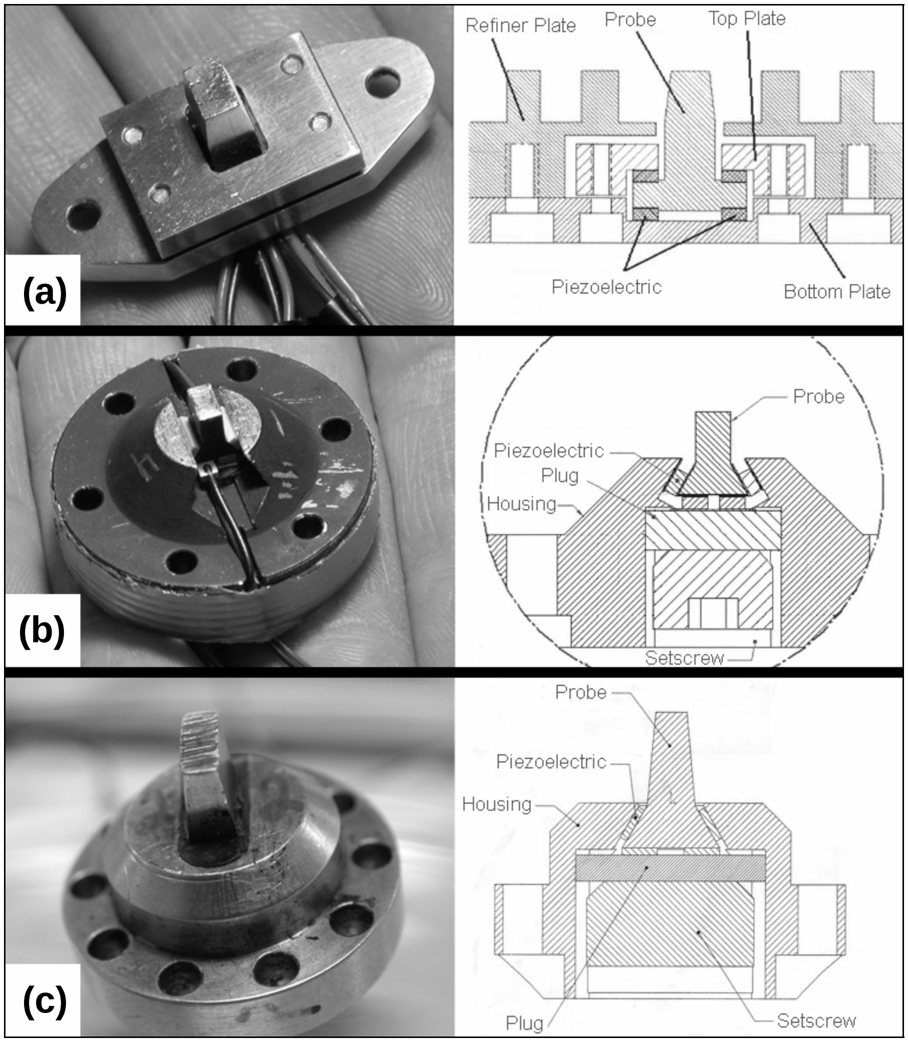

Figure 1: Photo and cross-section of (a) RFS1, (b) RFS2 and (c) RFS3.

The design that followed RFS1 is shown in Figure 1b. The RFS2 has a circular housing and, instead of sandwiching the sensor assembly between two plates as in RFS1, uses a plug and setscrew design. Tightening the setscrew forces the plug upwards, preloading the base of the probe and piezo elements against the sensor housing.

The features of the RFS2 provide a number of advantages over the RFS1. A more even pre-load is attained in the piezo-elements because the plug and setscrew configuration is self-aligning. This characteristic also makes it possible to pre-load the piezo-elements to a greater extent without cracking them. Further, assembly of the sensor is more repeatable, because the torque applied to the setscrew can be measured. Finally, the circular housing is more rigid, and provides a larger surface area for mating with the refiner plate.

The third generation of the sensor, RFS3 shown in Figure 1c, has the same basic shape as RFS2, but the scale of the sensor body and its internal components are significantly reduced. The portion of the housing that contains the piezo elements and captured the probe was strengthened by removing material on only one side during manufacture. More cap screw holes, used to mount the sensor to the refiner plate, have also been added to the housing. The setscrew and mating threads on the housing in the RFS3 design were also manufactured with extra fine threads.

The RFS3 design benefits primarily from the added rigidity of these modifications, but the reduction in size also allows for the sensors to be installed in closer proximity within the refiner plate. The increased pitch of the thread used on the setscrew increases the thread engagement within the housing, and provides for a more precise mate.

RFS3 was first tested in a 56 cm (22 in.) diameter pilot-scale chip refiner at the FPInnovations - Paprican Division in Pointe Claire, QC, CA [3], and later, in a 91 cm (36 in.) diameter pilot-scale chip refiner at the Andritz Ltd. Research Facility in Springfield, OH, USA. Two problems with the RFS3 design arose during the latter trials. The first problem was the presence of significant resonance in the force signal data. The resulting signal distortion was sufficient that clearly delineated force signals for individual bar-passing events could not be extracted. However, it was discovered that, after low-pass filtering, lower frequency components of the signal could be used to obtain consistent estimates of mean residence time [4].

The second problem became apparent when, after the first day of trials, no force signals could be obtained from any of the three installed sensors. The cause of this failure was unknown at the time, but it was suspected that the epoxy used to pot the assembly (seen in Figure 1c as the black substance between probe and housing) had failed to seal the piezo elements against the high pressure (approx. 0.5 MPa) saturated steam environment of the refiner. Subsequent laboratory testing of the recovered piezo elements showed high loss tangents and low d_{33}'s [19] for the piezo material used in RFS3, which was a modified lead metaniobate (PKI-100) supplied by Piezo-kinetics® [20]. The loss tangent is dimensionless, and measures the amount of charge lost to insulation breakdown in the piezo element. The d_{33} is a measure of the charge created per unit force in the primary poling direction. Average values of these two parameters from unused elements, labeled as "Control Elements" and those extracted from the sensors used in Ohio, are shown in Table 1.

Table 1: Average loss tangent and d_{33}'s measured from piezo elements used in RFS3 in Ohio trial before and after baking.

	Control Elements	Used Elements	Used Elements After Baking
d_{33} (pC/N)	86	10	55
loss tangent	0.005	1.2	0.015

To test the failure hypothesis, the elements removed from the sensor were baked at 150 ºC, well below the Curie temperature of 350 ºC for this material, for approximately 24 hours. The elements were again tested and loss tangents and d_{33}'s show significant recovery, as shown in Table 1. These findings confirm the original failure hypothesis, and the need for more effective sealing methods.

A third problem was not recognized during the trials, but found in laboratory testing. It was found that when the sensor was heated above 150 ºC it experienced a loss in sensitivity. Once cooled, the sensor behaved normally.

Fourth Generation Sensor (RFS4)

The fourth generation sensor (RFS4), shown in Figure 2, includes a number of improvements relative to the RFS3. The base of the probe contains both a cylindrical and conical portion. The cylindrical portion allows for the inclusion of an o-ring between probe and housing. A second o-ring is found between the setscrew and the housing. Both o-ring grooves are shown in cross-section in Figure 2b. Sensor wiring is routed to the outside through two small conduits in the housing. These conduits, not shown in the figure, were sealed with silicone. In combination, these systems were effective at sealing the piezo compartment in a 180 C and 10 MPa saturated steam test environment. Figure 2c shows a close-up of the probe and exposed housing of one installed sensor used in Port Alberni. Figure 2d shows the probe, O-ring used between probe and housing, conical spacer and plug, prior to assembly.

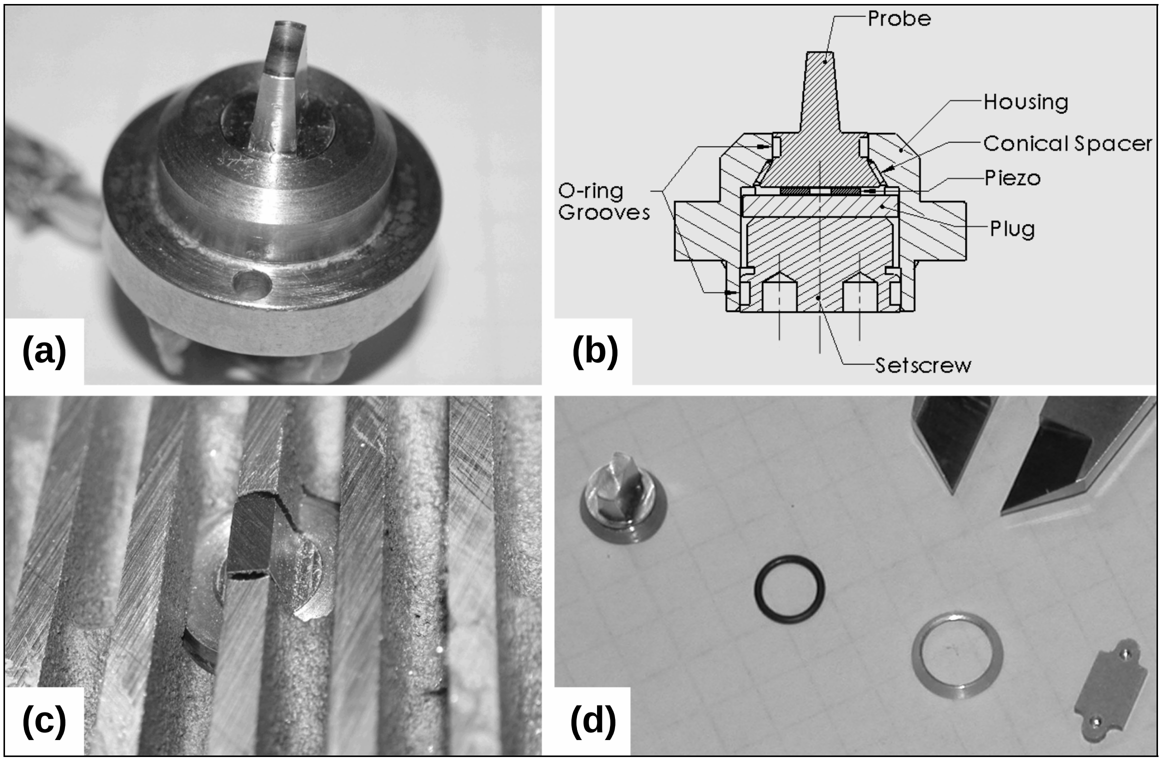

Figure 2: Photo (a) and cross-section (b) of the fourth generation sensor. A close-up (c) of the radially innermost sensor in the Port Alberni trial. View of the probe, O-ring used between probe and housing, conical spacer and plug (d), before assembly.

A new method of affixing the sensor to the refiner plate was also implemented for this sensor. The method uses a backing-screw, rather than many setscrews, to retain the sensor under compression in the plate, as shown in Figure 3. Also shown in Figure 3 is the castellated spacer, which provides the backing-screw with an uninterrupted mating surface. The backing-screw partially envelopes the sensor, and the assembly retains a low-profile as a result. This arrangement is necessitated by the limited thickness of the refiner plate.

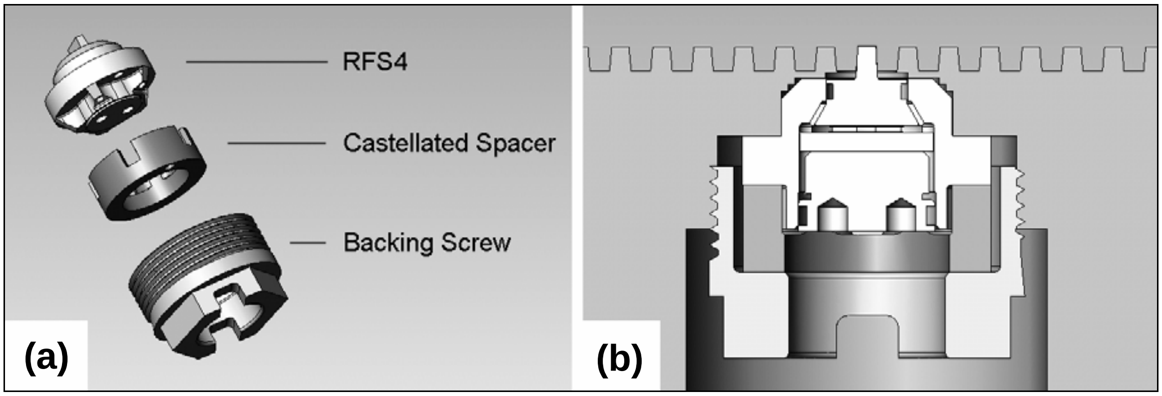

Figure 3: Exploded view (a) and assembled section view (b) of backing screw and castellated spacer used for fixation of RFS4 to refiner plate segment.

The loss of sensitivity found in the RFS3 as a function of temperature was at least partly caused by a loss of pre-load during thermal expansion. The coefficient of thermal expansion (CTE) of lead metaniobate is 1.3 x 10^{-6} m/mºC, an order of magnitude lower than the CTE of AISI 304 stainless steel (17 x 10^{-6} m/mºC), which is the material used for the housing and other components of the RFS3. The chamber that captures the piezo elements would therefore expand at a rate greater than those of the elements, unloading them. Finite element simulation of a 2D model of the RFS3 undergoing a 180 ºC increase in temperature showed that the pre-load loss was manageable, and would be limited to less than 10% of the initial estimated pre-load. To further reduce this effect in the RFS4 design, an aluminum alloy, which has a higher CTE than that of steel (AISI 316 was used in the RFS4), was used for the plug and conical spacer material.

Improvements to the sensor's electrical system were also made. A flexible copper-polyimide laminate was used to provide a conduction path for the piezoelectric elements. Past designs used insulating paints, and soldered wire leads directly to the elements. The specialized laminate, made by Dupont™ and known commercially as Pyralux®, offered defense against potential cracking, which using past methods would have rendered the cracked portion of the element ineffective. Custom charge amplifiers were also designed for each trial, which allowed the specification of system time constants [21] that were well-matched to bar-crossing frequencies. These amplifiers also included isolated power supplies to limit electro-magnetic interference found in industrial environments.

Dynamic Behaviour

The dynamic range, or bandwidth, of the sensor is an important design consideration, owing to the high-frequency excitation of bar-crossings, which range from 20 to 40 kHz in mill-scale refiners. From the point of view of frequency response, the sensor can be modeled as an under-damped, second-order instrument [21]. Instruments of this type are typically designed to record frequencies in a range well below their first natural frequency, to prevent phase and magnitude distortion of the signal due to sensor resonance. The frequency response functions (FRF) of the four sensor designs were measured using a miniature impact hammer (PCB Piezotronics Model 086D80). These measurements were made with the sensors mounted in a steel plate meant to simulate a refiner plate.

Sample FRFs are shown in Figure 4 for all generations of sensor. Each sensor build had a different sensitivity, which was based on many factors, including the d_{33} of the piezo material used, and the gain of the charge amplifier. To simplify comparison of the frequency response of the different sensors, the sensor's sensitivity was used to normalize its FRF. The first natural frequency of each sensor is labeled with the generation, the year and location of its trial, and the scale (or in the case of the LC sensor, type) of the refiner that was instrumented. In the case of the RFS4 trial in Port Alberni, two FRFs labeled “Inner” and “Outer” are shown. These are typical FRFs from the radially innermost and outermost sensors in the refining zone, which had coarse and fine bars respectively. These FRFs represent the full range of the first natural frequencies encountered in this refiner.

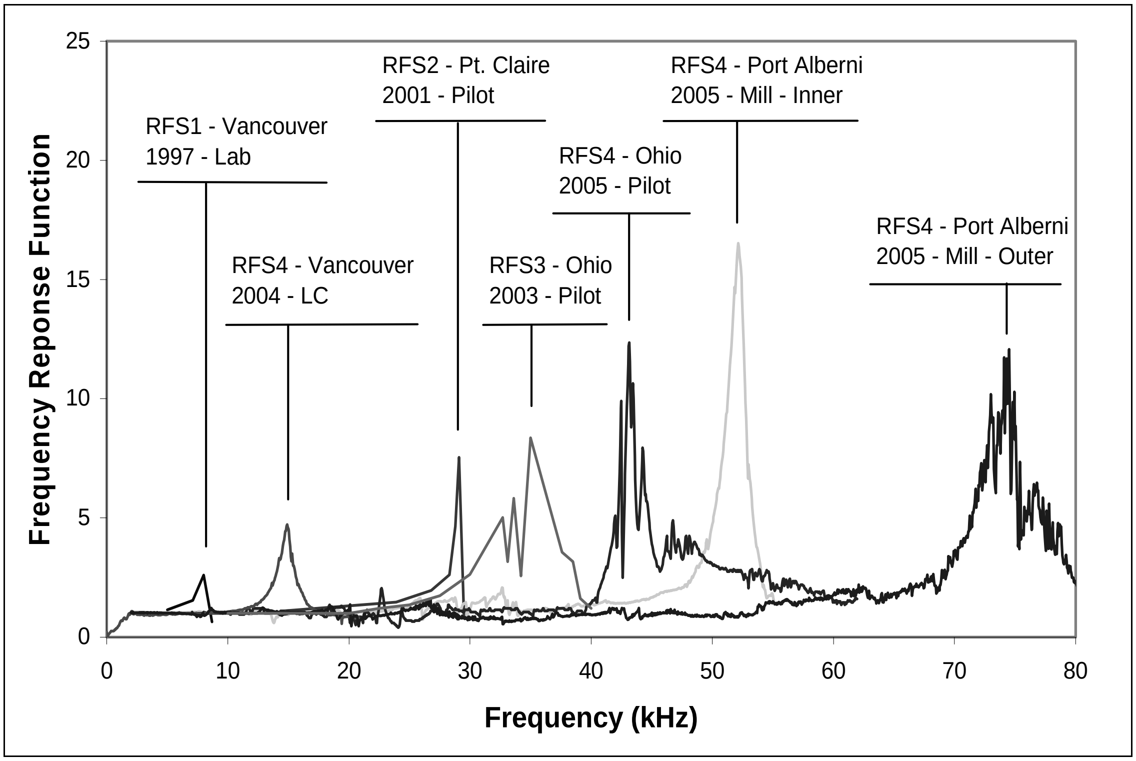

Figure 4: Sample frequency response functions from all four generations of refiner force sensor. Sensitivity of the sensors, which includes charge amplification, was used to normalize results.

RFS1 had a first natural frequency of approximately 8 kHz. Each subsequent model of the sensor improved upon its predecessor in this regard. RFS2 had first natural frequencies near 29 kHz and RFS3 had values near 35 kHz. The RFS4 clearly exhibits the widest dynamic range to date, with first natural frequencies from 44 to 74 kHz. Note that the RFS4 - LC installation was a special case involving an elongated probe and will be discussed later.

There are many resonant modes within the RFS system. The mode associated with the side-to-side "flapping" of the probe is the most dominant, as revealed in finite element modeling of the sensor, and sets its first natural frequency. This is exemplified in Figure 4 by comparing the fourth generation sensor installed in the LC refiner with those installed in the HC refiners. The probe in the LC sensor was over twice as long as the largest probe in the HC sensors. As a result, the first natural frequency of the LC sensor was approximately 15 kHz, far lower than the HC sensors.

A broad distribution of low amplitude frequency structures is also visible in the 20 to 30 kHz band in the FRFs of the HC sensors. These are believed to be a result of the stiffness of the fixation between sensor and refiner plate, as was originally discovered in the first generation sensor [1]. To increase the stiffness of fixation, more cap screws were added to the periphery of the RFS2 housing, and again to the RFS3 housing (as shown in Figure 1). The backing-screw fixation method used in the RFS4 is credited with further stiffening fixation between sensor and plate.

Quantifiable improvement to the dynamic range between the RFS4 and RFS3 without the influence of probe dimensions can be found in Figure 4 by comparing the first natural frequencies of sensors installed in the pilot-scale refiner in Springfield, Ohio, US. These two models had approximately identical probe dimensions - as they were designed for the same plate pattern - but a higher first natural frequency is observed in the RFS4. It is the belief of the authors that this improvement is largely due to the new geometry of the probe. Although the RFS4 probe is more massive than the RFS3 version due to the added conical section, it is now more firmly captured in three dimensions by the housing.

One further concern was the sensitivity of the sensor to the point of impact on the surface of the probe. Flocs are not necessarily expected to contact the probe at the midpoint along its length, for example, nor do flocs necessarily remain at the leading edge of the probe during a bar-crossing, but are dragged across its width. By calibrating the sensor while the impact hammer was positioned at different points along the length and width of the probe surface, the authors were able to quantify this sensitivity. These tests showed that the sensor was relatively insensitive to the point of impact; measured forces were found to vary by less than 10%.

Recent Mill Trial

An array of fourth generation sensors were installed in a 114 cm (45 in.) diameter refiner at a Catalyst Paper Corp. Mill, in Port Alberni, BC, CAN in 2005. A detailed account of the installation and the operating conditions are described elsewhere [5]. The installation was significant in both the scale of the machine and the duration of the tests, which lasted for the entire life of the plates (1800 hours, or three months). The refiner under study operates at high-consistency, but is specialized in that it reprocesses fibre material that has been rejected from a screening system following the original refining pass; these refiners are commonly referred to as reject refiners. As was noted earlier, a total of four sensors were installed at various radii in the refining plate. Calculated bar-crossing frequencies for the inner and outer sensor in the Port Alberni refiner, which runs at a constant rotational speed of 1800 RPM, were estimated to be 21 and 32 kHz, respectively. These excitation frequencies were less than half of the observed first natural frequencies in these sensors (as shown in Figure 4).

Results and Discussion

The sensors provided force data for the entire life of the plates, nearly three months of continuous operation. During this time the reject refiner was run at full capacity, and the sensors were subjected to multiple plate clashes, and stops and starts. Post-trial calibration of the sensors showed only a small drop in normal sensitivity, no more than 10%, while shear sensitivity decreased by as much as 30%. The additional loss in shear sensitivity corresponds closely to the reduction in height of the probes due to wear, which would decrease the available moment arm when the probe is struck. Before and after photographs of one of the outer sensors can be found in Figure 5b and 5c, respectively.

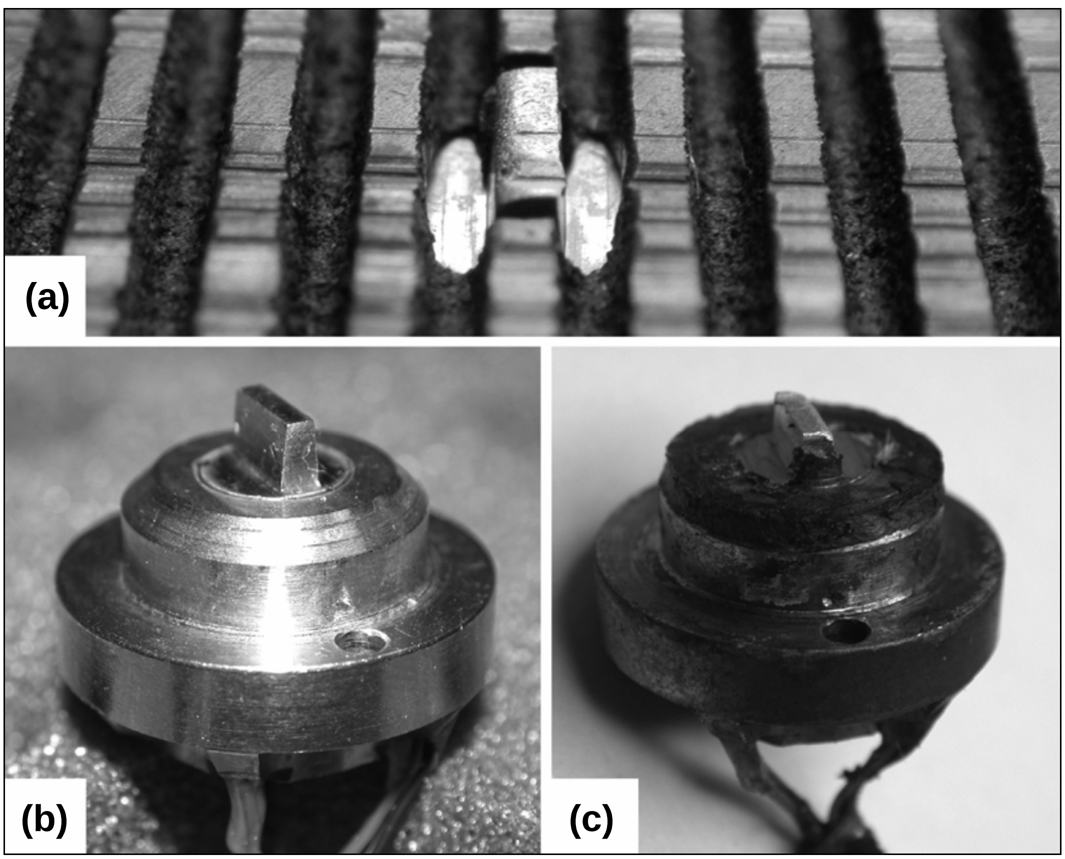

Figure 5: Close-up of an outer sensor (a) installed in the plate after three months of operation, (b) prior to installation in the plate, and (c) just after removal from the plate. The probe shows notable wear, along with tarnishing of the housing. A build-up of blackened pulp was also visible on the top surface.

A visual inspection of the sensor probes revealed that their height was similar to that of the surrounding bars, as seen in Figure 5a. Blunting of the leading edge of the sensor probes was accelerated relative to the surrounding bars on the plate because of a difference in hardness. The probes were machined from AISI 316, whose hardness is estimated at HRB 80. The Durametal™ 47209 plates used at the mill were found to have a hardness of approximately HRC 60 in tests undertaken by the authors. The interior of the sensors that were disassembled were found to be clean, confirming the integrity of the o-ring seals and silicone-laden wiring conduits.

Figure 6 shows force signals collected from the radially innermost sensor running at a motor load of 3 MW, production rate of 60 tonnes per day and dilution flow rate of 0.3 l/s (5 USGPM), which are typical operating conditions. These signals were gathered during trials conducted immediately following installation. The force signals have undergone filtering to eliminate any magnitude distortion and compensation for the loss of zero reference that occurs in piezoelectric systems [21]. In previous RFS work, the normal and shear force profiles have shown a distinct asymmetry. The first half of the impact, when crossing bars initially meet until they are directly overtop one another, is characterized by higher forces than the latter half. This asymmetry is associated with the ploughing force, first noted by Goncharov *et al.* [13], and is visible in Figure 6.

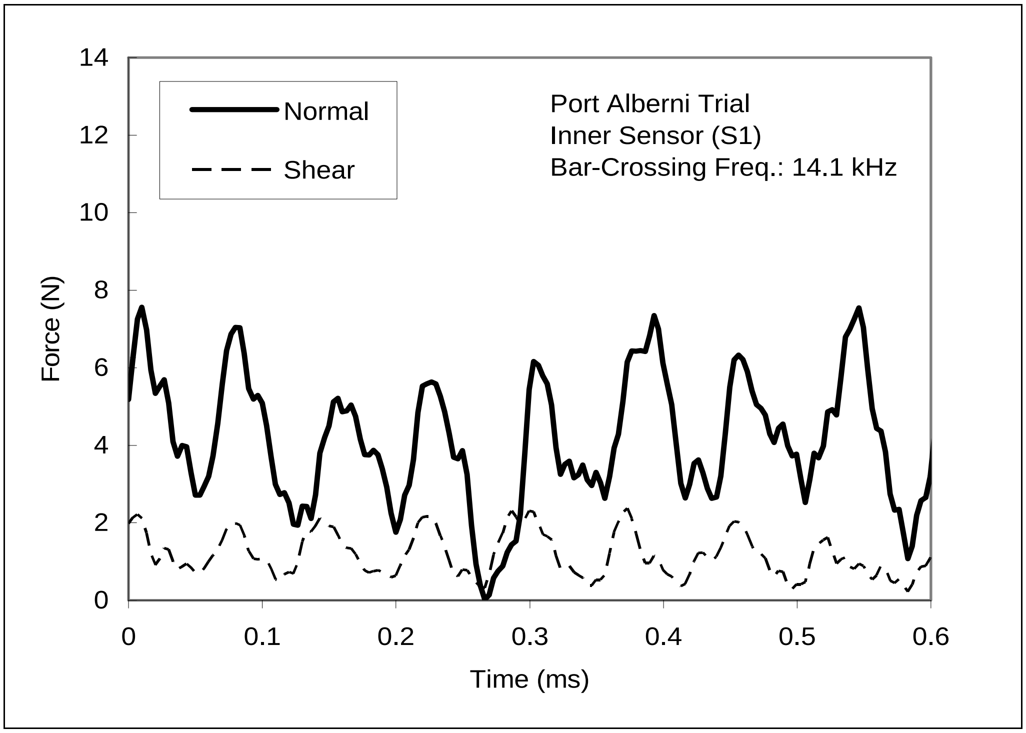

Figure 6: Sample of force signals taken from the inner sensor S1 in the Port Alberni trial under typical operating conditions. The force profiles show the characteristic asymmetry caused by ploughing.

Other features observed in the signals have been explained in part by plate geometry and probe width [5]. In general, the acquired force signals are believed to be accurate and representative of those experienced in the reject refiner. The new fixation method and stiffer design in the fourth generation sensor have dramatically improved frequency response, and have allowed capture of force profiles at the mill-scale.

More extensive analysis of the signal data was performed, including the development of software to isolate and catalogue hundreds of thousands of individual impacts from the signals [5]. With this information it has been possible to create frequency distributions of impact parameters, such as peak normal and shear forces. It has also been possible to estimate the fraction of bar-crossings in which fibres are captured and worked by comparing theoretical crossings versus recorded impacts. This information can be used to make an estimate of pulp quantity and distribution within the refiner. A study of the relationship between refining consistency and bar forces was also undertaken [22].

As noted earlier, plate clash is still a regular occurrence in refiners. The phenomenon is poorly understood, and is frequently responsible for reducing plate life, and causing operational delays. In some rare cases, an extreme plate clash will cause a catastrophic failure of the refiner. Existing accelerometer-based systems can provide some level of warning against these events by measuring vibrations that appear in the refiner prior to, or during, a clash. By using the RFS signal, plate clashes were predicted many seconds in advance of the existing accelerometer-based system at the mill in Port Alberni. An advantage of the RFS-based system is that it is a direct, rather than indirect, indicator of contact between the discs. The use of the RFS signals to predict clash is described in a separate report [16].

Conclusions

A piezoelectric-based sensor designed to measure bar forces in a chip refiner has been developed further to be able to withstand a saturated steam environment and to have a wider dynamic range. Wires are routed outside of the housing by way of small silicone-laden conduits. O-rings are now used to seal the two main orifices on the sensor housing, which complete the seal of the piezo compartment. The inclusion of an o-ring required a new probe geometry, which provides for a stiffer mate with the housing, and increases the dynamic range of the sensor. A single backing-screw replaces many cap screws to clamp the sensor to the refiner plate, and is credited with reducing resonance associated with fixation.

Bar force measurements were made by these sensors in the refining zone of a high-consistency, mill-scale refiner. Sensors were installed, and remained in the plates over a three-month period in a 45 in. (1143 mm) rejects refiner at a Catalyst Paper Corp. mill, in Port Alberni, BC, CA. A post-trial calibration revealed less than 10% loss in normal sensitivity and a loss of up to 30 % in shear sensitivity. The additional shear sensitivity loss is linked to the reduction in probe height caused by wear, which reduces the available moment arm. Disassembly revealed a clean piezo compartment, confirming the integrity of the sealing method.

Bar force profiles bear resemblance to those reported in previous smaller-scale refiners, showing the characteristic asymmetry of higher forces over the first half of the bar-crossing. Distributions of bar force magnitudes and estimates of pulp quantity and distributions have been recovered from the signal. The relationship between bar forces and consistency has also been explored. Finally, the force signal has been used to give advanced warning of plate clash.

Acknowledgements

The authors gratefully acknowledge funding provided by the Natural Sciences and Engineering Research Council, Andritz Ltd., and FPInnovations - Paprican; and access to experimental and commercial facilities provided by Andritz Ltd., Catalyst Paper Corp., and FPInnovations – Paprican. The authors would also like to thank Dr. Rolf Lueck for providing charge amplifier design and insightful discussions on signal conditioning.

References

[1] SIADAT, A., BANKES, A., WILD, P.M., SENGER, J., AND OUELLET, D., “Development of a Piezoelectric Force Sensor for a Chip Refiner,” Proc. IMechE, Part E, Journal of Process Mechanical Engineering, 217:133-140 (2003).

[2] SENGER, J., SIADAT, A., OUELLET, D., AND WILD, P., “Measurement of Normal and Shear Forces During Refining Using a Piezoelectric Force Sensor”, 2003 IMPC Preprints, 403 – 407.

[3] SENGER, J., OLMSTEAD, M., OUELLET, D. AND WILD, P.M., “Measurement of Shear and Normal Forces in the Refining Zone of a TMP Refiner,” J. Pulp Paper Sci., 30(9):247-251 (2004).

[4] SENGER, J., OUELLET, D., WILD, P.M., SABOURIN, M., AND OLENDER, D., “A Technique to Measure Mean Residence Time in TMP Refiners Based on Inherent Process Fluctuations,” J. Pulp Paper Sci., 32(2):83-89 (2006).

[5] OLENDER, D., WILD, P., BYRNES, P., OUELLET, D. AND SABOURIN, M., “Forces on Bars in High-consistency Mill-Scale Refiners: Trends in Primary and Rejects Stage Refiners,” J. Pulp Paper Sci., 33(3):163-171 (2007).

[6] KAPPEL, J., “Mechanical Pulps: From Wood to Bleached Pulp,” TAPPI Press, Atlanta, GA. (1999).

[7] SABOURIN, M., WISEMAN, N., AND VAUGHN, J., “Refining Theory Considerations for Assessing Pulp Properties in the Commercial Manufacture of TMP,” APPITA 55th Annual General Conference, Apr 30 – May 2, Hobart, TAS, 1:195-204 (2001).

[8] MILES, M., AND MAY, W.D., “The Flow of Pulp in Chip Refiners,” J. Pulp Paper Sci., 16(2):63-72 (1990).

[9] MURTON, K. AND DUFFY, G., “The Influence of Pulp Residence Time on Refining Intensity and Pulp Quality,” Appita J., 58(1):64-71 (2005).

[10] SENGER, J., AND OUELLET, D., “Factors Affecting the Shear Forces in High-consistency Refining,” J. Pulp Paper Sci., 28(11):364 – 368 (2002).

[11] VIFORR, S. AND SALMEN, L., “Optimal Shear/Compression Forces – A Way of Collapsing Coarse TMP Fiber,” J. Pulp Paper Sci., 33(1): 22-28 (2007).

[12] SVENSSON, B.A., RUNDÖLF, M., AND HOGLUND, H., “Sliding Friction Between Wood and Steel in a Saturated Steam Environment,” J. Pulp Paper Sci., 32(1): 38 – 43 (2006).

[13] GONCHAROV, V.N., "Force Factors in a Disk Refiner and their Effect on the Beating Process.", Bumazh. Promst. English Trans., 12(5):12-14 (1971).

[14] BACKLUND, H.-O., HOGLUND, H., AND GRADIN, P.A., “Study of Tangential Forces and Temperature Profiles in Commercial Refiners,” 2003 IMPC Preprints, 379- 388.

[15] PRAIRIE, B., WILD, P., BYRNES, P., OLENDER, D., FRANCIS, D.W., and OUELLET, D., "Forces During Bar-Passing Events in Low Consistency Refining: Effects of Refiner Tram,"Pulp Paper Can., 109(9):T153-T156 (2007).

[16] OLENDER, D., FRANCESCUTTI, P., WILD, P. AND BYRNES, P., "Refiner Plate Clash Detection Using an Embedded Force Sensor," NPPRJ, 22(1):124-130 (2007).

[17] PRAIRIE, B., WILD, P., BYRNES, P., OLENDER, D., OUELLET, D., AND FRANCIS, D.W., "Forces During Bar-Passing Events in Low Consistency Refining: Distributions and Relations to Specific Edge Load," J. Pulp Paper Sci. (2008).

[18] BANKES, A., "Design and Development of a Mechanical Wood Pulp Refiner Force Sensor," M.Sc. Thesis, Mechanical Engineering, Queen's University, Jan (2000).

[19] JAFFE, B., COOK, W.R., AND JAFFE, H., "Piezoelectric Ceramics," Academic Press, London (1971).

[20] PIEZO KINETICS INC., 660 East Rolling Ridge Drive, Bellefonte, PA., US., 16823, <http://www.piezo-kinetics.com>, Accessed September (2007).

[21] DOEBELIN, E. "Measurement Systems: Application and Design," McGraw-Hill Publishing Co., 5th Ed., ISBN: 0071194657, 768 pages (2003).

[22] OLENDER, D., WILD, P., BYRNES, P., OUELLET, D. AND SABOURIN, M., "Forces on Bars in High-Consistency Mill-Scale Refiners: Effect of Consistency," IMPC 2007, Minneapolis, MN.

Appendix B

Forces on Bars in High-Consistency Mill-Scale Refiners: Trends in Primary and Rejects Stage Refiners

(Published, Journal of Pulp and Paper Science, 2007)

Forces on Bars in High-Consistency Mill-Scale Refiners: Trends in Primary and Rejects Stage Refiners

D. OLENDER, P. WILD, P. BYRNES, D. OUELLET and M. SABOURIN

Arrays of piezoelectric-based force sensors were installed in two single-disc refiners. A pilot-scale machine operating as a primary stage and a mill-scale machine operating as a rejects stage were instrumented in independent trials. The installed sensors recorded normal and shear forces during individual bar-crossing impacts. In the rejects refiner, mean forces were highest at the periphery of the refining zone while, in the primary stage, mean forces were generally highest at the sensor closest to the refiner axis. Higher coefficients of friction were measured in the primary-stage refiner, which also showed less bar activity in the refining zone. Distributions of peak force values were generated for a range of standard operating conditions. Primary-stage refining showed near decreasing exponential distributions, while rejects refining showed skewed normal distributions. These results indicate a fundamental difference in the behaviours of these refiners, which is explained principally in terms of the processing stage of the wood fibre and the scale of the refiner.

Des séries de capteurs à force piézoélectrique ont été installés dans deux raffineurs à un seul disque. Une machine pilote fonctionnant comme étage primaire et une machine en usine fonctionnant comme un étage de refus ont été dotées d'instruments lors d'essais indépendants. Les capteurs installés ont enregistré des forces normales et des forces de cisaillement pendant les impacts individuels lors du passage des barres. Dans le raffineur de refus, les forces moyennes étaient les plus élevées en périphérie de la zone de raffinage, tandis qu'à l'étage primaire les forces moyennes étaient en général plus élevées au capteur le plus rapproché de l'axe du raffineur. Des coefficients de friction élevés ont été mesurés au raffineur de premier étage, qui a aussi montré moins d'activité aux barres dans la zone de raffinage. Les distributions des valeurs de pointe de la force ont été produites pour une variété de conditions d'exploitation standard. Le raffinage de premier étage a montré des distributions exponentielles presque décroissantes, tandis que le raffinage des refus a montré des distributions asymétriques normales. Ces résultats indiquent une différence fondamentale dans le comportement de ces raffineurs, ce qui s'explique principalement en termes d'étape de traitement des fibres de bois et d'échelle du raffineur.

INTRODUCTION

The energy requirements of thermomechanical pulp mills are set largely by the energy consumed during refining. This fact and the belief that large inefficiencies still exist within the process continue to be the primary motivations for research into refining. Unfortunately, the inaccessible nature of the refining zone has proven a formidable barrier to understanding the basic mechanisms governing operation. Current operational theory relies mainly on global process variables to model performance and, although its use has seen moderate success, issues remain [1,2]. Notable among these issues is the controversy surrounding the ways operating conditions such as consistency and production rate affect the process and also the limited performance of the models in predicting pulp quality.

Researchers are revisiting refining zone interactions in finer detail, in the hopes of revealing overlooked factors. The contact me-

JPPS

D. Olender and P. Wild
Univ. Victoria
Dept. Mech. Engin.
PO Box 3055, Stn CSC
Victoria, BC V8W 3P6
Canada
(pwild@uvic.ca)
P. Byrnes
Herzberg Inst. Astrophysics
5071 West Saanich Rd.
Victoria, BC V9E 2E7
Canada

D. Ouellet*
FP Innovations - Paprican Div.
3800 Wesbrook Mall
Vancouver, BC V6S 2L9
Canada
M. Sabourin
Andritz, Inc.
3200 Upper Valley Pike
Springfield, OH 45424, USA
*Now with:
Novadaq Technologies
6300 River Road
Richmond, BC V6X 1X5

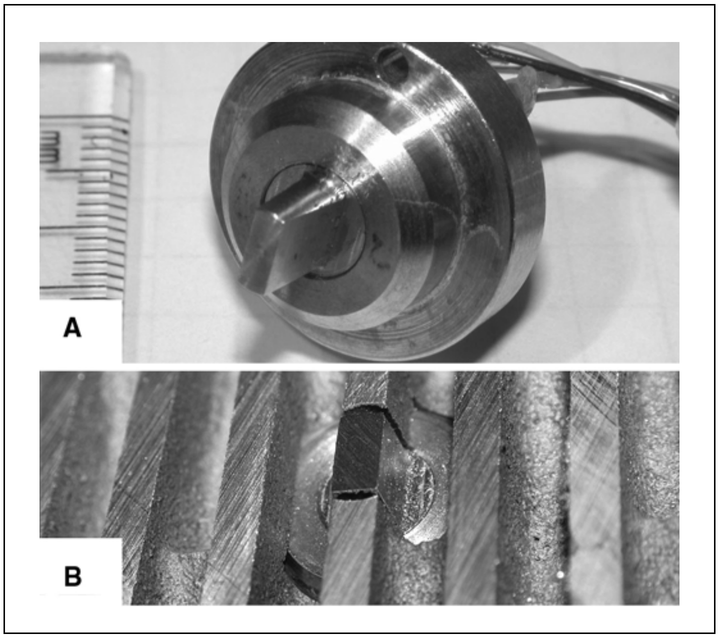

Fig. 1. Close-up of (A) RFS4 sensor used in the Springfield trial and (B) installed in plate prior to installation in Port Alberni.

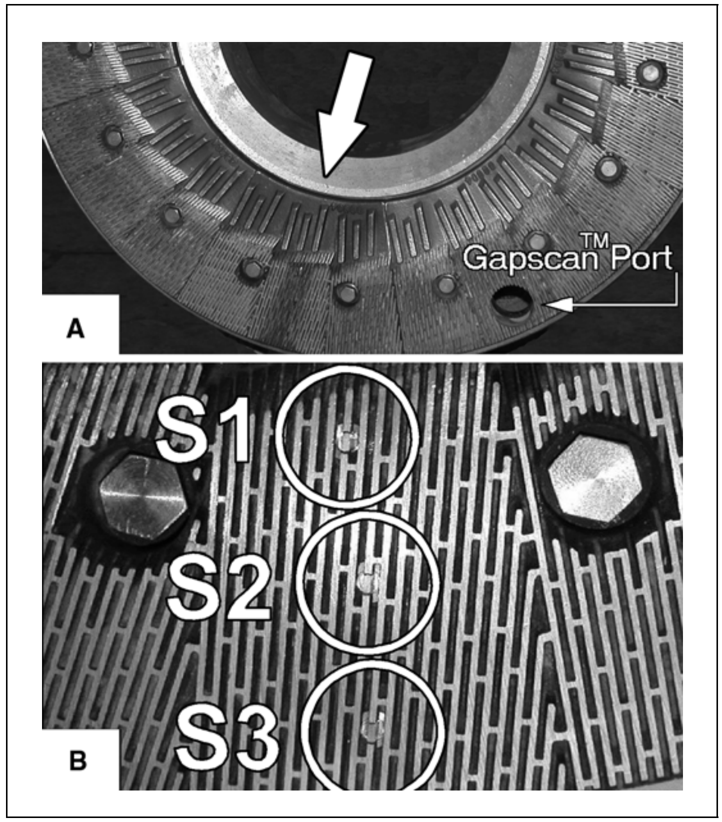

Fig. 2. Location of the instrumented plate segment and force sensors in the Springfield trial. (A) Instrumented segment in position. (B) Location and identification of the sensors in the instrumented plate.

chanics of refiner bar-crossings have received much attention, including mechanisms of fibre development [3], fibre quantity in the refining zone [4] and tribological tests [5]. Also falling under this category are bar force measurements which, in a laboratory setting, have provided recent insights into previously unexplainable phenomena [6]. The observation of a potential link between transitions in the shear-force levels and in the behaviour of the energy–quality relationship known to exist in refiners is particularly compelling. This work has inspired the development of a new force sensor [7]. Tested in a lab-scale high-consistency (HC) refiner [8] and in a pilot-scale HC refiner [9], the sensors provided detailed information on bar forces experienced during refining and spurred interest in further development. In this pursuit, the piezoelectric-based sensor from these earlier trials, known as a refiner-force sensor (RFS), has been adapted to operate in the harsh environment found in mill-scale refiners. This paper presents the results of the latest RFS trials, in which sensors were installed in two HC refiners.

Bar forces were first measured over three decades ago in a low-consistency (LC) refiner using a bending-beam load cell by Goncharov [10]. In situ measurement of bar forces was not undertaken again until more recently by Gradin et al. [11]. Strain gauges were again used but, in this case, the gauges were applied in the exposed grooves of the refining zone. Backlund et al. [12] converted a commercial piezoelectric sensor to measure tangential forces over a circular section of the refining zone, spanning multiple bars. Bar forces were influenced significantly by radial location in the refining zone, with forces being highest at the periphery. Senger et al. [9] also observed a significant dependence on radius, but found that forces were smallest at the periphery. Because of the limited amount of empirical evidence, Senger et al. could only speculate on the cause of this conflicting result. A third-generation RFS has also been employed to measure mean residence time [13] and, most recently, a fourth-generation RFS was tested successfully in an LC refiner [14]. Commercial pressure sensors have also been used extensively to capture the pressures that develop in the refining zone [15–18]. Eriksen [19] has performed the most recent tests with pressure sensors in pilot and Eriksen et al. [20,21] in mill-scale HC refiners.

In the work presented here, sensors were installed in a primary-stage refiner at the Andritz, Inc. pilot plant in Springfield, OH, USA and in a rejects refiner at a Catalyst Paper Corp. mill in Port Alberni, BC, Canada. The sensors used were the fourth generation of the sensor described by Siadat et al. [7]. Each sensor contained two piezoelectric elements and a thermocouple, and replaced a short (5 mm) segment of bar in the refiner plate. The sensors were capable of measuring normal and shear forces experienced by pulp during bar-crossing impacts. The Port Alberni campaign marked the first time a force sensor of this capability has ever been installed in a mill-scale production machine for an extended length of time. This paper presents bar forces measured during standard operating conditions in both primary- and rejects-stage HC refiners, and identifies general trends.

EXPERIMENTAL

Figure 1A is a photograph of one fourth-generation RFS (RFS4) used in the Springfield trials. This sensor is sealed hermetically, and was tested to withstand a saturated steam environment of 1 MPa and 180ºC. RFS4 also has a higher first natural frequency than its predecessors. Figure 1B shows an RFS4 installed in the plate segment prior to installation in the refiner in Port Alberni. Each sensor probe replaces a 5 mm segment of bar. The sensor housing was exposed in grooves adjacent to the sensor probe and therefore would have partially obstructed the flow of pulp. However, the exposed portion of the sensor housing did not exceed surrounding dams and therefore is expected to allow sufficient flow of pulp around the sensor probe.

Springfield Trial

Shown in Fig. 2A is the stator disc of the Andritz 36-1CP refiner (Springfield) after removal from the casing for a change of plates. This is a single-disc pressurized refiner with a variable speed motor. The arrow indicates the

TABLE I
LIST OF SPRINGFIELD EXPERIMENTS

Sample Identification	Target Motor Load (kW)	Actual Motor Load (kW)	Production Rate (t/d)	Specific Energy (kWh/t)	Plate Gap (mm)	Discharge Consistency (%)
A15	550	561	21.1	562	0.76	38.1
A16	650	659		673	0.56	38.6
A17	750	701		721	0.43	43.3
A18	850	857		899	0.25	48.0
A19	450	454	18.4	505	1.07	37.3
A20	550	547		626	0.94	38.4
A21	650	605		702	0.74	41.9
A22	750	750		891	0.46	47.6
A23	600	601	26.4	521	0.94	40.0
A24	700	702		620	0.64	43.0
A25	800	786		701	0.53	54.0
A26	900	883		796	0.36	55.9

plate segment instrumented with sensors, which is installed at approximately the 7 o'clock position on the stator. Figure 2B shows the location and identification of the three sensors within the instrumented plate segment. Clearly visible in this figure is the directional bar pattern of the Durametal 36604 (Andritz) plates, which have a cutting-edge length of 31 km/revolution and an average bar angle of 7º from radial. The plates have a 0.2% taper. The width of the top of the bars is 1.7 mm, and the pitch of the bars, or space between leading edges, is 4.3 mm. Sensors S1, S2 and S3 were positioned at radii of 0.358, 0.395 and 0.437 m, respectively.

Data acquisition hardware consisted of two National Instruments (Austin, TX, USA) PCI high-speed boards and one low-speed board, installed in a personal computer. Custom acquisition software was created using Labview (National Instruments). To resolve bar-crossing impacts accurately, a sampling rate of 300 kilo samples/s (kS/s) was used on the high-speed boards. This sampling rate was greater than ten times the highest bar-crossing frequencies encountered in the trial.

The setup and experiments in Springfield took place over one week in early January 2005. Table I lists the process conditions of the experiment considered in this work. While holding production rate constant, four levels of motor load were tested. This pattern was repeated for three production rates: a nominal rate of 21.1 o.d. mt/d, a low rate of 18.4 o.d. mt/d and a high rate of 24.6 o.d. mt/d. After reaching stable refining conditions, force signals were recorded for 15–30 s to allow representative force data and pulp samples to be acquired. The casing environment was held constant at a gauge pressure of 350 kPa (3.5 bar) and a temperature of 148ºC. The refiner was run at a constant speed of 1900 rpm in hold-back mode during all tests. Hold-back mode is defined by the direction of rotor rotation that causes crossing bars to scissor radially inward. Spruce wood chips having a moisture content of 48.6% were used. Retention in the presteaming tube was 120 s at a gauge pressure of 100 kPa (1 bar).

Port Alberni Trial

Figure 3A is a photograph of the stator disc in the Andritz 45-1B refiner instrumented in Port Alberni. This is a single-disc atmospheric discharge refiner running at 1800 RPM. The photograph was taken just prior to installation of the instrumented plate segment. Also indicated in Fig. 3A is the wiring port, located directly behind the plate segment that was refitted for the trials. The wiring port already existed in this refiner model, and allowed for the RFS wiring to be routed outside without any modifications to the casing. The instrumented plate segment was installed during a scheduled plate change. Figure 3B shows a close-up of the installed plate segment, showing the location and identification of the four RFS. Sensors S1, S2, S3 and S4 were positioned at radii of 0.478, 0.523 and 0.556 m. Sensors S3 and S4 share the same radius. The plates used in this trial were Durametal model 47209, which have a bidirectional bar pattern with a cutting-edge length of 74.9 km/revolution and taper of 0.2%. These plates are 119 cm (47 inch) in diameter, greater than the nominal size for the refiner, and are considered overhung. The plates had three regions of bar, requiring three unique sensor probes to be designed. The width of the top of the bars for the three regions, starting with the innermost region, was 2.54, 1.91 and 1.4 mm.

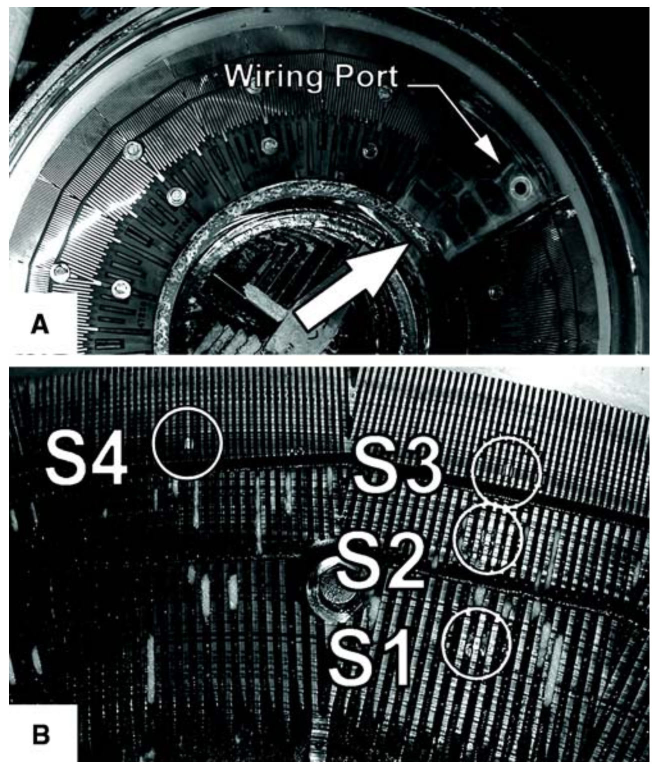

Fig. 3. Location of the instrumented plate segment, wiring port and force sensors in the Port Alberni trial. (A) Vacant segment position, just prior to installation of the instrumented plate. (B) Location and identification of the sensors in the instrumented plate.

The pitch of the bars, starting with the innermost region, for the three regions was 6.35, 4.7 and 3.31 mm.

Data acquisition hardware consisted of one National Instruments high-speed board and one low-speed board installed in a PXI system. A sampling rate of 300 kS/s was used again on the high-speed board to record RFS signals. A sampling rate of 50 S/s in the low-speed board was adequate to record the signal from the RFS thermocouples and from the plate protection accelerometer. Signals for process variables such as motor load, production rate and dilution flow were not available; these were recorded directly from the operator's monitor.

The RFS were installed for the entire life of the plates, a period of approximately three months (1800 h), from September to November 2005. Immediately following installation of the instrumented plate segment, two experiments were performed and are listed in Table II. In these two experiments, motor load and production rate were varied while keeping other process variables constant. The consistency of incoming reject pulp was ~28%. Dilution flow was held constant at 19 L/min (5 USGPM). Once process conditions were stabilized at the target point, settings were held for ~3 min as forces were recorded and inlet and discharge pulp samples were taken. Post calibration of the sensors after 1800 h of operation revealed less than 10% loss of sensitivity.

Signal Conditioning

Each sensor generates two voltage signals, which are converted to normal and shear force signals based on a method described elsewhere [7]. Instruments having a second-order response [22], such as the RFS, are subject to recording a false rise in amplitude at measured frequencies near their first natural frequency. In the refiners tested in these trials, bar-crossing frequencies as high as ~32 kHz were encountered. All sensors used in these trials had first natural frequencies of at least twice the bar-crossing frequencies occurring in the trials. As an example, the outer sensors S3 in Springfield and Port Alberni had first natural frequencies of ~44 and ~75 kHz, respectively. The first natural frequency of each sensor was estimated from the frequency response function (FRF) obtained during calibration. Based on this information, a digital filter was designed to attenuate any increase in signal amplitude associated with resonance for each sensor's unique FRF. The Springfield sensors all had similar FRFs because they were physically identical. In contrast, the Port Alberni sensors each had different probes to match the local bar dimensions, which altered the FRF and required a different filter in each case.

TABLE II
LIST OF PORT ALBERNI EXPERIMENTS

Sample Identification	Motor Load (kW)	Production Rate (o.d. mt/d)	Specific Energy (kWh/t)
A1	2700	61.2	1055
A2	2900		1137
A3	3100		1216
A4	3300		1294
A5	3000	55.0	1309
A6		59.3	1214
A7		61.4	1173
A8		65.5	1099

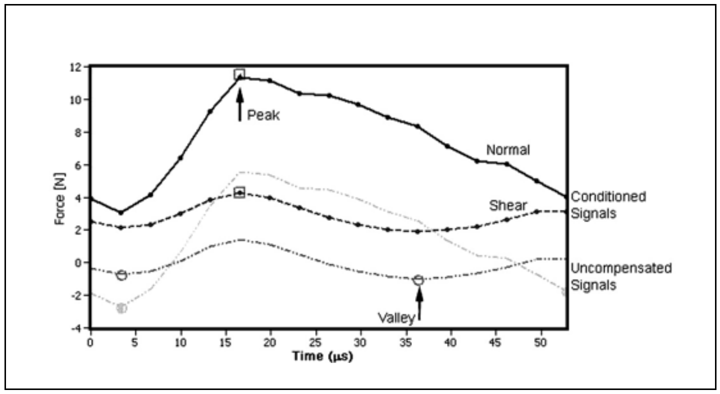

Fig. 4. One bar-crossing impact recorded in Port Alberni. Peaks and valleys are indicated on normal and shear force profiles. Uncompensated signals are those that have been filtered but have not received final offset.

One further signal-conditioning step relating to the frequency response of these sensors was necessary. Piezo-based transducers cannot measure direct current or constant signals, because the small amounts of charge generated at the electrodes dissipate through the signal-conditioning circuit and through the internal resistance of the piezo itself. As a result, some low-frequency components of the signals are lost. This behaviour can be modelled as a first-order, high-pass filter [22]. An inverse filter, similar to that tested in past RFS trials [9], was used to compensate for this loss. A complete recovery of the lost signal was not possible using this method, as it would have involved amplification of signals that were below the noise threshold of the system. A final manual correction therefore was necessary. The reference for this correction is the valley between adjacent force peaks, based on the assumption that the force signal returns to zero. In some cases, the signal does not return to zero between each impact and it is necessary to discard these valleys as zero references. The way this situation arises is discussed further in the results section. To identify valleys that do not give an accurate zero reference, a characteristic of the piezo-amplifier system is used. Assuming no new impacts after a certain point, it is known that the piezo signal will decay to zero at a certain rate due to charge loss. It is also true that, if the piezo signal is below zero, a maximum growth rate to zero based on charge gain also exists. These rates are defined by the system time constant, which was ~1.6 ms (after inverse filtering) for both campaigns. Starting with a known zero reference, a line representing the maximum growth rate then can be calculated. If the next valley in the signal exceeds this line, this valley can be discarded as a reference. This logic is used until the next zero reference is found. Thus it is possible for the zero reference of an impact to be based on valleys not immediately adjacent to its peak, which is the case in Fig. 4. The resulting filtered and compensated force signals are an accurate representation of the bar forces experienced in the refiner.

Processing Techniques

Classification software was created to identify bar-crossing impacts automatically and to measure their characteristic features. First, the algorithm filters the conditioned force signals with a fourth-order, low-pass filter using a cut-off frequency near the bar-crossing frequency at the location of the sensor. Then this heavily filtered signal is phase-matched to the conditioned signal to allow the identification of the three primary extrema making up a bar-crossing impact, considered to be a maximum (peak) surrounded by two minima (valleys). Valleys mark the boundaries of the impact. Normal force impacts are targeted first, as they offer the best signal-to-noise ratio and are identified initially by their peaks. Peaks below the system noise threshold (0.2 N) were discarded. The boundaries of the normal force impact guide the search for the corresponding shear impact. An example of one identified impact is shown in Fig. 4. Fully conditioned normal and shear force signals are shown in dark, while the faint, dashed lines below show the signals prior to compensation for lost low-frequency components. Peaks are indicated on both conditioned signals by a square, while valleys are indicated on their uncompensated counterparts by circles.

As noted, a number of features of the bar-crossing impacts, known as impact parameters, were stored for further analysis: normal and shear force peak values and the equivalent tangential coefficient of friction μ_{teq}. The equivalent tangential coefficient of friction was defined by Senger and Ouellet [6] as the average shear force divided by the average normal force over the duration of the impact. An indicator of bar activity, occurrence ratio, was also defined. Occurrence ratio is the number of impacts recorded divided by the theoretical number of impacts predicted by the bar-crossing frequency and test duration.

Distributions of impact parameters were created to characterize hundreds of thousands of bar-crossings, spanning many seconds of operation. Due to the high sampling rate (300 kS/s) these distributions were based on data taken from three intervals of 5 s spaced evenly throughout each experiment. In the sections below, all results are based on data extracted in this manner unless otherwise noted. A four-parameter Weibull distribution was found to be an accurate fit to the observed data. Sigmaplot 9.0 [23] graphing software was used to perform the regression.

RESULTS AND DISCUSSION

Force Signals

Figures 5A and 5B show force signals measured by the outer sensor S3 during the Springfield and the Port Alberni trials, respectively. Vertical dashed lines, spaced evenly in time at the bar-crossing period and aligned with the impact peaks, have also been added to both figures. Immediately apparent in these two figures is the difference in force magnitude, which will be given a more quantitative treatment in sections below. Of interest here is the general composition and quality of the force signals.

In the primary-stage refiner, forces consisted of many small-force impacts interspersed with relatively few large-force impacts. It was common to observe groupings of large-force impacts, such as B, C and D in Fig. 5A. As shown in Fig. 5B, bar-crossing impacts are more regular in the rejects refiner. Groupings of impacts were also reported in earlier RFS work by Senger et al. [8]. But, in that case, the impacts showed periodicity with the rotor and supported the physical interpretation that flocs were being stapled to rotor bars over multiple rotations. The grouping of large-force impacts B, C and D shown in Fig. 5A can be interpreted in several ways, one of which is that a floc has become stapled to the sensor probe on the stator. The stapling of flocs to stator bars has been photographed in separate works [3,24]. A further point of interest in this sequence of impacts is the change in μ_{teq}. By visually comparing the normal and shear force peaks, one can see that μ_{teq} would decrease with each successive impact until, presumably, the floc is released or carried away by the rotor.

It is clear from Figs. 5A and 5B that the force signal does not return to zero after every impact. This blending of impacts is believed to be a consequence, in part, of the bar-crossing angle of the plates. For large bar-crossing angles, it is possible for the trailing edge of a receding bar and the leading edge of an approaching bar to overlap the sensor probe simultaneously. This condition effectively increases the width of the sensor probe and is similar to phenomena encountered with pressure transducers installed in refiners [18]. The recording of blended impacts would also depend largely on the amount and homogeneity of the material in the refining zone. Blending is present in both Springfield and Port Alberni signals, but is more pronounced in the Springfield data. This is expected, as the 36604 pattern used in Springfield is a directional plate and experiences higher bar-crossing angles than the pattern used in Port Alberni. The surface dams found in the 36604 pattern would further add to the blending effect in Springfield.

Impact peaks between normal and shear forces are not consistently in phase with each other, nor do they always appear in the position predicted by the calculated bar-crossing period. These phase irregularities could be explained by the geometry of the nip of crossing bars, which varies throughout the rotation of the discs. This also highlights the fact that the calculated bar-crossing period is an average. Changes in relative bar angle away from parallel alter the geometry of intersection of the nip from a line to a point. Further compounding

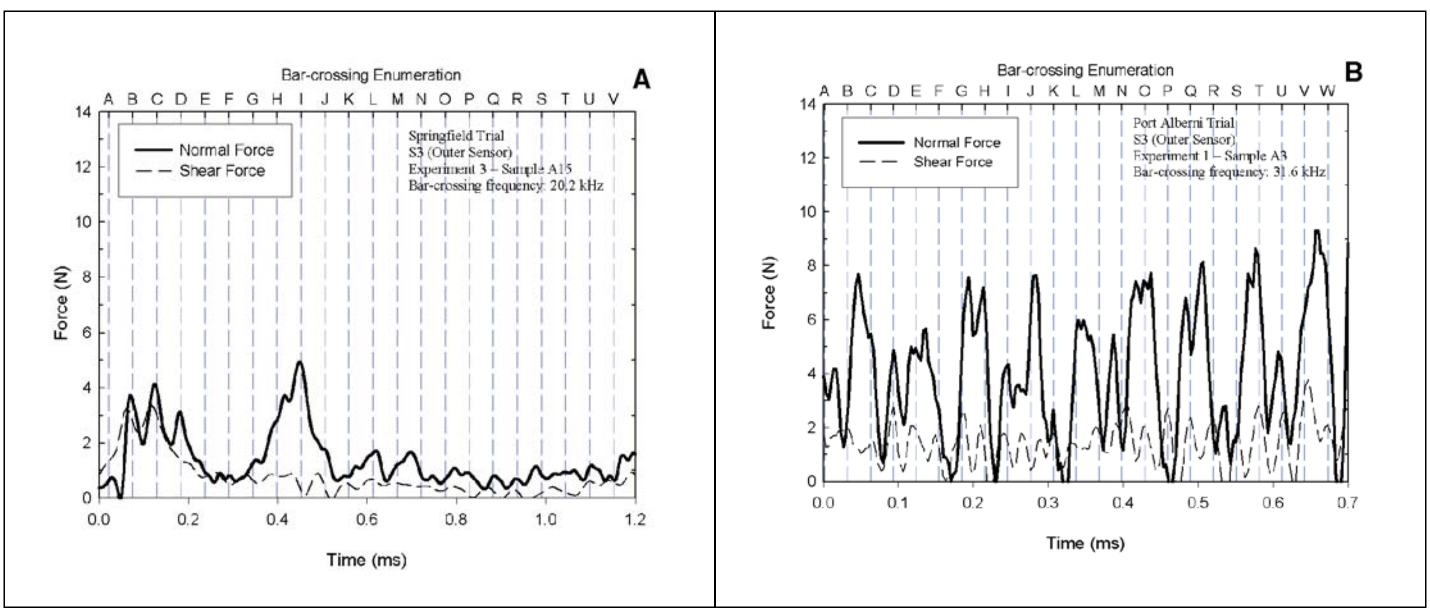

Fig. 5. Representative sample of force profiles from the outer sensor S3 in (A) the Springfield and (B) the Port Alberni trials. Vertical dashed lines are spaced at the calculated bar-crossing period.

this contact variability is the presence of the fibre material.

Impact Distributions

A comparison of peak shear-force distributions measured by the outer sensor S3 at high and low motor loads under nominal production rates is shown in Fig. 6. Distributions in this figure were taken from samples A15, A17 and samples A1, A3 from the Springfield and Port Alberni trials, respectively. Each distribution was formulated from a single 5 s interval from the sample. Solid lines indicate the Weibull curve in the case of high motor loads, while dashed lines indicate the curve at low motor loads. The r^2 was at least 0.99 for all regressions. For clarity, experimental data histograms are shown only for the high motor load cases.

Superimposed on Fig. 6 are data from an outer sensor in earlier tests at Paprican's research facility in Pointe Claire, QC, Canada [9]. These tests were conducted in an Andritz 22-1CP single-disc refiner and used a third-generation RFS. The bin size of the histogram was adapted to match Springfield and Port Alberni data. The shape parameter β is indicated for all curves. As a reference, a β value of 1.0 specifies a decreasing exponential distribution, while a β value of 3.0 specifies a normal distribution.

Noticeable in Fig. 6 is an increase in both the magnitude and spread of the force distributions from Pointe Claire to Port Alberni. In terms of Weibull parameters, this is quantified by the location and scale parameters. Of more immediate interest is the progression in the shape of the distributions between the three trials, from decreasing exponential to near normal, which is reflected in an increase in β. This trend remains if one considers the mean β for all sensors over each trial. The mean β found for all sensors, in all Springfield experiments listed in Table I, was 1.4. The mean β found for all sensors, in all Port Alberni experiments listed in Table II, was 2.5. This trend also exists in the peak normal force data, where the mean β for Springfield and Port Alberni were 1.3 and 2.6, respectively. There was no significant difference in β between individual sensors in either trial.

The theory of a decreasing exponential distribution of forces has been advanced, but only in the context of LC refining [25,26]. Recent RFS tests in an LC refiner by Prairie et al. [14] have shown a near normal distribution of forces, which does not support this earlier theory. Prairie et al. proposed that the normal distributions found in their work could be explained by the composition of the mixture in the refining zone. It was postulated that the fibrous solution found in LC refining offers a continuous stream of flexible material into the nip of crossing bars, resulting in a more regular impact history. This was in contrast with the irregular three-phase mixture of coarse wood fibre, water and steam found in primary-stage HC refiners. This mixture may cause an unevenly distributed pulp pad, resulting in null or glancing impacts, and may create the distribution found in the Pointe Claire trial. This hypothesis was also postulated earlier by Backlund et al. [12] as one reason for the large scatter in the recorded data from their innermost sensor.

The findings of the current RFS trials support this hypothesis. Distributions found in Springfield and Port Alberni are consistent with the notion that the degree of refining and therefore the processing stage of the pulp are important factors in determining the magnitude and frequency of bar-crossing impacts in the refining zone.

Another factor to be considered in comparing these trials is the scale of the refiner. Comparison of the Pointe Claire and Springfield trials offers potential isolation of this effect. The procedures in the two trials in Pointe Claire and in Springfield processed chips under similar casing pressures and temperatures and, aside from plate pattern, scale is the most noteworthy difference. One of several aspects of the increasing scale was an increase in throughput. This may result in an increase in the amount of fibre between the plates. Calculations done according to Miles and May [27] indicated that the amount of pulp per unit area around the outer sensor locations was about twice as high in the 45-1B refiner as in the 36-1CP refiner. The observed increase in β from Pointe Claire to Port Alberni could be partly explained by this effect of scale.

The discovery of a decreasing exponential distribution of bar forces in HC refining could have implications for efficiency. As Giertz [25] proposed in the context of LC refining, an optimal range of bar forces exists that performs useful work in the refining zone. In his description, a normal distribution centered on the mean of this useful range permits more impacts than an exponential distribution, whose tail extends out over this optimal range. If this logic were applied to HC refining, improvements in efficiency could be gained by moving toward a normal distribution of forces in the refining zone. Sabourin et al. [28] reported an average specific energy reduction of 11%

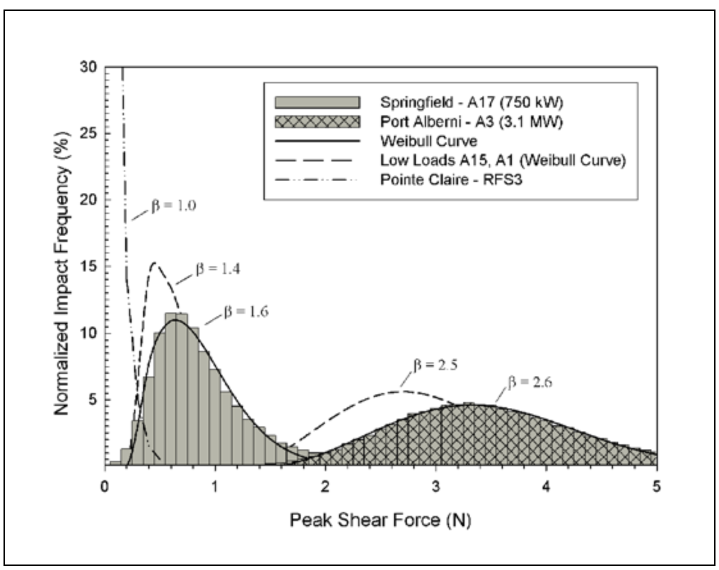

Fig. 6. A comparison of peak shear-force distributions measured in the outer sensor S3 at two motor loads while running at nominal production rates. Weibull curves, and their corresponding β, are also indicated. Data for low motor loads were removed for clarity.

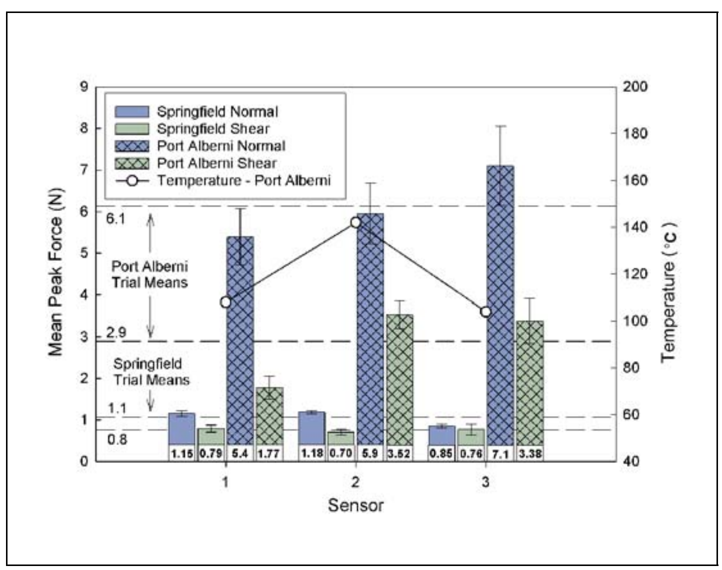

Fig. 7. Mean peak normal and shear forces measured at sensors S1, S2 and S3 in Springfield and Port Alberni. Peak forces have been averaged for all experiments in each trial. Measured temperatures from Port Alberni are also included.

in the Springfield refiner by increasing chip defibration prior to refining. One might expect a more uniform fibre flow as a result, which could be an example of expected efficiency gains. Regardless, the present findings indicate that different distributions do exist, and that it might be worth investigating their relationship to refining efficiency.

General and Radial Trends

Mean peak normal force, peak shear force, μ_{teq} and occurrence ratio, measured at each sensor, are presented in Figs. 7, 8 and 9, respectively. Means were calculated for each sensor from all experiments in the trial. Error bars report the standard deviation between the three intervals of 5 s sampled from each experiment. Also included in each of these figures as a dashed line is the average of the three sensor means, called the trial mean. In Fig. 7, temperature readings from Springfield are not included due to a thermocouple insulation breakdown that caused signal error and intermittency.

Trial means for peak force, shown in Fig. 7, are approximately five times greater in Port Alberni than in Springfield. This factor is similar to the ratio of motor loads between the two refiners, and suggests that forces are generally proportional to power. A good correlation between force and power was also reported by Backlund et al. [12]. The motor load increase from Pointe Claire to Springfield is also consistent with this trend, at least in the case of the outer sensor. The Pointe Claire refiner operated at between 50 and 190 kW.

From Fig. 8, the trial mean μ_{teq} in Springfield was 0.83 while the trial mean in Port Alberni was 0.49. The higher trial mean μ_{teq} observed in Springfield can be explained by the difference in the stage of refining. The coarse, more intact wood fibre in the primary stage is mechanically stronger, but also is at higher consistency, which has been reported to increase μ_{teq} [6]. These are thought to be the dominant factors causing the difference in trial mean μ_{teq} between Springfield and Port Alberni.

Figure 9 shows the occurrence ratio, which was defined previously, and represents the fraction of bar crossings in which fibres are captured and worked. The trial mean occurrence ratio for Springfield was 0.66 while, in Port Alberni, it was 0.82. These findings show that bar activity was less in Springfield, which further supports the existence of a more heterogeneous mixture in this refiner. The reported occurrence ratios can be compared to earlier work by Stationwala et al. [29]. In these experiments, the bar coverage in the refining zone of an Andritz 42-1B was estimated using photography and image analysis, and was observed to be between 50 and 85%. This gives confidence in the observed occurrence ratios, which are within this range. However, it should be noted that the lower occurrence ratios observed in Springfield could be due to blended impacts in small part. In extreme cases, these impacts would have been misinterpreted by the classification software as a single impact.

Both the increasing and decreasing radial force trends observed in Fig. 7 have been reported in the literature. Backlund et al. [12] reported an increase in tangential forces with radius in mill-scale single-disc and conical-disc refiners, while Senger et al. [9] observed a decrease in forces in the Pointe Claire trial. One explanation for the difference in these trends considers that chips or intact wood segments such as shives induce larger force impacts than refined pulp for a given plate gap. Primary-stage refining in Pointe Claire and Springfield would contain more intact wood fibre at the entrance to the refining zone, which would undergo a pronounced change in mechanical properties before exiting the refiner. This transformation would be the most important factor in determining the radial force trend. In Port Alberni, the rejects fibre has been separated largely from its original wood matrix, and mechanical properties such as modulus and strength are already reduced greatly. Therefore, radial force trends in Port Alberni might have been determined principally by other factors in the refining zone, such as an increase in tangential velocity of crossing bars as postulated by Backlund et al. [12], or a reduction in plate gap as a result of taper. Prairie et al. [14] reported a three-fold increase in forces in LC refining linked to a rotor misalignment of only 0.06 mm. The 0.2% plate taper found in Springfield and Port Alberni could cause a far larger reduction in gap over the radial span of the sensors.

Radial trends of occurrence ratio in Fig. 9 point to an accumulation of fibre at S2 in both refiners, most probably near the stagnation point. The stagnation point is approximately located in the Port Alberni trial by the recorded temperature maximum at S2.

An explanation of the radial μ_{teq} trends in Fig. 8 has yet to be developed. The increase in fibre material could partially explain the maximum in μ_{teq} found in Port Alberni, but cannot be the principal factor in Springfield, whose minimum μ_{teq} is found at S2. Other potential factors, such as an increase in consistency and temperature, are expected to cause an increase in friction [5,6]. Both are expected to rise at the stagnation point [27,30], which again supports the trends in Port Alberni but not in Springfield. It can only be assumed that the stagnation point was located near the middle of the plate in Springfield, as no useful sensor

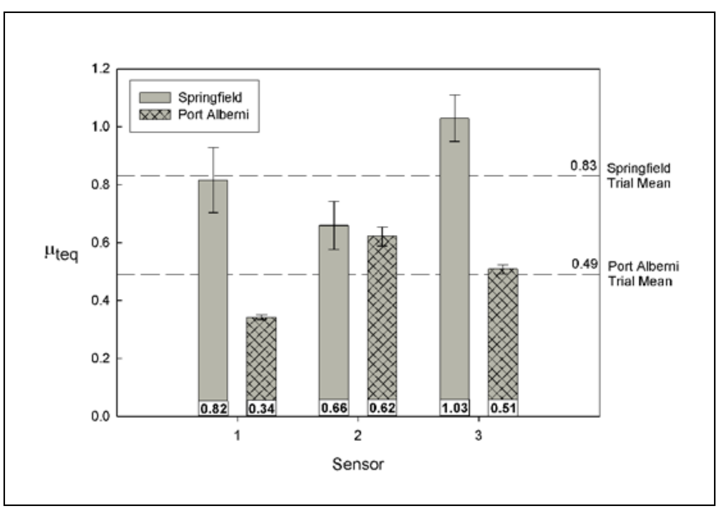

Fig. 8. The equivalent tangential coefficient of friction μ_{teq} found at each sensor for Springfield and Port Alberni. The values of μ_{teq} were averaged over all experiments for each trial.

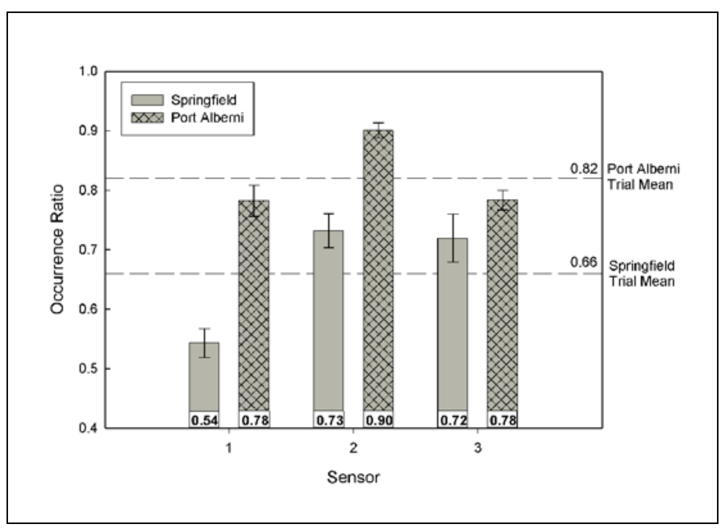

Fig. 9. Occurrence ratio measured at each sensor for the Springfield and Port Alberni trials. The occurrence ratio was averaged over all experiments in the trial.

temperature data was recorded during the actual trial. Thus, it is difficult to speculate on the factors causing the radial μ_{teq} trend in Springfield.

CONCLUSIONS

Bar-force measurements were made by a dual-axis sensor in the refining zone of two HC, mill-scale refiners in separate field campaigns. Tests were conducted in a 914 mm (36 inch) pressurized refiner, processing chips at the Andritz pilot plant in Springfield, OH, USA and in a 1143 mm (45 inch) rejects refiner at a Catalyst Paper Corp. mill in Port Alberni, BC, Canada. Experiments that varied motor load and production rate were carried out following sensor installation. Post-campaign calibration of the sensors revealed only marginal loss in sensitivity, verifying their survivability in mill-scale refiners.

Force signals in Springfield showed many small-force impacts, interspersed with relatively few large-force impacts. A more regular impact history was found in Port Alberni. This was confirmed quantitatively through the use of classification software, which was created to automatically identify and characterize thousands of individual impacts spanning many seconds of operation. Four-parameter Weibull curves showed a good fit to the distributions of impact parameters, such as peak normal and peak shear force. Primary-stage refining in Springfield displayed near-decreasing exponential distributions. Conversely, reject refining displayed skewed normal distributions. We postulate that the processing stage of the wood fibre and the scale of the refiner are the primary cause of this difference. Primary-stage wood fibre is mechanically stronger and less likely to promote capture between crossing bars. In terms of scale, a higher production rate per unit area is postulated to increase the amount of fibre in the refining zone and to improve regularity of the flow. We propose that both of these factors contribute to the homogeneity of the fibre–water–steam mixture in the refining zone and determine the magnitude and frequency of bar-crossing impacts.

Mean peak forces in Springfield were approximately five times lower than in Port Alberni, which roughly corresponds to the ratio of power between the two refiners, and suggests that bar-force levels are proportional to motor load. Primary-stage refining in Springfield showed higher friction and ~20% less bar activity based on the occurrence of bar-crossing impacts. Higher coefficients of friction were attributed to greater mechanical properties and higher consistency of the fibre in the refining zone. Lower bar activity further elucidated the nature of heterogeneity in the Springfield refiner, and was attributed to a combination of chip- or shive-induced null-impacts and a refining zone less densely packed with fibre material. Both refiners showed their highest bar activity in the middle of the plate segment, presumably near the stagnation point, which was attributed to an accumulation of fibre material.

Mean peak forces in Port Alberni increased with increasing radius while, in Springfield, mean peak normal forces slightly decreased with radius and shear forces were relatively constant throughout the refining zone. The difference in radial trends observed in Springfield and in Port Alberni are explained principally by the difference in mechanical properties of the captured wood material. Larger force impacts are expected from chips or intact wood segments such as shives than from refined pulp for a given plate gap. In Springfield, the transition from chip to pulp drives the radial trend while, in Port Alberni, the rejects fibre has already undergone a significant decrease in its mechanical properties. In this case, force levels are postulated to be determined by other factors such as the increase in tangential velocity of crossing bars or a reduction in gap caused by plate taper.

ACKNOWLEDGEMENTS

The authors gratefully acknowledge funding provided by the Natural Sciences and Engineering Research Council, Andritz Ltd. and Paprican; and access to experimental and commercial facilities provided by Andritz Ltd. and Catalyst Paper Corp. The authors would also like to thank John Senger for valuable discussions during the projects, Keith Miles for providing pulp-flow calculations and to Ingunn Omholt for support and discussion throughout the project and during the preparation of this paper. All are from FPInnovations - Paprican Division, Pointe Claire, QC, Canada.

REFERENCES

1. SABOURIN, M., WISEMAN, N. and VAUGHN, J., “Refining Theory Considerations for Assessing Pulp Properties in the Commercial Manufacture of TMP”, Proc. Appita 55th Ann. Gen. Conf., 1:195–204 (2001).
2. MURTON, K. and DUFFY, G., “The Influence of Pulp Residence Time on Refining Intensity and Pulp Quality”, *Appita J.* 58(1):64–71 (2005).
3. OUELLET, D., BENNINGTON, C.P.J. and POTKINS, D., “Wood Comminution and Material Flow in a Laboratory Chip Refiner”, *J. Pulp Paper Sci.* 21(12):415–421 (1995).
4. ALAHAUTALA, T., LASSILA, E., HERNBERG, R., HARKONEN, E. and VUORIO, P., “Optical Measurement of Pulp Quantity in a Rotating Disc Refiner”, *Measurements Sci. Technol.* 15(11):2256–2261 (2004).
5. SVENSSON, B.A., RUNDÖLF, M. and HOGLUND, H., “Sliding Friction Between Wood and Steel in a Saturated Steam Environment”, *J. Pulp Paper Sci.* 32(1):38–43 (2006).
6. SENGER, J. and OUELLET, D., “Factors Affecting the Shear Forces in High-Consistency Refining”, *J. Pulp Paper Sci.* 28(11):364–368 (2002).
7. SIADAT, A., BANKES, A., WILD, P.M., SENGER, J. and OUELLET, D., “Development of a Piezoelectric Force Sensor for a Chip Refiner”, Proc. Inst. Mech. Engin., Part E, *J. Proc. Mech. Engin.* 217:133–140 (2003).
8. SENGER, J., SIADAT, A., OUELLET, D. and WILD, P., “Measurement of Normal and Shear Forces During Refining Using a Piezoelectric Force Sensor”, Preprints Intl. Mech. Pulping Conf., PAPTAC, 403–407 (2003).
9. SENGER, J., OLMSTEAD, M., OUELLET, D. and WILD, P.M., “Measurement of Shear and Normal Forces in the Refining Zone of a TMP Refiner”, *J. Pulp Paper Sci.* 30(9):247–251 (2004).
10. GONCHAROV, V.N., "Force Factors in a Disk Refiner and their Effect on the Beating Process", *Bumazh. Promst.,* English Trans. 12(5):12–14 (1971).
11. GRADIN P.A., JOHANSSON, O., BERG, J.-E. and NYSTRÖM, S., “Measurement of the Power Distribution in a Single-Disc Refiner”, *J. Pulp Paper Sci.* 25(11):384–387 (1999).
12. BACKLUND, H.-O., HOGLUND, H. and GRADIN, P., “Study of Tangential Forces and Temperature Profiles in Commercial Refiners”, Preprints Intl. Mech. Pulping Conf., PAPTAC, 379–388 (2003).
13. SENGER, J., OUELLET, D., WILD, P.M., SABOURIN, M. and OLENDER, D., “A Technique to Measure Mean Residence Time in TMP Refiners Based on Inherent Process Fluctuations”, *J. Pulp Paper Sci.* 32(2):83–89 (2006).
14. PRAIRIE, B., WILD, P., BYRNES, P., OLENDER, D., FRANCIS, D.W. and OUELLET, D., “Forces During Bar-Passing Events in Low Consistency Refining: Effects of Refiner Tram”, Preprints 92nd Ann. Mtg., PAPTAC, B157–B160 (2005).
15. ATACK, D. and STATIONWALA, M.I., “On the Measurement of Temperature and Pressure in the Refining Zone of an Open Discharge Refiner”, *Trans. Tech. Sect., Can. Pulp Paper Assoc.* (3):71–76 (1975).
16. CAUCAL, G., CHAUSSY, D. and RENAUD, M., “Etude Physique et Hydraulique du Raffinage”, *Revue ATIP* 45(5):187–199 (1991).
17. NORDMAN, L., LEVLIN, J., MAKKONEN, T. and JOKISALO, H., “Conditions in an LC-Refiner as Observed by Physical Measurements”, *Paperi ja Puu* (4):169–180 (1981).
18. BERG, D. and KARLSTRÖM, A., “Dynamic Pressure Measurements in Full-Scale Thermomechanical Pulp Refiners”, Proc. Intl. Mech. Pulping Conf., PTF, Oslo, Norway, 42–49 (2005).
19. ERIKSEN, O., “Diagnosis of a First-Stage Mill-Scale TMP Refiner by Means of Refining Zone Pressure and Temperature Measurements and Blow-Line Pulp Analysis”, Preprints Intl. Mech. Pulping Conf., PAPTAC, 389–398 (2003).
20. ERIKSEN, O., GREGERSON, Ø. and KROGSTAD, P.-Å., “High-Speed Measurements of Pressure and Temperature in the Refining Zone of a High-Consistency Refiner”, *Nordic Pulp Paper Res. J.* 20(4):459–467 (2005).

21. ERIKSEN, O., GREGERSON, Ø. and KROGSTAD, P.-Å., “Pressure and Vibration in the Refining Zone of a TMP Refiner – Influence of the Fibre Flow”, *Nordic Pulp Paper Res. J.* 21(1) (2006).
22. DOEBELIN, E., Measurement Systems: Application and Design, 5th ed., McGraw-Hill Publishing Co., New York, NY, USA (2003).
23. SYSTAT Software, Sigmaplot 9.0 User’s Manual, San Jose, CA, USA (2004).
24. ATACK, D., STATIONWALA, M.I. and KARNIS, A., “What Happens in Refining”, *Pulp Paper Can.* 85(2):303–308 (1984).
25. GIERTZ, H.W., “A New Way to Look at the Beating Process”, *Norsk Skogindustri* 18(7):239–248 (1964).
26. MAYADE, T.L., “Statistical Theory of Chemical Pulp Refining – An Innovative Combined Approach”, *Appita J.* 50(3):237–244 (1997).
27. MILES, K.B. and MAY, W.D., “The Flow of Pulp in Chip Refiners”, *J. Pulp Paper Sci.* 16(2):63–72 (1990).
28. SABOURIN, M., AICHINGER, J. and WISEMAN, N., “Effect of Increasing Wood Chip Defibration on Thermomechanical and Chemi-Thermomechanical Refining Efficiency”, Preprints Intl. Mech. Pulping Conf., PAPTAC, 163–170 (2003).
29. STATIONWALA, M.I., ATACK, D. and KARNIS, A., “Distribution and Motion of Pulp Fibres on Refiner Bar Surface”, *J. Pulp Paper Sci.* 18(4):131–137 (1992).
30. HARKONEN, E., RUOTTU, A. and JOHANSSON, O., “A Theoretical Model for a TMP Refiner”, Proc. Intl. Mech. Pulping Conf., SPCI, Stockholm, Sweden, 95–101 (1997).

REFERENCE: OLENDER, D., WILD, P., BYRNES, P., OUELLET, D. and SABOURIN, M., Forces on Bars in High-Consistency Mill-Scale Refiners: Trends in Primary and Rejects Stage Refiners, Journal of Pulp and Paper Science, 33(3):XXX-XXX July/August/September 2007. Paper presented at the 93rd Annual Meeting of the Pulp and Paper Technical Association of Canada, February 5-8, 2007. Not to be reproduced without permission from the Pulp and Paper Technical Association of Canada. Manuscript received December 4, 2006; revised manuscript approved for publication by the Review Panel June 27, 2007.
KEYWORDS: To come from Glen

Appendix C

Forces on Bars in High-Consistency Mill-Scale Refiners: Effect of Consistency

(Under review, Journal of Pulp and Paper Science)

Forces on Bars in High-Consistency Mill-Scale Refiners: Effect of Consistency

D. Olender[1*], P. Wild[1], P. Byrnes[2], D. Ouellet[3†], and M. Sabourin[4]

[1.]Department of Mechanical Engineering, University of Victoria, PO Box 3055 Victoria, BC, V8W 3P6, Canada
[2.]Herzberg Institute of Astrophysics, Victoria, BC, Canada
[3.]FPInnovations – Paprican, Vancouver BC, Canada
[4.]Andritz Inc., Springfield, OH, USA

[*]Corresponding author (dolender@uvic.ca)
[†]Now with Novadaq Technologies, Richmond, BC, Canada

Abstract

Past laboratory experiments in a single-bar refiner have shown that pulp consistency in the thermomechanical pulping process can greatly affect the contact mechanics of bar-crossing impacts. The effect was observed as a change in magnitude of the shear force in the recorded impact, and quantified using the equivalent tangential coefficient of friction μ_{teq}. A positive correlation between μ_{teq} and the mass fraction of fibre to water, known as the consistency, was found above a certain threshold consistency. In the present work, arrays of piezo-based sensors capable of measuring normal and shear forces on bars were installed in two high-consistency refiners, in two separate trials. In the first trial, a pilot-scale machine was instrumented and operated as a primary stage. The second trial took place at a mill, where the instrumented refiner was operating as a rejects stage. An increase in refining consistency in the primary refiner, measured at the discharge, was observed to cause an increase in μ_{teq} near the refining zone entrance. No significant changes in μ_{teq} were observed in the rejects refiner, but only a small range of consistencies could be tested. These initial findings suggest

relationships found in past laboratory tests in a single-bar refiner may translate to larger-scale equipment.

Keywords

bar forces, consistency, refiner, mechanical, TMP, pulp, sensor, piezo

Introduction

The contact mechanics that arise during bar-crossing impacts are responsible for inducing the stresses, and corresponding strains, that develop raw wood fibre into useful papermaking pulp. Enhancing our knowledge of the interactions that make up these impacts, and how they are affected by process variables, is therefore a necessary step to advancing refiner technology. Experiments by Senger and Ouellet [1] involving individual fibre bundles, or flocs, in a single-bar refiner have indicated that bar forces are dependent on floc consistency, floc grammage and bar edge sharpness. These results offered insight into previously unexplainable behavior, but investigation of these relationships in mill-scale refiners was restricted by lack of available measurement technology. This investigation is now possible with the development of a refiner force sensor (RFS) that replaces a small segment of refiner bar, and is capable of measuring normal and shear forces experienced during individual bar-crossing impacts. Bar forces from RFS tests in one pilot-scale and one mill-scale refiner under nominal operation have already been reported [2]. During the same installations, consistency within the refining zone was also varied in individual experiments. The principal goal of this work is to report on the effects of refining consistency on recorded bar forces in these two trials.

Goncharov *et al.* [3] first measured the rapid spike in force encountered as crossing bars meet in low-consistency refining. This *ploughing force* component creates an asymmetry in the recorded bar-crossing force profile, with higher forces associated with the initial part of the bar-crossing. The authors recognized this force as the primary driver of pulp quality. Senger and Ouellet [1] recently renewed interest in the shear forces encountered at bar edges, recognizing that they are directly responsible for working captured fibres. In investigating these shear forces, they define the equivalent tangential coefficient of friction, μ_{teq}, as the ratio of average shear force to average normal force during a bar-crossing impact. This definition emphasizes that the shear force is not solely a linear friction component of the normal force, but also contains a significant ploughing force component. During their tests in a single-bar refiner, the authors observed a dependency in μ_{teq} only when floc consistencies were increased above approximately 35 %. Above this value, μ_{teq} was found to increase with increasing floc consistency. Senger and Ouellet note that this consistency matches the discharge consistency reported [4, 5] to induce a new energy-quality relationship in tests involving mill-scale refiners. Senger and Ouellet also demonstrated that bar wear and floc thickness have a pronounced effect on μ_{teq}.

Researchers have since attempted to measure the forces on bars in operating refiners. Backlund [6] used a converted commercial force sensor that replaces a circular section spanning multiple-bars to measure shear forces. In tests where dilution flow rate was varied, it was found that the sensor positioned closest to the rotational axis of the refiner was the most sensitive.

Prior to these trials, the most recent successful recording of forces in high-consistency refining using the RFS took place in a pilot-scale refiner [7]. Although no attempts were made to vary consistency during these tests, the asymmetry of the recorded force profile due to ploughing was clearly visible. This characteristic profile has also been found in RFS tests in low-consistency refining [8]. In the current research, the latest generation RFS were installed in two high-consistency, single-disc refiners in separate field trials. Tests were conducted in a 36 in. (914 mm) pressurized refiner, processing chips at the Andritz Pilot Plant, in Springfield, Ohio, and in a 45 in. (1143 mm) rejects refiner at a Catalyst Paper Corp. mill, in Port Alberni, BC. Refining consistency in both trials was varied by altering the flow rate of the dilution water, and also, in the case of Port Alberni, by varying the pressure developed in the dewatering press. A range of discharge consistencies between 20-55% was found in the primary stage refiner, while the best measurement of the range was between 20-27% in the rejects refiner. Experiments considered in this study were performed over a two-day period in the primary stage refiner, and over a single day in the operational rejects refiner.

Experimental

An earlier companion report [2] has already detailed the installation process in Springfield and Port Alberni, including photographs of sensor locations within the instrumented plate, as well as the plate pattern and relevant dimensions. In brief, the array of sensors installed in each refiner were labelled S1, S2 and S3 in both trials, and were located at increasing radii, respectively, within the refining zone. S1 was the innermost sensor, while S3 was located in the outer region of the plate.

The trial in Port Alberni took place over the entire life of a set of plates, and represented an opportunity to measure the effects of bar wear on μ_{teq}. Unfortunately, although all the RFS probes were worn to the same height as surrounding bar, they experienced accelerated rounding of their leading edge. Photographs of the sensors before and after the trial are presented and discussed in a separate report [9]. Accelerated wear of the probes was expected, as the stainless steel used in their manufacture was considerably softer than the nickel-hardened plate material. For this reason, only the sensor data from the trial immediately following the installation of the sensors, when rounding would have been negligible, is considered.

Springfield and Port Alberni Trials

During the trials in Springfield and Port Alberni, all experiments were enumerated in chronological order. The enumeration scheme used in this report continues from the previous report [2].

The setup and experiments in Springfield took place over one week in early January 2005. Table 1 lists the process conditions of the experiments considered in this work. In these experiments, dilution flow rates were varied between 5 and 11 USGPM (19 and 42 l/m). At each dilution flow rate, two motor loads were targeted: 650 and 800 kW. After reaching equilibrium in each case, process conditions were held constant for between 15 to 30 s to allow a representative force signal and pulp sample to be acquired. The casing environment was held constant at a gauge pressure of 3.5 bar (350 kPa) and temperature of 148 ºC. The refiner was run at a constant speed of 1900 rpm in hold-back mode during all tests. Hold-back mode is defined by the direction of rotor spin that causes crossing bars to scissor radially inward. Spruce wood chips, having a moisture content of 48.6%, were used. Retention in pre-steaming tube was 120 s at a gauge pressure of 1 bar (100 kPa).

Table 1: List of Springfield experiments.

Sample ID	Target Motor Load (kW)	Actual Motor Load (kW)	Dilution Flow Rate USGPM (l/m)	Specific Energy (kWh/t)	Plate Gap (mm)	Discharge Consistency (%)
A1	650	653	5 (19)	725	0.64	42.8
A2	800	794	5 (19)	899	0.36	54.9
A3	800	890	7 (27)	1018	0.36	44.2
A4	650	670	7 (27)	746	0.66	35.7
A5	650	639	9 (34)	708	0.89	27.1
A6	800	800	9 (34)	899	-	30.9
A7	800	834	11 (42)	949	0.86	25.2
A8	650	665	11 (42)	740	1.47	22.4
A9	650	616	9 (34)	679	1.19	27.0
A10	800	829	9 (34)	943	0.69	31.1
A11	800	800	7 (27)	932	-	37.7
A12	650	650	7 (27)	721	0.81	34.1
A13	650	642	5 (19)	711	0.64	46.4
A14	800	817	5 (19)	928	0.41	53.8

It is worth noting that during the Springfield experiments, the gap increased with increasing dilution water, which is non-standard behavior. This implies that an increase in the water content between the plates caused more fibre material to flow into the refining zone, and as a result, it was necessary to increase the gap to maintain the same motor load. Mill-scale refiners typically exhibit the reverse relationship, where gap decreases with an increase in dilution water [4].

The trial in Port Alberni took place over a three-month period, starting in September and finishing in November of 2005. Following installation of the plate segment, a first trial consisting of two experiments was performed and for the reasons noted above, is the focus of this work. In these two experiments, dilution flow rate and the pressure developed in the dewatering press were varied, while keeping other process variables constant, as shown in Table 2. Production rate was held constant at approximately 60 odmt/d, and motor load at 3 MW. Once process conditions were stabilized, settings were held for approximately three minutes, as forces were recorded, and inlet and discharge pulp samples were taken. Inlet samples were taken following the dewatering press, prior to entering the refiner.

Table 2: List of Port Alberni experiments.

Sample ID	Dilution Flow Rate USGPM | (l/m)	Pressure in De-watering Press (psig)	Inlet Consistency (%)
A9	5 (19)	1500	26.4
A10		1600	28.1
A11		1700	29.3
A12		1800	29.4
A13	3 (11)	1700	29.8
A14	4.3 (16)		29.8
A15	5.6 (21)		29.1
A16	7 (27)		28.5

No measurements of discharge consistency were taken from the samples recovered in the first Port Alberni trial, but measurements were taken during a later trial, which used the same operating conditions. Values of discharge consistency in the later trial ranged from 20 to 27 % over the experiments. The historical average discharge consistency for the reject refiner under study is 33 %.

Signal Conditioning and Processing Techniques

The conditioning steps used to convert the two voltages from the RFS into normal and shear force signals are detailed in the previous report of these trials [2]. The same steps were taken in the analysis of these experiments. In brief, the voltages were first transformed into forces, using the method of superposition described elsewhere [10]. Secondly, the force signals were filtered to remove any magnitude distortion associated with operating near the RFS first natural frequency. Lastly, the signals were compensated for the loss of low-frequency components associated with piezoelectric transducer systems. This last step included inverse-filtering, and a final manual offset, which assumed the minima, or valleys of the force signals, are an accurate zero reference.

As detailed in the previous report [2], software was written to identify and record individual bar-crossing impacts. Impact parameters, such as peak forces and μ_{teq} were also catalogued. Impacts with a normal force below the 0.2 N system threshold (referred to as “low threshold” data in the following sections) were discarded. It was also recognized early on that very high-force impacts were of interest, as will be presented, and these impacts were segregated from the main data set. To achieve this, impacts with very high forces were isolated using a high-force threshold (referred to as “high threshold” data). These high-force data sets contained less than 5 % of the total number of recorded impacts in each sample.

The averages reported in this work are based on data processed from three 5-second intervals spaced evenly throughout each experiment. Sigmaplot® 9.0 [11] graphing software was used to perform all regressions. S1 data for samples A2, A3 and A4 in Springfield were of poor quality, possibly due to a plate clash, and are not included.

Results

Force Profiles

As noted, the ploughing force that occurs as crossing bars meet creates an asymmetry in the recorded bar-crossing force profile, with higher forces associated with the initial part of the bar-crossing. Bar force measurements in past RFS trials have shown this asymmetry [7, 8] and profiles in both these trials have also shown this asymmetry. It was this characteristic shape of the profile that was used as one indicator of the successful performance of the RFS [9]. In the current work, an example of the ploughing force asymmetry is shown in Figure 2. It should be noted that the classification software mentioned in the previous section selects the highest peak in the profile for characterization, and thus naturally selects the ploughing force peak. In this case, the ploughing force peaks are approximated by the bar-crossing period dashed lines.

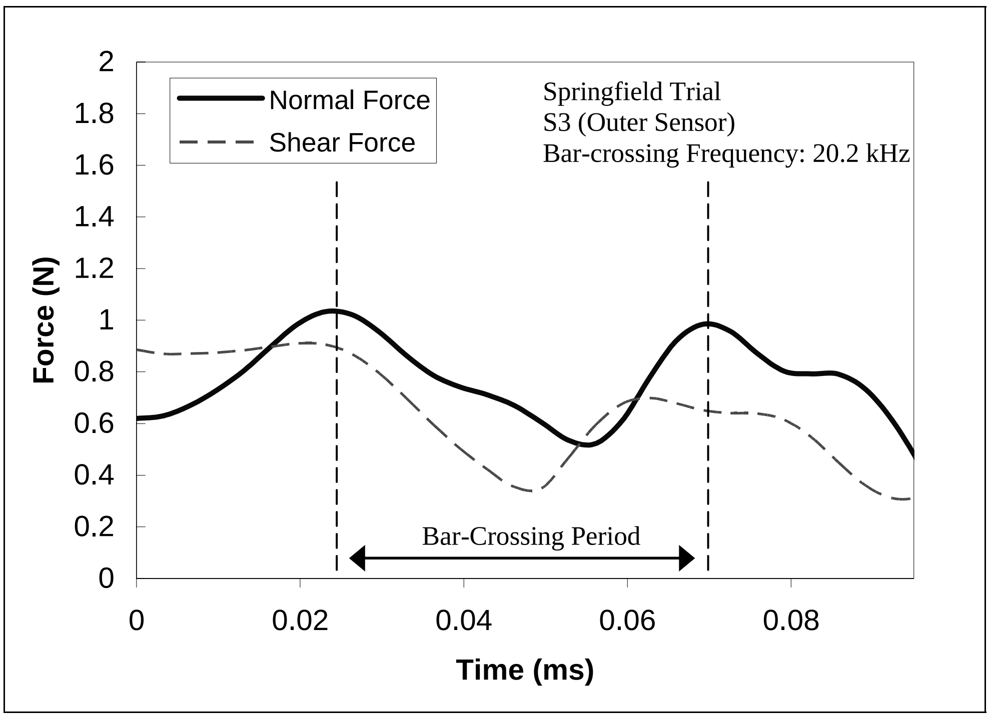

Figure 2: Close-up of force profiles from outer sensor S3 in Springfield. Characteristic asymmetry attributed to ploughing force is visible in both impacts.

Springfield Trial

Figures 3, 4 and 5 present mean μ_{teq} recorded by sensors S1, S2 and S3, respectively, for all Springfield experiments listed in Table 1. Results using both low and high threshold settings are included. All three sensors show an increase in μ_{teq} with increasing consistency at the high threshold, but only the inner sensor S1 shows this relationship at the low threshold. Values of` μ_{teq} at the high threshold are also observed to be lower than those found using the low threshold in both S1 and S3.

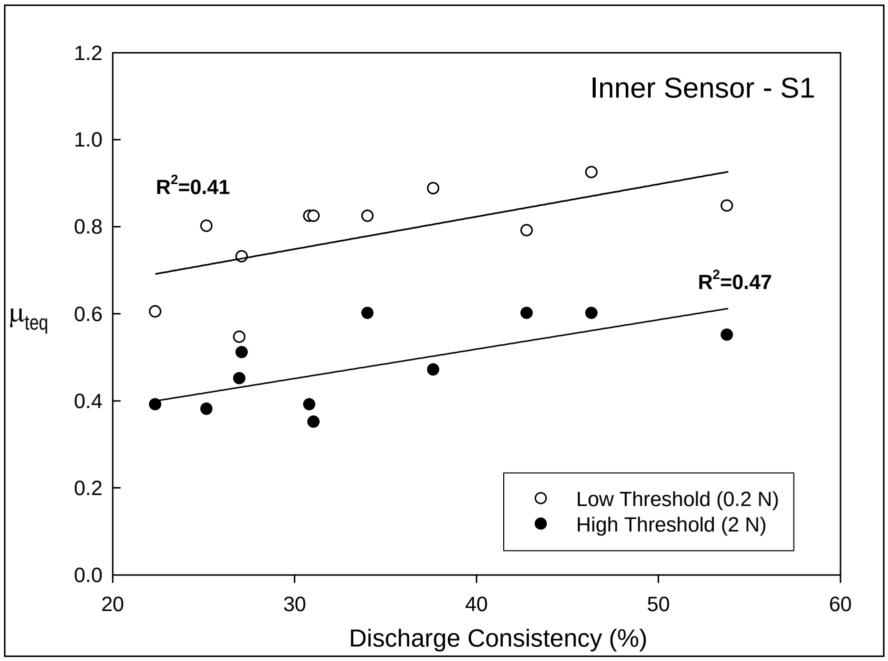

Figure 6.1: Effect of discharge consistency on μ_{teq}, measured by inner sensor S1 in Springfield.

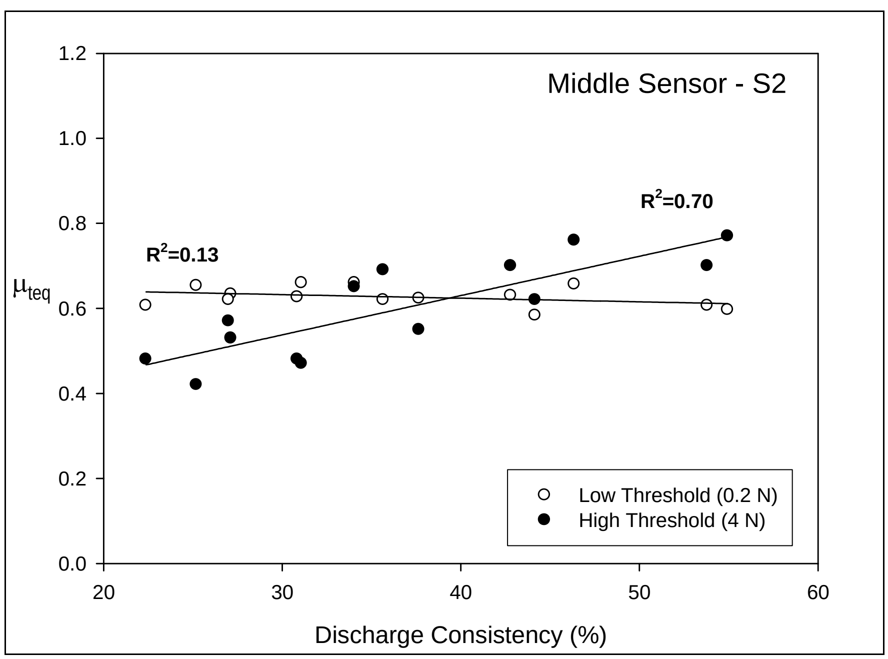

Figure 6.2: Effect of discharge consistency on μ_{teq}, measured by middle sensor S2 in Springfield.

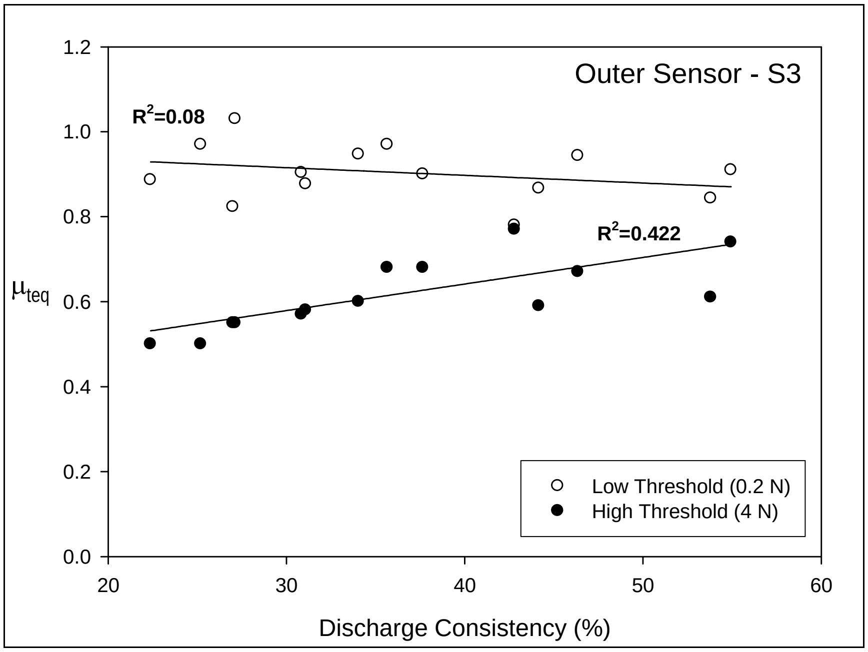

Figure 5: Effect of discharge consistency on μ_{teq}, measured by outer sensor S3 in Springfield.

Figure 6 is a plot of the mean normal and shear forces recorded by sensor S1 at the low threshold. It is observed that the trend in μ_{teq}, shown in Figure 2, is primarily caused by a drop in normal force. Figure 7 is a plot of the mean normal and shear forces recorded by sensor S1 at the high threshold. In this plot it is observed that the increase in μ_{teq}, shown in Figure 4, is caused by a rise in shear force with increasing discharge consistency. A rise in shear force with discharge consistency is also responsible for the observed increase in μ_{teq} at the high threshold setting for sensors S2 and S3. Mean normal force levels for the inner, middle and outer sensors were, respectively, 1.38 N, 1.52 N, and 0.93 N. Listed in the same sensor order, mean shear force levels were 0.78 N, 0.86 N, and 0.75 N.

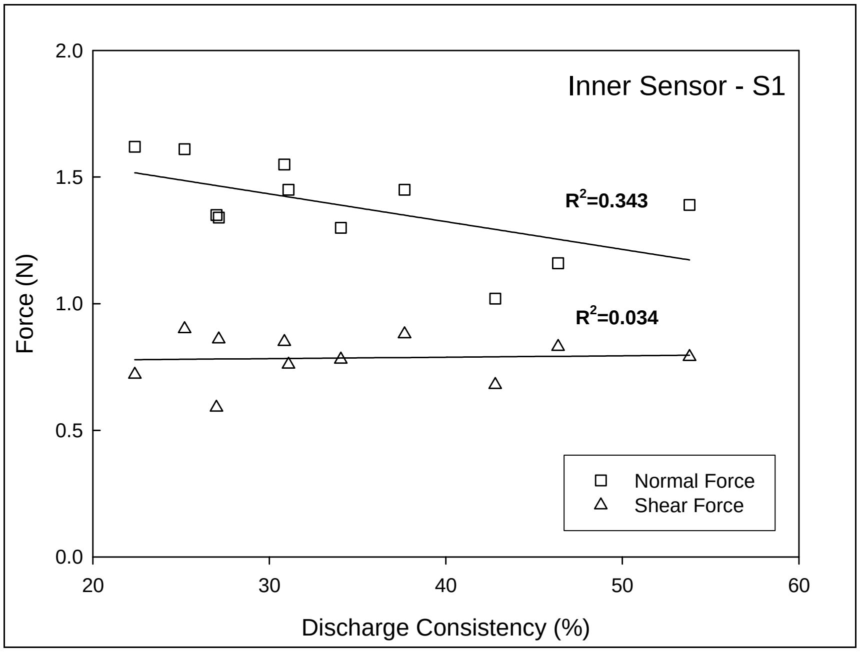

Figure 5: Effect of discharge consistency on mean forces recorded by inner sensor S1 in Springfield. Results were processed using the low threshold.

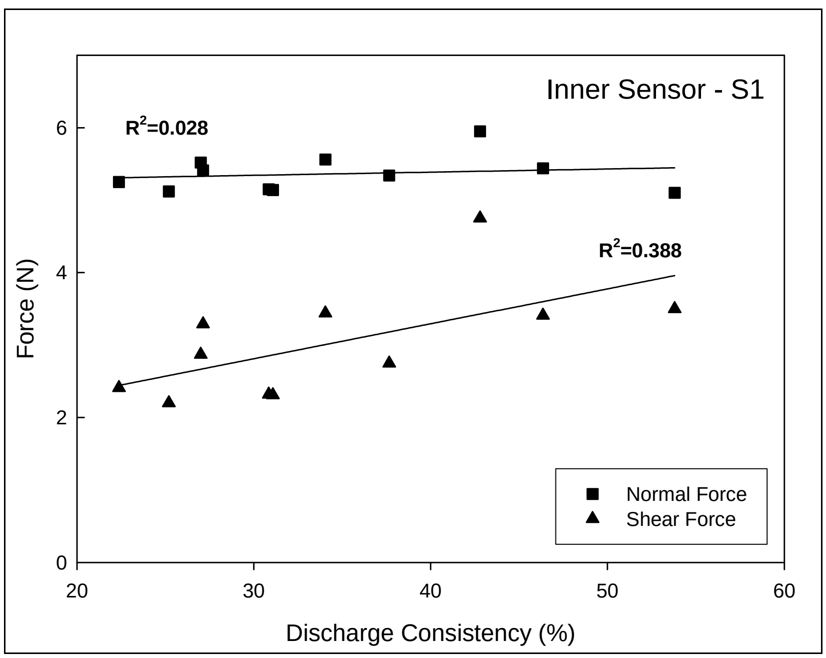

Figure 6: Effect of discharge consistency on mean forces recorded by inner sensor S1 in Springfield. Results were processed using the high threshold.

Figure 8 plots mean values of μ_{teq} at the inner sensor with discharge consistency for the low threshold setting, but in this case separates the experiments by low and high motor loads. As seen in this figure, μ_{teq} at the low motor loads is observed to be more sensitive to the effects of consistency and records a higher coefficient of determination. This effect was not observed in the middle and outer sensors.

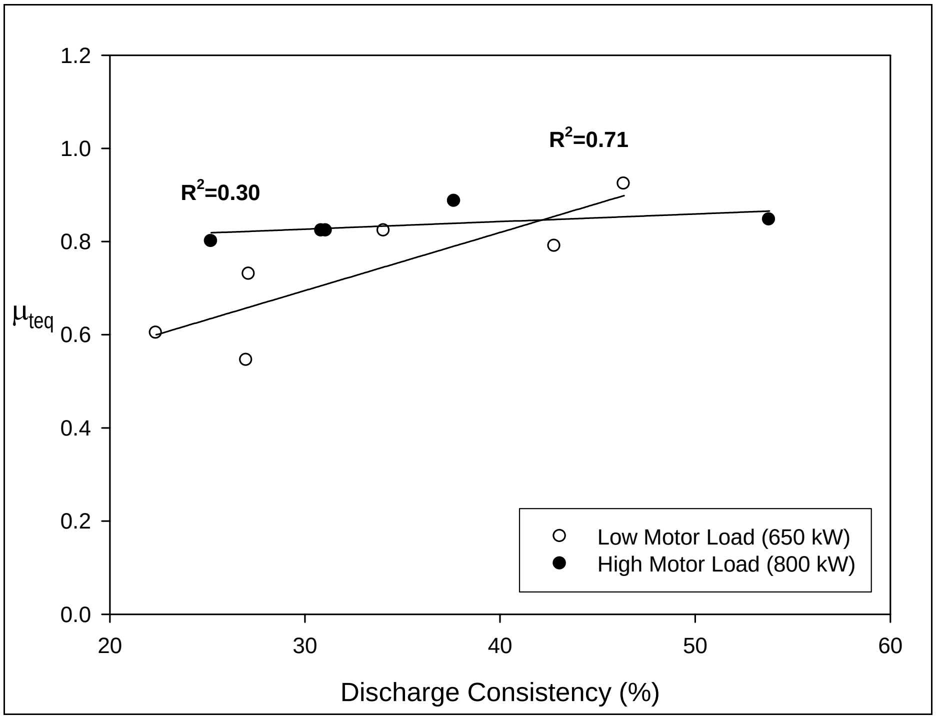

Figure 7: Additional motor load effect on mean values of μ_{teq} for the inner sensor S1 at low threshold. Low and high motor load experiments have been isolated and separate regressions performed.

Port Alberni Trial

Over the operating conditions tested, the sensors in Port Alberni measured no significant change in μ_{teq} at either threshold setting. Mean values and standard deviations of μ_{teq} at the low threshold were 0.34±0.006, 0.64±0.015, and 0.53±0.017 for S1, S2 and S3, respectively. As mentioned previously, a measurement of discharge consistency was not performed on samples from the first trial, but was at a later date at the same operating conditions. This sampling took place on November 17, 2005, which was within one week of failure of the plates. Discharge consistencies measured in these samples ranged from 20 to 27 %.

Discussion

The measured values of μ_{teq}, which ranged from approximately 0.3 to 1.1, were near those reported in previous findings [6, 7]. Also worth noting is that the characteristic asymmetry found in past measurements of bar forces, which is due to the ploughing of flocs as crossing bars meet, has been found at the mill-scale. This finding supports the ploughing phenomenon as significant, and one worth further study.

Senger and Ouellet [1] observed that an increase in consistency of a floc trapped between crossing bars leads to an increase in μ_{teq} during the impact, but this effect was only observed at consistencies above 35 %. The authors relate this behaviour to the ploughing component of friction. The shear force required to plough through a floc will increase with an increase in inter-fibre friction, which is dependent on the amount of water in the floc. This increase in μ_{teq} was more pronounced with higher grammage (thicker) flocs subjected to the same normal force. In this case, the higher grammage flocs have more fibres in front of the crossing bar, and thus require a larger ploughing force to allow the floc to pass between crossing bars. It was proposed that these higher grammage interactions are therefore more sensitive to consistency based on the increased quantity of fibre between the bars.

The results of the current work support many elements of this hypothesis in mill-scale refiners. The measurements taken in Springfield by sensor S1 show that impacts in the inner region of the refining zone experienced an increase in μ_{teq} with increasing consistency. As the Springfield refiner was processing chips, the inner sensor would encounter more intact wood segments, such as shives. One hypothesis is that impacts which capture this less processed material show a higher sensitivity to changes in dilution flow, which is analogous to the floc thickness effect found by Senger and Ouellet. A further factor could be the location of the dilution water injection. Backlund [6] also found that forces recorded in the inner region of the refining zone were the most sensitive to changes in dilution flow rates, but he observed the opposite correlation. No explanation was given for this behaviour by the author. The positive correlation between μ_{teq} in higher force impacts and consistency, which was found in all sensors, is also consistent with the effect of floc thickness proposed by Senger and Ouellet; one would expect higher-force impacts to be associated with the capture of thicker flocs.

As shown in Figure 6, the increase in μ_{teq} recorded by the inner sensor at the low threshold is driven by a drop in normal force. Senger and Ouellet performed their tests over similar ranges of normal forces, and found that the recorded trends in μ_{teq} were primarily driven by an increase in the magnitude of the shear force. These findings therefore contradict this earlier work on this point. One possible explanation could be that the laboratory experiments were performed at constant gap, while these tests were performed at constant motor load. This implies that these tests were performed at constant shear load. This behaviour stands in contrast to the high threshold findings, which for all sensors showed the expected result: an increase in μ_{teq} was caused principally by a rise in the shear force.

A further point of interest is the effect of motor load on the inner sensor's recorded increase in μ_{teq} at the low threshold setting. As shown in Figure 8, by isolating the low and high motor load experiments it is clear that the low motor load experiments drive the relationship with μ_{teq}, showing a higher degree of positive correlation with changes in consistency. Physical interpretation on this point is reserved until more data can be collected.

The lack of any significant change in μ_{teq} in Port Alberni is not unexpected. The best available measurements of discharge consistencies encountered in this trial were below the 35 % threshold discovered by Senger and Ouellet known to affect μ_{teq}. Although the measured values of discharge consistency are lower than anticipated, it is known that the discharge consistency of the refiner under study has a historical average (since 2003) of 33 %; this discharge consistency is slightly lower than the other two reject refiners used at the mill, which process the same material. Further speculation as to the observed insensitivity of μ_{teq} in Port Alberni may also be related to the small range of consistencies explored.

Conclusions

Bar force measurements were made by dual-axis sensors in the refining zones of two high-consistency refiners in separate field campaigns. Sensors were installed and tests were conducted in a 36 in. (914 mm) pressurized refiner, processing chips at the Andritz Pilot Plant, in Springfield, Ohio, and in a 45 in. (1143 mm) rejects refiner at a Catalyst Paper Corp. mill, in Port Alberni, BC. Variation of refining consistency was accomplished by altering dilution flow rates in both refiners. In the case of the rejects refiner the pressure developed in the dewatering press, which controls the consistency of incoming pulp, was also varied in a separate experiment.

Software was used to catalogue many thousands of individual bar-crossing impacts during each experiment condition from which a mean μ_{teq} could then be calculated. Mean values of μ_{teq} calculated solely from higher force impacts, which made up less than 5 % of total recorded impacts, were also explored.

Measured values of μ_{teq}, which ranged from approximately 0.3 to 1.1, where consistent with those reported in previous findings. Further, the characteristic asymmetry found in past measurements of bar forces has also been found in mill-scale refiners, promoting the ploughing force as significant, and one worth further study.

The findings of these experiments can generally be attributed to the relationships observed in laboratory work in a single-bar refiner. An increase in discharge consistency from approximately 20 – 55 % in the primary stage refiner caused an increase in μ_{teq}, but only in the innermost sensor. The hypothesis offered for this behavior was that less processed wood material, such as shives, is more sensitive to changes in water content, and also more likely to appear in the inner part of the refining zone. This effect would be analogous to the effect of floc thickness observed in the laboratory. An increase in μ_{teq} with discharge consistency for the middle and outer sensors was not observed in most impacts, except for those few with very high forces. High force impacts in the inner sensor also showed this trend. The sensitivity of high force impacts to consistency was further attributed to the floc thickness effect, as these high-force impacts likely involve the capture of thicker material.

The trends in μ_{teq} at the inner sensor over the bulk of the impacts were shown to be caused by a drop in normal force, which was contrary to laboratory experiments. This is explained by the fact that the laboratory experiments were performed at constant gap, while these tests were performed at constant load, which implies a constant shear force. It was also noted that μ_{teq} was more strongly correlated with consistency at lower motor loads. No explanation for this behavior is currently given, and it is hoped further experimentation will provide an answer. In contrast, the increase in μ_{teq} in the higher force impacts behaved as expected. These trends were driven by a rise in shear force and attributed to an increase in the ploughing force.

In the Port Alberni trial, no significant change in μ_{teq} was observed over the tests and this was the result predicted by laboratory experiments. Although no measurements of discharge consistency were taken, the range of consistencies explored would be near the range, below 35 %, where μ_{teq} was observed in laboratory experiments to be insensitive to changes in consistency. The small range of explored consistencies also likely contributed to the observed insensitivity in Port Alberni.

Acknowledgements

The authors gratefully acknowledge funding provided by the Natural Sciences and Engineering Research Council, Andritz Ltd., and FP Innovations - Paprican Division; and access to experimental and commercial facilities provided by Andritz Ltd., and Catalyst Paper Corp.. The authors would also like to thank John Senger for valuable discussions during the campaigns and to Ingunn Omholt for support and discussion throughout the project.

References

[1] SENGER, J., AND D. OUELLET, “Factors Affecting the Shear Forces in High-consistency Refining,” J. Pulp Paper Sci., 28(11):364 – 368 (2002).

[2] OLENDER, D., WILD, P., BYRNES, P., OUELLET, D. AND M. SABOURIN, “Forces on Bars in High-Consistency Mill-Scale Refiners: Trends in Primary and Rejects Stage Refiners,” J. Pulp Paper Sci., 33(3):163-171(2007).

[3] GONCHAROV, V.N., "Force Factors in a Disk Refiner and their Effect on the Beating Process," Bumazh. Promst. English Trans., 12(5):12-14 (1971).

[4] MURTON, K.D., “Effect of primary stage consistency on TMP pulp quality and energy consumption,” 51st Appita Annual General Meeting, s.1.:87-94 (1997).

[5] ALAMI, R., BOILEAU, I., HARRIS, G., LACHAUME, J., KARNIS, A., MILES, K.B., AND A. ROCHE, “Impact of refining intensity on energy reduction in commercial scale refiners: effect of primary stage consistency,” Tappi J., 80(1):185-193 (1997).

[6] BACKLUND, H.-O., “Measurement of shear force, temperature profiles and fibre development in mill-scale TMP refiners,” PhD Thesis, Mid Sweden University (2004).

[7] SENGER, J., OLMSTEAD, M., OUELLET, D. AND P.M.WILD, “Measurement of Shear and Normal Forces in the Refining Zone of a TMP Refiner,” J. Pulp Paper Sci., 30(9):247-251 (2004).

[8] PRAIRIE, B., WILD, P., BYRNES, B., OLENDER, D., FRANCIS, B., AND D. OUELLET, “Forces During Bar-Passing Events in Low-Consistency Refining: Distributions and Relationships to Specific Edge Load,” In press, J. Pulp Paper Sci. (2008).

[9] OLENDER, D. WILD, P., and P. BYRNES, “A Piezo-Electric Force Sensor for Mill-Scale Chip Refiners,” Under review, Proc. IMechE, Part E, Journal of Process Mechanical Engineering.

[10] SIADAT, A., BANKES, A., WILD, P.M., SENGER, J., AND D. OUELLET, “Development of a Piezoelectric Force Sensor for a Chip Refiner,” Proc. IMechE, Part E, Journal of Process Mechanical Engineering, 217:133-140 (2003).

[11] SYSTAT SOFTWARE, “Sigmaplot 9.0 User’s Manual,” ISBN: 1568272510, 852 pages (2004).

Appendix D

Refiner Plate Clash Detection Using an Embedded Force Sensor

(Published, Nordic Pulp and Paper Research Journal, 2007)

Refiner plate clash detection using an embedded force sensor

Dustin Olender, **Paul Francescutti** and **Peter Wild**, University of Victoria, **Peter Byrnes**, Herzberg Institute of Astrophysics, Victoria, Canada

KEYWORDS: Clash, Pad-collapse, Refiner, Mechanical, TMP, Pulp, Sensor, Piezo

SUMMARY: Plate clash in disc refiners continues to detract from the efficiency of mills, reducing plate life and affecting production. The work presented here examines the potential of a piezoelectric-based force sensor for clash prediction. Four sensors were installed in an operational rejects refiner over a three-month period at the Catalyst Paper Corp. mill in Port Alberni, B.C., Canada. Signals from these sensors were processed for prediction of plate clash and the results were compared to the accelerometer-based plate protection system currently in use at the mill. The force sensors consistently gave advanced warning of a clash event, many seconds before the accelerometer. A sensitivity study showed that the new system was able to outperform the accelerometer system over a range of detection settings, and that the accelerometer could not be tuned to match the performance of the new system.

ADDRESSES OF THE AUTHORS: **Dustin Olender** (dolender@uvic.ca), **Paul Francescutti** (pfrances@engr.uvic.ca) and **Peter Wild** (pwild@uvic.ca): University of Victoria, Department of Mechanical Engineering, P.O. Box 3055 STN CSC, V8W 3P6, Victoria, BC, Canada. **Peter Byrnes** (peter.byrnes@nrc-cnrc.gc.ca): Herzberg Institute of Astrophysics, Astronomy Technology Research Group, 5071 West Saanich Rd., V9E 2E7, Victoria, BC, Canada.
Corresponding author: Dustin Olender

Plate clash occurs when the gap between refiner plates is reduced to zero. The resulting metal-to-metal contact causes large forces between the bars on these plates, accelerating wear and disrupting operation (Allison et al. 1995, Dumont, Astrom 1988). This destructive event is thought to be caused by the breakdown of the pulp pad between the refiner plates, and is sometimes called “pad collapse”. The exact mechanisms that induce pad collapse are unknown, but disruptions in pulp flow caused by back-flowing steam are often blamed (Allison et al. 1995). Variations of forces in the refining zone could be associated with such a breakdown of the pulp pad. These variations could be used to detect an imminent plate clash and then trigger a reduction of the load on the refiner plates to prevent the clash. Current plate protection systems rely on gap sensors or vibration monitors to detect the onset of clashes. While these devices have proven useful, they do not consistently prevent plate clash (Dumont, Astrom 1988). The importance of a reliable and effective plate protection system lies in its ability to extend refiner plate life and produce uniform pulp quality (Jack et al. 1981). Accordingly, the goal of this work is to evaluate the potential of a force sensor to predict clash events.

Past efforts to detect clashes include the system currently used in the Port Alberni reject refiners. This method was first developed and tested in 1977 (Rogers, Butler 1977). The system is based on the measurement of vibrations in the refiner body. It was found that a range of vibrational frequencies showed an increase in amplitude prior to, and during, a plate clash (Jack et al. 1981). An accelerometer-based system is used to monitor this frequency range and warn of an impending clash if an increase in the amplitude of vibration is detected. Another system that uses information gathered from an accelerometer was developed by Whyte (Whyte 1986). Whyte’s method detects a drop in vibrational amplitude associated with a reduction in the flow of pulp between refiner plates prior to clash. A third clash detection system was developed by Brenholdt (Brenholdt 1997). This system measures electrostatic discharges through the refiner caused by impacts of charged particles in the pulp. Electric impulses are measured directly from the refiner body and have been successfully correlated to pulp properties and gap width.

In the work presented here, four piezo-electric force sensors, known as Refiner Force Sensors (RFS), were installed in an operational rejects refiner at a Catalyst Paper Corp. mill in Port Alberni, B.C, Canada. Trials were carried out at regular intervals over the three month installation, each trial consisting of a set of controlled experiments. The sensors used in these trials were the fourth generation of sensor described in previous work (Siadat et al. 2003). The sensors each contain two piezoelectric elements and a thermocouple, and replace a short (5 mm) segment of bar in the refiner plate segment. The sensors are capable of measuring the normal and shear forces experienced by pulp during bar-crossing impacts. High sampling rates are necessary to resolve these impacts, whose durations are on the order of microseconds. However, the resulting force signals also contain information regarding larger timescale phenomena, such as the flow of pulp in the refining zone (Senger et al. 2006). Signals from the RFS could therefore contain information regarding process fluctuations associated with plate clash.

Current plate protection system

The plate protection system in use on the Port Alberni refiners is based on the signal from an accelerometer mounted on the outboard bearing block of the refiner. The accelerometer signal is conditioned to produce a plot of the amplitude of vibration in a frequency range known to be associated with clashes (Jack et al. 1981). An impending clash is detected using two alarm types. The first alarm type, *Alert*, is triggered when the acceleration exceeds a specified *static threshold*. The second alarm type, Danger, is triggered when the acceleration exceeds a *dynamic threshold*. This dynamic threshold is based on

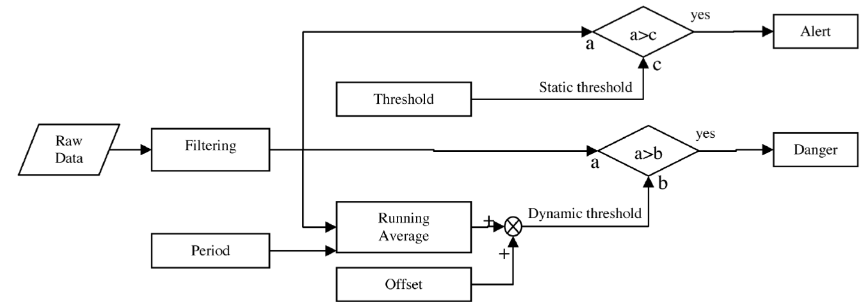

Fig 1. Accelerometer *Danger* and *Alert* alarm detection methods.

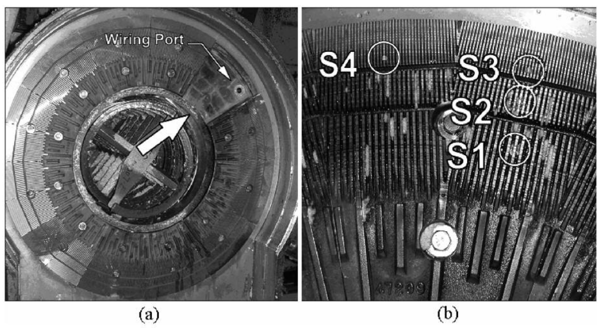

Fig 2. Location of instrumented plate segment, wiring port and force sensors.
(a) Vacant segment position, just prior to installation of the instrumented plate.
(b) Location and identification of the sensors in the instrumented plate.

the running average which is defined as the average of the accelerations recorded during a prescribed and immediately preceding time period. The dynamic threshold is the sum of the running average and a prescribed fixed offset. The accelerometer-based plate-protection system is illustrated in *Fig 1*.

During the trials, the static threshold for the Alert was 40 g while the offset for the Danger was set at 5 g over the 50 s running average. According to operators at the Port Alberni mill, the alarm of importance is the Danger alarm. The Alert alarm is seldom triggered during normal operation.

Sensor installation, data acquisition and preprocessing

Four sensors were installed in one plate segment on the stator disc of an Andritz 45-1B refiner. This is a single-disc, atmospheric refiner running at 1800 RPM on which plate gap is controlled mechanically by a lead screw. The instrumented Durametal™ 47209 plate segment remained installed for the entire life of the plates, which was approximately three months (~1800 hours), starting in September and ending in November 2005. The installation took place during a regularly scheduled plate change, and as a result, required little additional downtime. *Fig 2a* shows the location of the instrumented plate segment and the port used to route wiring outside of the refiner housing. *Fig 2b* shows the location and identification of each sensor on the plate.

In the fine bar region of the refiner plates, the bar-crossing frequency was as high as 32 kHz. Because of this, a high sampling rate of 300 KSamples/s was used. Data acquisition hardware used to record the signals from all sensors consisted of a National Instruments high-speed PXI-6251 board and a low-speed PXI-6133 board installed in a PXI system. Software was developed using National Instruments Labview™ to record data from all four sensors, their thermocouples, and the refiner's plate protection accelerometer.

It was apparent from manual inspection of the recorded RFS signals that the high sampling rate used to resolve individual bar-crossing impacts was not necessary to record the low frequencies associated with the increase in forces preceding a plate clash. The first step in processing the RFS signal was, therefore, to decimate the data files to a more manageable size. All data processing was performed using National Instruments Labview™ software. As mentioned previously, the data from each sensor was recorded at a sampling rate of 300 KSamples/s. The decimated data was equivalent to data sampled at a rate of 300 Samples/s, allowing for a larger time span to be viewed using a desktop computer. In addition to the decimation, the data was rectified to cast all data points into the positive domain.

Clash events

As mentioned above, the sensors were operational for the entire plate life of ~1800 hours. However, because of the high sampling rate and finite data storage space, long-term continuous data collection over this period could not be achieved. Instead, data from the four sensors was collected continuously during five short-term periods consisting of daylong controlled experiments. In between these periods, data collection software automatically recorded 10 seconds of data on 15-minute intervals. This data was supplemented with data from the refiner's plate protection accelerometer as well as notes taken during continuous trials. Data was stored in several files, the largest of which contained approximately seven minutes

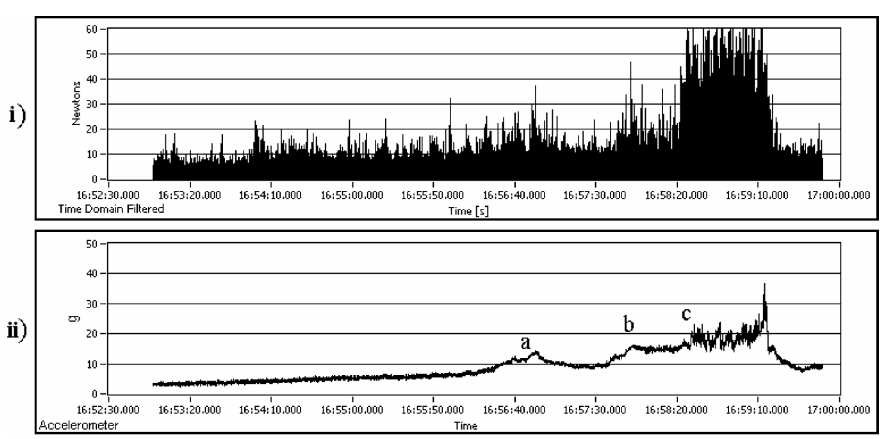

Fig 3. Samples of i) the decimated and rectified RFS data, and ii) the accelerometer data.

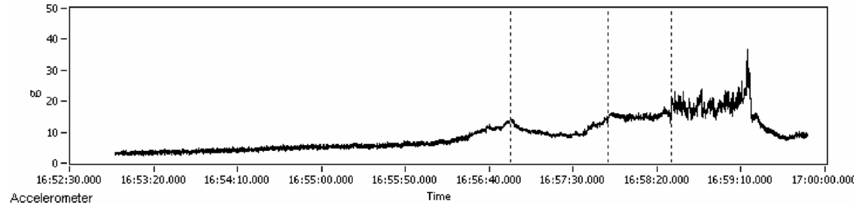

Fig 4. Accelerometer signal with danger alarms indicated as dashed lines.

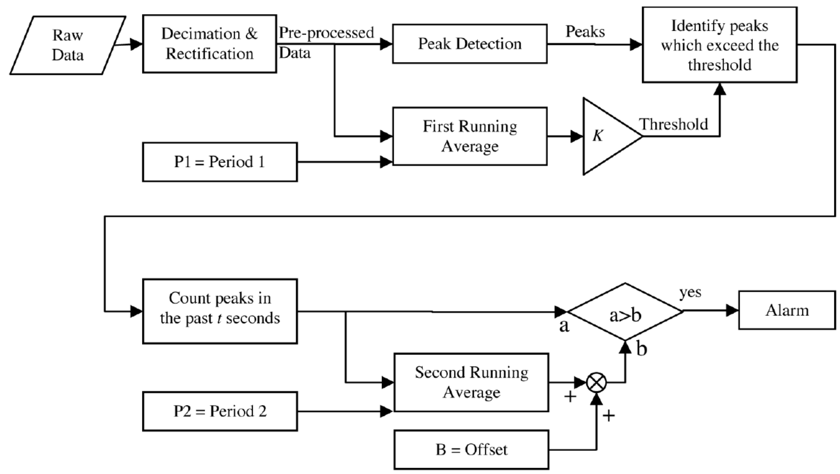

Fig 5. Data processing strategy used for the *Peak density* method.

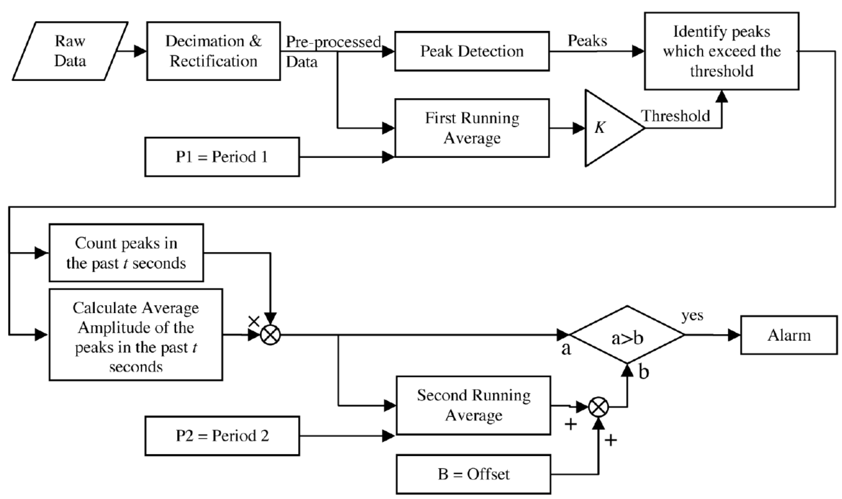

Fig 6. Data processing strategy used for the *Weighted peak density* method.

of continuous data. Of all the data files collected, only four contained clash events, all of which were found early in the trial period. These events were manually classified as either "clashes", or "interrupted clashes". The later describes events where the accelerometer successfully detected and prevented a clash from occurring. In total, nine events were observed including 6 clashes and 3 interrupted clashes. These events were verified using the trial notes.

Fig 3i shows 412 s, or approximately 6.9 minutes, of continuous decimated and rectified data produced by all RFS. *Fig 3ii* shows the signal recorded from the accelerometer system for the same period of time. Three events of interest are contained in this data. The first two are interrupted clashes, which are easily observed in the accelerometer data as two peaks at points a and b in the figure. The third event occurs at point c, marking the onset of a suspected clash. It is believed that physical contact between plates occurred at or soon after point c, based on the response of the RFS signals shown in *Fig 3i*. It is not understood why the third event was not averted as the previous two were. All three events can be observed in both the RFS and accelerometer data.

It is important to note that all clash events analyzed in this work occurred in the first trial period, during run-in of the new refiner plates. Clash events were recorded later in the three-month installation, but none during the continuous acquisition used in the trial periods. These records were therefore incomplete, showing only portions of the clash events, and could not be included in this analysis. It is unknown whether the process conditions in the refining zone that facilitated early detection of plate clash would be affected by plate wear, and this deserves further attention. However, the ability of the RFS to detect these process fluctuations later in the life of the plates was not diminished. All four sensors showed a minimal loss of sensitivity during calibration following the trials.

Detection Methods

Several clash detection algorithms were explored using the RFS data and each was judged based on its ability to predict the clashes before the accelerometer-based plate-protection system. Labview™ software was developed to scan data files and identify clash events. This software also simulated the operation of the accelerometer-based plate-protection system. The accelerometer data was processed and alarms were generated using the threshold and offset definitions described earlier. *Fig 4* shows an example of the accelerometer signal and the alarms generated using the simulated clash detection system.

In this figure, each of the three vertical lines indicates a Danger alarm as described earlier. The first two peaks are believed to be instances where the accelerometer detected and prevented clashes as previously discussed. The third alarm corresponds to the beginning an event in which the plate protections system failed to avert a clash. These results give confidence that the simulated accelerometer-based warning system is an accurate simulation of plate protection.

The RFS-based clash detection methods explored in this work are: *Peak density*, *Weighted peak density*, *Running average* and *Combined running average*. In all of these methods, the data is first decimated, as mentioned earlier, and then rectified. In the following descriptions of the individual methods, this decimated and rectified data is referred to as the pre-processed data.

Peak density method

The *Peak density* method is based on an *adaptive threshold*. This adaptive threshold is defined as a multiple of the running average of the pre-processed data. A LabView™-based peak detection algorithm[1)] is used to identify peaks in the pre-processed data. Each peak that exceeds the adaptive threshold is counted and the number of peaks counted in a prescribed period of time is defined as the *Peak density*. This method is illustrated in *Fig 5*.

An example of the parameters used to generate the peak density signal is as follows: The number of peaks in the past t = 1.65 s which exceed the first running average, taken over a period P1 = 60 s, by a factor K of 4. Alarms are triggered using a second running average, taken over a period P2 = 30 s, and offset value B of 9 peaks.

Weighted peak density method

The *Weighted peak density* method is an extension of the *Peak density* method. In the *Peak density* method, all peaks above the dynamic threshold, regardless of amplitude, contribute equally. In the *Weighted peak density* method, the contribution of each peak above the dynamic threshold is weighted according to its height. More specifically, *Weighted peak density* is defined as the *Peak density* multiplied by the average peak height during the period over which density is calculated. This method is illustrated in *Fig 6*.

An example of the parameters used in the *Weighted peak density* method is as follows: The number of peaks in the past t = 1.65 s which exceed the first running average, taken over a period P1 = 60 s, by a factor K of 4 multiplied by the average height of those same peaks. Alarms are triggered using a second running average, taken over a period P2 = 10 s, and offset value B = 80 N peaks.

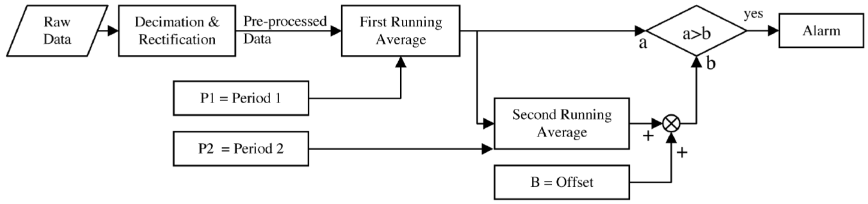

Fig 7. Data processing strategy used for the *Running average* methods.

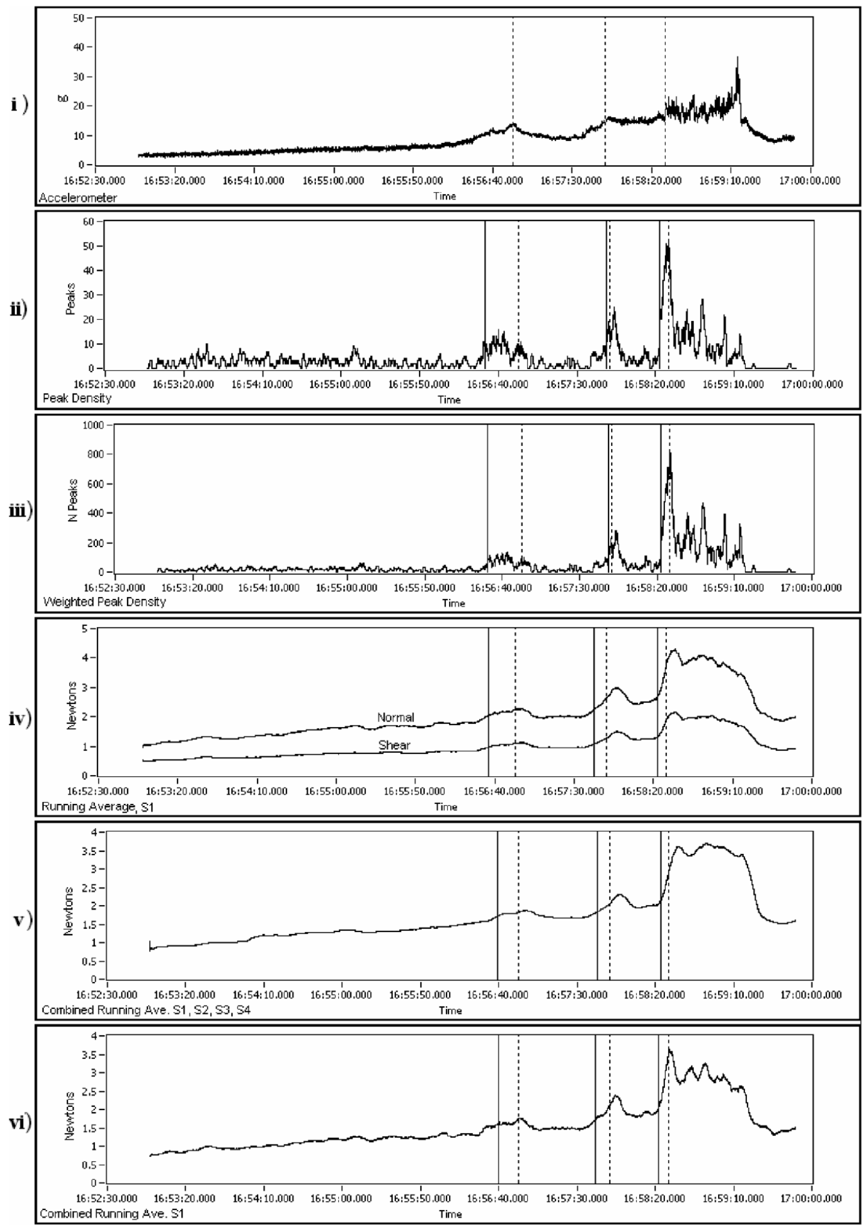

Fig 8. Examples of the output from i) the accelerometer, ii) *Peak density*, iii) *Weighted peak density*, iv) *Running average* v) *Combined running average* S1, S2, S3, S4 and vi) *Combined running average* of S1. In all figures accelerometer-based Danger alarms are shown by dashed lines, while RFS-based alarms are shown by solid lines.

Running average method

This method is essentially the same as the method used for the accelerometer-based detection system. In this method, a *first running average* of the pre-processed data is calculated. A *second running average* is then performed on the first running average data. The period over which each of these averages is calculated is longer for the second running average than for the first. Thus, the second running average data is subjected to more "smoothing" than the first running average data. A dynamic threshold is then calculated as the sum of the second running average data and a prescribed fixed offset. When

[1)] The core of the peak-finding algorithm consists of fitting a parabola to successive groups of points. The function checks whether each parabola is at a local maximum, determines the sign of the quadratic coefficient, which indicates the parabola's concavity, and finally checks that the peak is above the designated threshold.

the first running average exceeds this dynamic threshold, an alarm is generated. This process is performed on each sensor signal, two signals per sensor, such that eight independent alarm signals are produced. This method is illustrated in *Fig 7*.

Combined running average method

The *Combined running average* method is based on the *Running average* method. Shear and normal force data for the eight signals from the four sensors are pre-processed. The averages of the pre-processed signals are then calculated for each sensor (i.e. the average of the pre-processed shear and normal force signals) and for all four sensors (i.e. the average of the pre-processed shear and normal force signals for all four sensors). These average pre-processed signals are then used to detect impending plate clashes using the *Running average* method, as described above.

Table 1. Lead times[2)] for nine clash events using the five clash detection methods.

[2)] The accelerometer danger alarm, which is the base-case for calculation of lead time, was triggered by accelerations greater than 5 g over the 50 s running average

	Detection Methods				
Event designation	Peak density (S1-normal force)[3]	Weighted peak density (S1-normal force)[4]	Running average (S1-normal force)[5]	Combined running average (S1, S2, S3 & S4 - normal & shear force)[6]	Combined running average (S1-normal & shear force)[7]
a	21.1	22.3	16.8	13.7	12.9
b	2.1	1.4	7.8	7.6	9.3
c	5.9	6.1	5.5	5.2	6.1
d	9.7	9.7	-4.5	5.9	7.5
e	20.0	20.0	23.1	23.1	24.7
f	13.43	-0.84	-1.7	-2.6	11.2
g	-0.57	-0.27	3.2	2.5	15.9
h	-0.020	0.013	1.6	2.3	1.86
i	8.7	9.62	7.4	7.7	8.71
Average Lead Time	**8.9**	**6.3**	**6.6**	**7.9**	**10.9**

[3] Data is generated based on the number of peaks in the past 1.65 s which exceed the current 60 s running average by a factor of 4. Alarms triggered using second running average period of 30 s and offset value of 9 peaks

[4] Data is generated based on the number of peaks in the past 1.65 s which exceed the current 60 s running average by a factor of 4 multiplied by the average height of those same peaks. Alarms triggered using second running average period of 10 s and offset value of 80 N·peaks

[5] Data is generated using a first running average period of 10 s on normal force signal from S1. Alarms triggered using second running average period of 15 s and offset value of 0.20 N

[6] Data is generated using average of signals generated using a first running average period of 10 s on all 8 force signals. Alarms triggered using second running average period of 15 s and offset value of 0.12 N

[7] Data is generated using average of signals generated using a first running average period of 5 s on normal and shear force signals from S1. Alarms triggered using second running average period of 20 s and offset value of 0.20 N

Results

The plots shown in *Fig 8* show 412 s, of data from the accelerometer (*Fig 8i*) and force sensors (*Figs 8ii-8iv*), as processed with the methods described in the previous section. Note that, in this figure, dashed lines indicate the point at which the simulation of the accelerometer-based method detects an imminent clash and the solid lines indicate the point at which RFS-based methods detect an imminent clash. The time between a solid line and a corresponding dashed line indicates the time by which each RFS-based method leads the accelerometer-based method for each event. From this point forward, this time will be referred to as the lead time.

The performance of each of the five RFS-based detection methods for each of the nine clash events is summarised in *Table 1*. The lead times presented in *Table 1* are based on parameters which were chosen to provide maximum sensitivity without the appearance of false triggers. The accelerometer danger alarm, which is the reference-case for calculation of lead time, was triggered by accelerations greater than 5 g over the 50 s running average. This is the setting used in the mill during the sensor trials.

To further elucidate the performance of the RFS clash detection system, two sensitivity studies were performed. These studies examined the effects of adjusting the key data-processing parameters away from their optimum or reference values. As mentioned above, these optimum

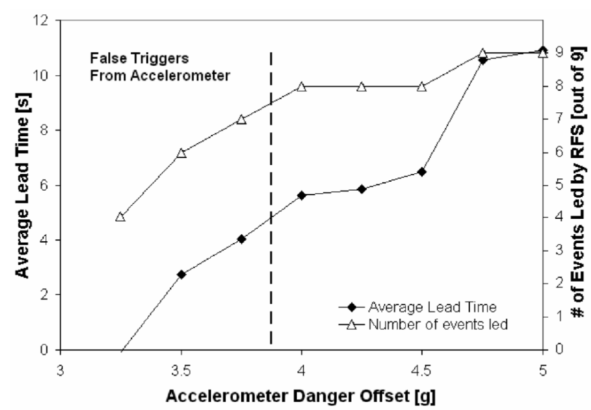

Fig 9. Average lead time and *Number of events led* vs. Accelerometer danger offset.

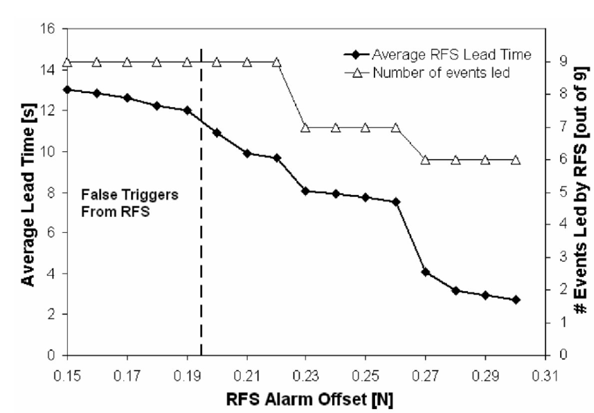

Fig 10. Average lead time and *Number of events led* vs. RFS-alarm offset.

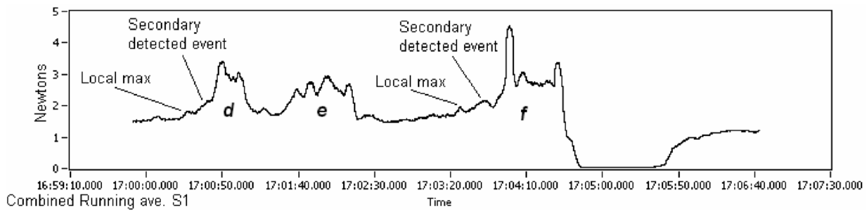

Fig 11. Detail of local maximums and their potential effect on peak detection performance. Events d, e and f indicated.

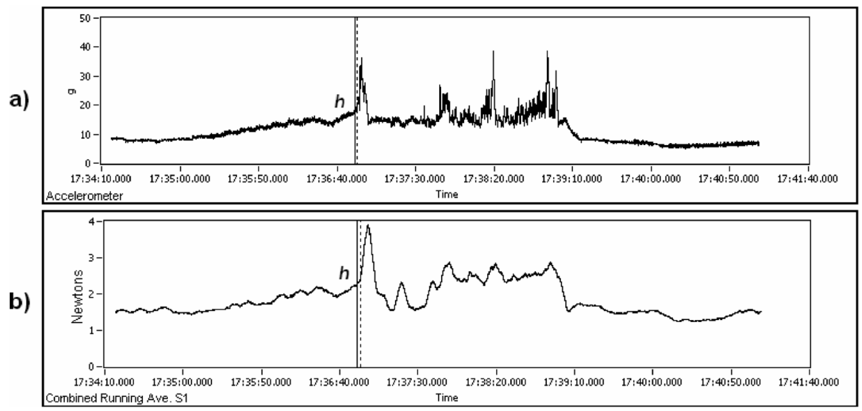

Fig 12. Detail of event h in a) the accelerometer data and b) the RFS-data. The sudden increase in forces leads to a relatively small lead time for this event.

values were used to calculate the data in *Table 1*.

In the first study, the accelerometer Danger offset was incrementally reduced from its reference value of 5.0 g to a minimum value of 3.25 g. Lead time was calculated relative to the *Combined running average* method based on S1 using the optimum settings listed for *Table 1*.

In the second study, the RFS alarm offset of the *Combined running average* method based on S1 was incrementally adjusted around its optimum or reference setting of 0.20 N, over the range from 0.15 N to 0.30 N. Lead time was calculated relative to the accelerometer-based method using the settings that were used at the mill during the trials.

In each study and for each incremental adjustment of the key data-processing parameters, the lead time for each of the 9 events was recorded. The average lead time and *Number of events led* were then determined. *Number of events led* method is defined as the number of events (out of 9) for which the lead time is positive.

The results of the first study are shown in *Fig 9*. In this figure, the dashed line denotes the offset below which false triggers occur. The results of the second study are shown in *Fig 10*. As in *Fig 9*, the dashed line in *Fig 10* indicates an offset setting below which false triggers occur.

Discussion

The performance of the RFS-based detection methods is superior to the performance of the accelerometer-based system. The average lead times for all of the RFS-based methods are at least 6 seconds. All of the RFS-based detection methods provide positive lead time in at least 7 of 9 events while the *Combined running average* method can detect all 9 events before the accelerometer based method using a single sensor. Each sensor was tested individually as well as in various combinations with other sensors using the *Combined running average* method. It was found that a sensor in the location of S1 provides the greatest increase in clash detection performance based on the number of events led and the average lead time.

The significance of the larger lead times provided by sensor S1 is not completely understood. One hypothesis considers radial location. S1 is the innermost sensor, and the only sensor believed to be completely inside the stagnation point, or the point at which steam velocity is zero. If back-flowing steam is a contributor to the disruption of the pulp pad, it would suggest a restriction of pulp flow radially inward from the stagnation point. This restriction could result in an accumulation of material in the inner part of the refining zone prior to a clash, which would explain the early rise in forces recorded by S1.

The lead time data in *Table 1* for events a, b, c, e, g, h and i are relatively consistent across all of the detection methods. The data for events d and f, however, is less consistent. Inconsistencies include the relatively large distribution of lead times found for event f as well as the large negative lead time found using the *Running average* method on event d. These inconsistencies are caused by the presence of local maxima in the processed data as shown in *Fig 11*. A local maximum may be missed by a small margin leading the detection algorithm to select a second rise in forces following it. Other methods may detect the first maximum leading to a significantly different detection time. This behaviour is the result of the characteristics of each detection method and the characteristics of the data surrounding each clash event.

Another notable characteristic found in the tabulated results is the relatively small lead times for event h across all detection methods. This event is characterised by an abrupt increase in force and acceleration amplitudes, as shown in *Fig 12*. The RFS and accelerometer based system detect the event almost simultaneously, just before the spike in their respective signals. Also noticeable is the similarity in shape between the accelerometer and RFS signals which could also lead to similar detection performance.

The sensitivity results in *Fig 9* show that the accelerometer based system cannot out perform the RFS for more than one event without also causing false triggers. The event for which the RFS system lags is suspected to be an interrupted clash and occurs at relatively low force amplitude. The study also shows a decrease in average lead time from the RFS as the accelerometer offset is reduced from its initial value. Despite this reduction in advantage, the RFS still outperforms the accelerometer by a significant margin.

The sensitivity results shown in *Fig 10* show that any increase in the RFS alarm offset results in a reduction in the average lead time. However, the RFS system is still able to pre-detect all events for offsets up to 0.22 N. When the offset is further increased to 0.23 N, two events show negative lead times. The average lead time of these two events is -1.65 s. This negative lead time is small when compared to the remaining seven events, whose average lead time is 9.45 s. As the offset is further increased in increments to 0.26 N, the average lead time of these two events decreases to -2.13 s. However, this is still small compared to the average lead time of 8.93 s for the remaining seven events. A decrease in the RFS offset below 0.20 N results in an increase in the average lead time, but is accompanied by false triggers.

Conclusions

Four Refiner Force Sensors (RFS) were installed in a mill-scale pulp refiner at the Catalyst Paper Corp. mill in Port Alberni, B.C., Canada. These sensors replace a short segment of a refiner bar and measure normal forces and tangential shear forces that are applied to the bar by the pulp. The refiner used for these experiments is an Andritz 45-1B refiner which is a single-disc type. The sensors were installed at different locations along the same radius in a Durametal™ 47209 plate segment. The experiments were performed over a three-month period starting in September of 2005. Data was collected at regular intervals over the installation and consisted of four day-long trials of continuous collection and four long periods of intermittent, short term data collection intervals. In total, the data collected contains 9 clash events all of which occurred in the first day of testing.

The data recorded from the sensors was processed to detect the onset of refiner plate clash. Several methods of processing the data to produce a predictive tool were explored. These methods included a running count of the density of high force peaks, a weighted version of the peak density method which also accounted for peak height, the running average of RFS data, and the combined running average of RFS data based on the average of the forces measured by one or more sensors. Of the methods explored, the combined running average yielded the best performance.

The combined running average algorithm computes the running averages of the RFS shear and normal force signals. These running averages are then averaged, producing a single signal. The combined running average of the shear and normal force signals from S1 can predict all events before the accelerometer-based system with an average lead of 10.9 s. Sensor 2 through 4 could also predict all the events but not with the same performance as S1. It is speculated that this is due to S1's unique location on the refiner plate, inside of the stagnation point.

A sensitivity study revealed that the accelerometer could not match the performance of the RFS for any event, other than one, without also causing false triggers. The study also showed that the RFS system could offer improved detection performance for a broad range of offset values.

Literature

Allison, B.J., Ciarniello, J.E., Tessier, P.J.C. and Dumont, G.A. (1995): Dual adaptive control of chip refiner motor load, Pulp Paper Can. 96(3), 39.

Brenholdt, I.R. (1997): Apparatus and method for particle size classification and measurement of the number and severity of particle impacts during comminution of wood chips, wood pulp and other materials, United States Patent 5,605,290, issued February 25.

Dumont, G.A. and Astrom, K.J. (1988): Wood chip refiner control, IEEE Control Systems Magazine, 8(2), 38.

Jack, J.S., Mills, C. and Baas, P.H. (1981): A device for detection and prevention of plate clash in disc refiners, Pulp Paper Can. 82(9), 89.

Rogers, J.H. and Butler, D.J. (1977): Method and system for detecting plate clashing in disk refiners, United States Patent 4,233,600, issued November 11.

Senger, J., Ouellet, D., Wild, P., Byrnes, P., Sabourin, M. and Olender, D. (2006): A technique to measure mean residence time in TMP refiners based on inherent process fluctuations, J. Pulp Paper Sci. 32(2), 83.

Siadat, A., Bankes, A., Wild P.M., Senger, J. and Ouellet, D. (2003): Development of a piezoelectric force sensor for a chip refiner, Proc IMechE Part E: Journal of Process Mechanical Engineering, 217(2), 133.

Whyte, D.M. (1986): Methods of and/or apparatus for detecting and controlling refiner plate clashing, United States patent 4,627,578, issued December 9.

Manuscript received October 18, 2006
Accepted November 6, 2006

Appendix E

Description of Signal Conditioning Steps

Each sensor generates two raw voltage signals, which are converted to a normal and shear force signal according to the relation described in the flowchart in Figure 1. Piezo-based transducers are second-order instruments [], and are therefore subject to recording a false rise in amplitude as measured frequencies near the first natural frequency. The magnitude of this rise can be calculated using Equation E.1:

$$\left|FRF\right| \cong \frac{K}{\sqrt{\left[1-\left(\frac{\omega}{\omega_n}\right)^2\right]^2+\left(\frac{1}{Q^2}\right)\left(\frac{\omega}{\omega_n}\right)^2}} \quad \text{(E.1)}$$

where:
$\left|FRF\right|$ = magnitude of frequency response function,
K = static sensitivity (V/N),
ω = frequency (Hz),
ω_n = first natural frequency (Hz),
Q = factor of amplitude increase at resonance.

The parameters K, Q and ω_n are estimated from the empirical *FRF* measured during calibration (see Figure A.4 for examples of FRF). Once an accurate model of the *FRF* has been found, an inverse filter can be designed to counter the effects of resonance. An infinite impulse response (*IIR*) filter is perfectly suited for this task, as it can be designed to match an arbitrary frequency response []. Design of the *IIR* filter proceeds according to:

$$\left|IIR\right| = \frac{K}{\left|FRF\right|} \quad \text{(E.2)}$$

where:
$\left|IIR\right|$ = magnitude of frequency response of filter.

While the IIR filter is used to extend the upper limit of useable bandwidth of the sensor, and counter the effects of resonance, the second conditioning step extends the lower limit of useable bandwidth, and compensates for the loss of low-frequency components inherent to all piezo-based transducers. The low frequency response of the sensor and charge amplifier is modeled as a first-order, high-pass filter [Doebelin]. A compensation filter can then be used to recover these lost components, effectively lowering the cut-off frequency of the system. The custom charge amplifier used in both campaigns has a cut-off frequency ω_{cAMP} of 400 Hz. An effective cut-off frequency ω_{cEFF} of 100 Hz was chosen according to the relation described in Figure 1. A complete recovery is not possible, as it requires infinitely high gain *G*. The effect of the compensation filter is primarily visible as a positive offset of the force signals in the time domain.

Because it is not possible to recover all of the low frequency components using the compensation filter, a final manual correction is necessary. A reference for this correction can be found in the valleys between adjacent force peaks, based on the assumption that the force signal returns to zero in between bar-crossing impacts. This assumption is valid in most instances, but not in plate patterns that contain high bar-crossing angles. The directional plates used in the Springfield campaign are an example of this pattern. At specific angular positions between rotor and stator, observed bar-crossing angles make it possible for two bars to be over the sensor probe at once, causing the recorded force profiles to blend together. The force signal would therefore not completely return to zero during impacts of this nature, and corresponding valleys cannot be used as an accurate reference.

To avoid using these "blended" valleys when reconstructing the true zero of the signal, a threshold based on the time constant was developed. Analogous to the rate of charge decay, it was discovered through simulation that the rate of increase of the system's true zero is also governed by the time constant. The correct valleys V_t can then be chosen based on the logic described in Figure 1.

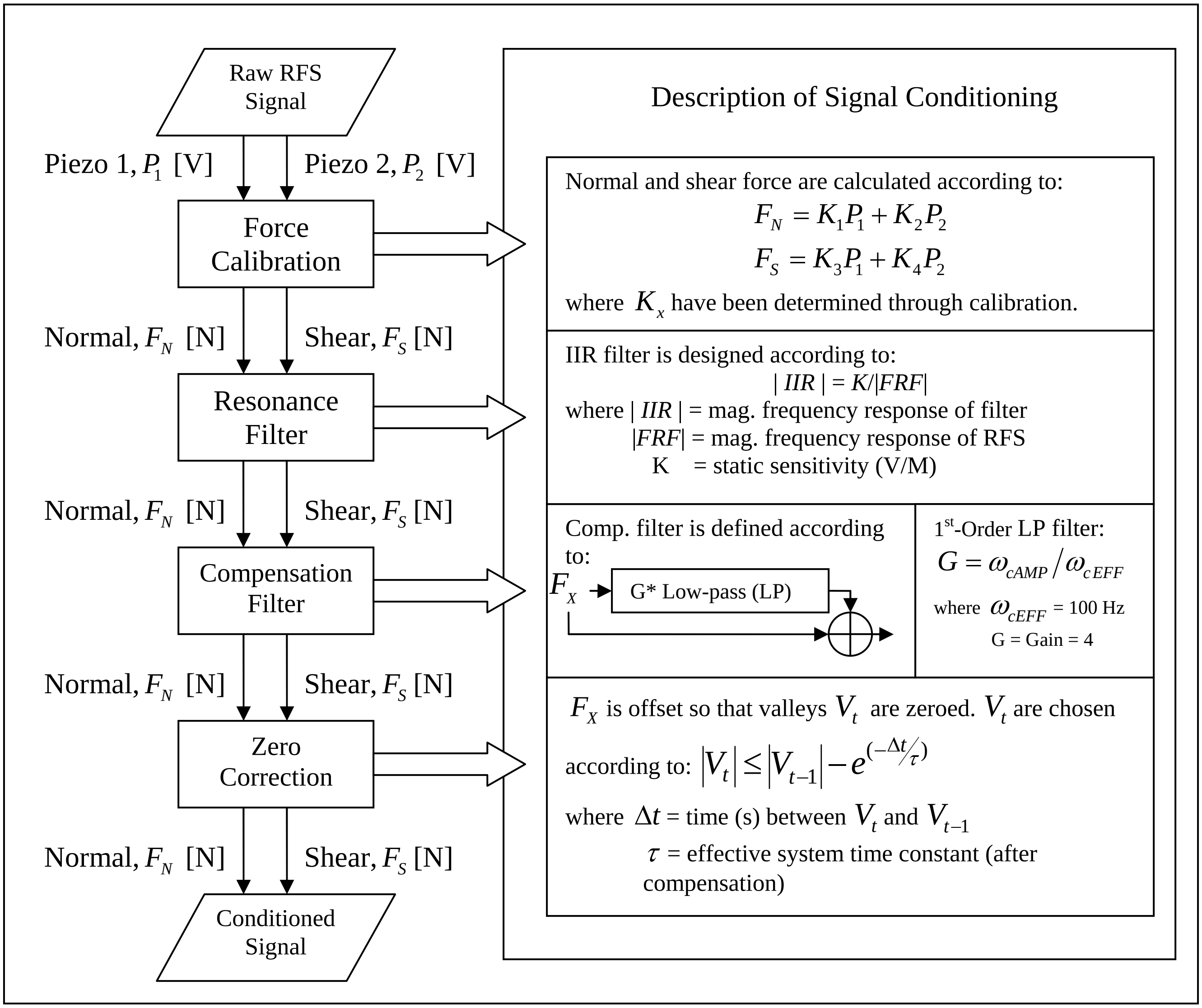

Figure 1: Flowchart of signal conditioning steps used to reconstruct normal and shear force signals.

Appendix F

Port Alberni Trial Data Acquisition System and Setup

A National Instruments PXI system with 8-slot chassis and embedded controller was purchased for the Port Alberni campaign. The system is rugged, portable and offers scalability, should more sensor channels be necessary in future experiments. The PXI system was outfitted with one PXI-6133 high-speed board, one PXI-6220 low-speed board, and one IEEE-1394 (Firewire™) board. The high-speed board is capable of handling 3 MSample/s on 8 channels simultaneously, but for each of the RFS channels, would only be sampling at 300 KSamples/s. The low-speed board would record thermocouple data, and refiner parameters, at reduced sampling rates. In this case, an accelerometer was affixed to the refiner, and was part of a control system to warn of impending plate clash. This was the only piece of refiner information available to be recorded. Because of the volume of data that would be accumulated during the trials, portable hard-drives were purchased and would connect to the DAQ system through the IEEE-1394 ports. The IEEE-1394 ports would support real-time streaming of the recorded data to the hard-drives, which could then be exchanged when full. Figure 1a shows the DAQ system as it was setup at the mill.

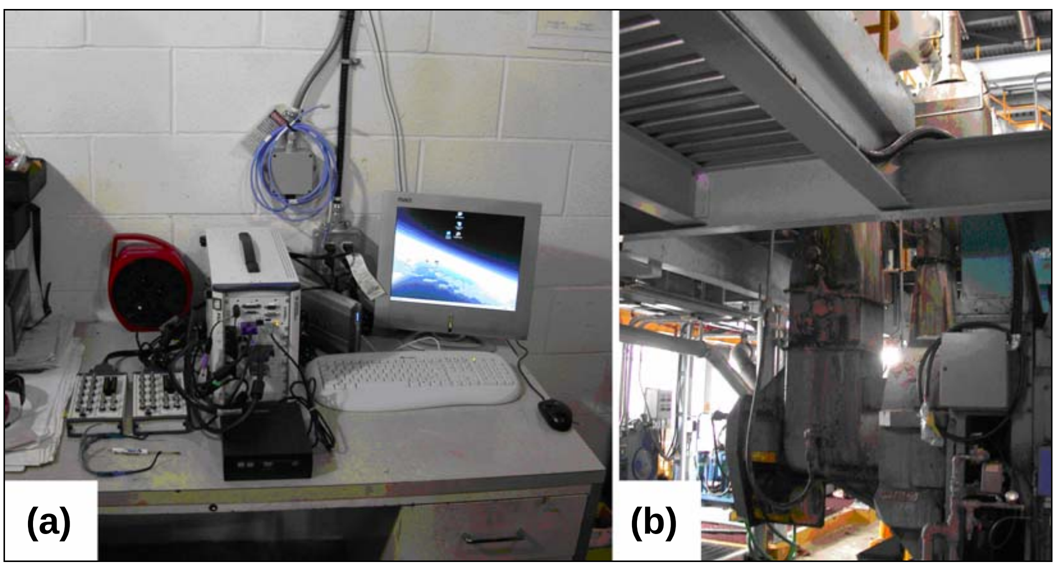

Figure 1: (a) The data acquisition system as it was setup at the mill, and (b) a view of the refiner, wire-routing conduit and charge amplifier enclosure.

The DAQ system was located in a clean room that was adjacent to the test refiner, and isolated from the regular activity of the production floor. Figure 1b shows a view of the test refiner, from the doorway of the room housing the DAQ equipment. Also seen in this photograph, is the black conduit that was used to route coaxial cabling from the DAQ system to the charge amplifier enclosure, which was bolted directly to the refiner. The charge amplifier enclosure also housed two 12 V batteries, which were its source of power, and a number of thermocouple signal conditioners. The smaller black conduit, which is coiled around the enclosure in the photograph, was eventually connected to the RFS wire bundle exiting the refiner. The installation of all these auxiliary systems was undertaken a week prior to the installation of the instrumented plate.

Vita

Name

Dustin James Olender

Place and year of birth

Winnipeg, Manitoba, Canada, 16 June 1979

Education

Bachelors of Applied Science, Mathematics and Engineering Applied Mechanics Option, Queen's University, Kingston, Ontario, 2001

Masters of Applied Science, Mechanical Engineering, Royal Military College of Canada, Kingston, Ontario, 2004